

22nd International Conference on
Condensed Matter Nuclear Science (ICCF22)

Book of Abstracts

(Updated Monday, 26 August 2019)

Copyright 2019

The International Society for Condensed Matter Nuclear Science



ICCF22

ASSISI

2 0 1 9

Contents

Conference Patrons!	5
Outline Program at a glance	5
Map of Hotel Domus Pacis	6
Local Map	6
Excursion	7
Lost?	7
Questions?	7
Trains:.....	7
Returning home:	7
Renaissance Banquet:	7
Companions.	7
Open Bar:	7
Meals:.....	7
IAC Meeting.....	7
Other Meetings	7
Questionnaire.....	8
Poster papers	8
Takahashi: Latest Progress in Research on AHE and Circumstantial Nuclear Evidence by Interaction of Nano-Metal and H(D)-Gas	9
Kasagi: Possible radiation from thin film metal surface with anomalous excess heat: Can we observe hot spots or Bremsstrahlung?	10
Grimshaw: LENR Research Documentation Initiative: Progress in Methods and Participants Oral & Poster	11
Kotsyubynsky: Synthesis and characterization of Pd and Ni nanoparticles confined in microporous structures for the LENR applications	12
Dubinko: Nuclear Fusion of Hydrogen Isotopes Induced by the Phason Flips in Pd and Ni Nanoclusters	13
Konagaya: Supercomputer simulation and experiment clarifying the maximum level of focusing compression due to pulsed supermulti-jets colliding: in weak cold-fusion engine (Fusine)	14
Konagaya: Development of weak cold-fusion engine (Fusine) assisted by molecular chemical reaction: based on double focusing-compression over 1,000 bar and 7,000 K due to pulsed supermulti-jets colliding	15
Greenyer: Leveraging observations of patterns in transmutation data from multiple experiments and nature to drive the development of a predictive tool Poster	16
Szumski: Initial Simulations Using The Least Action Nuclear Process [LANP] Computer Model for Electrode Design Poster	17
Szumski: The Least Action Nuclear Process [LANP] Computer Model of Cold Fusion Poster.....	18
Kobayashi: Quasi-stability theory with multi-dimensional Taylor expansion: revealing transmutation of atoms in cold fusion.....	18
Rusetskii: Investigation LENR Processes in Condensed Matter on the HELIS Setup - Overview and Prospects.	20
Mastromatteo: LENR evidence with hydrogen and deuterium loading in thin palladium films	21
Ruer: Experimental setup to detect hydrinos	22
Ruer: How LENR can change the World	23

Carpinteri: Earthquake neutrons and Earth-Crust LENR: From seismic precursors to Geochemistry evolution 24

McKubre: Thirty Years On. 25

Bannister: The limits to growth: the intersection of energy and economics. Oral & Poster 26

Meulenberg: Deep-level atomic orbitals and more 27

Garai: Physical Model for Lattice Assisted Nuclear Reactions 28

Nagel: Review of Seebeck Calorimeters Used in LENR Experiments 29

Hagelstein: HD/He-3 phonon-nuclear coupling matrix element Poster 30

Hagelstein: Recent Progress on Phonon Coupling Models 31

Metzler: Observations of delocalized gamma emission from Co-57/Fe-57 samples during application of mechanical stress 32

Forbes: Initial report on low-energy ion beam experiments with various metal targets..... 33

S Dana Seccombe: Phonon Assisted Nuclear Fusion Mode 34

Uchikoshi: Laser Condensed-Matter Fusion Experiments. Oral and Poster 35

Miles: Thermodynamic Basis For The Power Term For Work in Electrochemical Calorimetry Poster 36

Miles: The Thermoneutral Potential In Electrochemical Calorimetry For The Pd/D2O System Poster 37

Nagel: The LENRIA Experiment and Analysis Program (LEAP) 38

Nagel: Comparison of the Theoretical Results of Kálmán and Keszthelyi with LENR Experimental Results 39

Roggeri : Opportunities and aid from the European community for the development of scientific cooperation projects: horizon 2020 and new horizon Europe programs 40

Tanzella: Mass Flow Calorimetry in Brillouin’s Reactor 41

Celani: Progress understanding LENR-AHE effects, using thin, long Constantan wires multi-elements coated, under D2 gas mixtures at high temperatures, by DC/AC voltage stimulation in coiled coaxial geometry. 42

Stankovic: Nuclear Transmutation with Carbon and Oxyhydrogen Plasma 43

Garai: Speculation on the size of the electron poster 44

Jaitner: Condensed Plasoids – The Nuclear Active Environment in LENR Oral & Poster..... 45

Carat: Fiery Science of Cold Fusion comic book Poster 46

Rothwell: Increased Excess Heat from Palladium Deposited on Nickel..... 47

Kovacs: The Zitterbewegung Orbit of Electrons..... 48

Kovacs: Maxwell-Dirac Theory and Occam’s Razor: Unified Field, Elementary Particles, and Nuclear Interactions Poster 49

Klimov: Power Balance in Water Plasma Reactor 50

Klimov: Review of the Proceedings of the 25th Russian Conference on Cold Nuclear Transmutation of Chemical Elements and Ball Lightning..... 51

Klimova: Thermal Energy Release in a Swirl Heterogeneous Reactor at Pulsed Repetitive Electrical Discharge52

Bowen: Primary and Secondary Reactions in a LENR with a Li Electrolyte Solution 53

Iwamura: Excess Energy Generation using a Nano-sized Multilayer Metal Composite and Hydrogen Gas..... 54

Hatt: Cold Nuclear Transmutations Light Atomic Nuclei Binding Energy Oral and Poster 55

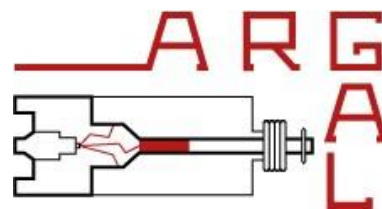
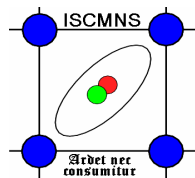
Tarasenko: Planet Earth - cold fusion reactor poster 56

Narita: Investigating Thermal Behavior of Pd Foil Coated with Metal Membrane in Deuterium Diffusion Poster 57

Ruer: Basics of air flow calorimetry 58

Albertini: ^{228}Th , ^{63}Ni , ^{57}Co : three anomalous decays suggesting the feasibility of radionuclide neutralization .	59
HuangC: Temperature Dependence of Maximum Excess Power in 3 New Experiments (Letts, Parkhomov, & Mizuno).....	60
Varaprasad: Experiments to observe Excess Heat in Ni-LAH, Ni-H ₂ , Pd-D ₂ systems Poster.....	61
Kaal: Nuclear Transmutation and Mass Defect explained with the Structured Atom Model (SAM) Oral & Poster	62
Wytttenbach: SO(4) Physics and LENR poster.....	63
Bowen: An Examination of the Updated Empirical Data in Support of the Shell Model.....	64
Vysotskii: Anomalous LENR effects and its justification based on the method of coherent correlated states..	65
Vysotskii: Formation, evolution, collapse and application of correlated packets in LENR experiments	66
Gaydamaka: THE POSSIBLE ROLE OF LENR IN DENTISTRY (EFFECTS AND PREVENTION) Poster.....	68
VysotskiiV: Distant behind-screen generation, X-Ray stimulation and LENR action of undamped heat waves	69
Vysotskii: Periodic structure of Fe-Mn natural geology crusts with anomalies of the isotopic ratio as the results of self-controlled global biostimulated isotope transmutation in oceans and lakes	71
Vysotskii: New (pre-industrial) stage of applied research on isotope transmutation in biosystems Poster.....	72
Alexandrov: Cold nuclear fusion in lithium compound alloy	73
Collis: An Empirical Global Calculator of Atomic Masses.....	74
Zeiner-Gundersen : Electricity production from ultra dense deuterium.....	75
Huang BJ: Excess Energy from a Vapor Compression System.....	76
Greenyer: Nickel-hydrogen heat generator continuously working for 7 months	77
Greenyer: LENR as Appearance of Weak Interactions Poster	77
Hatt: Cold Nuclear Transmutations Theoretical basis for the calculation of binding energy. Poster.....	78
Hatt: Cold Nuclear Transmutations - Examples of Fe Isotopes Binding Energies Poster.....	79
Swartz: Superhyperfine Structure of the Deuteron Line Emission from Active ZrO ₂ PdD Heralds an FCC Vacancy	80
Swartz: Atomic Deuterium in Active LANR Systems Produces 327.37 MHz Superhyperfine RF Maser Emission	81
Swartz: Buoyant heat transport can produce unreliable estimates of heat generation	82
Swartz: Pulsing Sideband at 327.37 MHz May Herald Movements within an Active Loaded PdD Lattice.....	83
Fredericks: Elliptical tracks: evidence for superluminal electrons?.....	84
"Beyond Hydrogen Loading"	85
Paillet: Highly relativistic deep electrons and the Dirac equation	86
Bowen: The Electromagnetic Considerations of the Nuclear Force	87

Conference Patrons!



Outline Program at a glance

<h2 style="text-align: center;">ICCF22 Outline Program 2019</h2> <p style="text-align: center;">www.iscmns.org/iccf22</p>								
Date	08:00-10:30	10:30-11:00	11:00-13:00	13:00-14:30	14:30-16:00	16:00-16:30	16:30	19:00
Sunday 8 September							Registration	Welcome Reception
Monday 9 September	SESSION 1	Coffee	SESSION 2	Lunch	SESSION 3	Coffee	SESSION 4	Dinner
Tuesday 10 September	SESSION 5	Coffee	SESSION 6	Lunch	Excursion			Dinner
Wednesday 11 September	SESSION 7	Coffee	SESSION 8	Lunch	Poster Session	Coffee	SESSION 9	Dinner
Thursday 12 September	SESSION 10	Coffee	SESSION 11	Lunch	SESSION 12	Coffee	SESSION 13	Banquet
Friday 13 September	SESSION 14	Coffee	SESSION 15	Lunch				

N.B.Refer to the conference program for more details.

Map of Hotel Domus Pacis



Local Map

S. MARIA DEGLI ANGELI



Excursion



Coach leaves 14:30 from the hotel carpark. We will tour Assisi on foot.

- Basilica of St. Francis*
- Piazza del Comune (central square)
- Minerva temple
- Chiesa Nuova
- Oratory of St. Francesco Piccolino
- Basilica of St. Claire
- San Rufino Cathedral (option)



If you want to smoke, please go outside. You may not smoke anywhere indoors.

Lost? The address and phone numbers of the hotel Domus Pacis are on the map page.

Questions? Do ask one of the hostesses at the ICF22 reception desk outside the conference hall.

Trains: You can book trains and find the timetable at <http://www.trenitalia.it> Assisi railway station is shown on the map 10 minutes' walk from the hotel.

Returning home: We may be able to coordinate coach transport directly to Fiumicino airport on Friday. Please give your flight details to the conference desk well in advance.

Renaissance Banquet: Weather permitting, will be held in the gardens at the back of the hotel. There will be an appetitive at 19:00.

Companions. Please ask at the conference desk for details of excursions for which there may be a modest charge. (possibly Perugia, Foligno). Or why not walk round the Basilica just 200m from the Hotel and also visit the Rose Garden? N.B. Companions resident in the hotel are entitled to all the privileges of participants including meals and coffee breaks.

Open Bar: From 20:30 to 22:00 at the bar in the hotel foyer. Take advantage of the convivial atmosphere to discuss science! Make sure you wear your badge to show your entitlement.

Meals: Please respect the timetable. Lunches are at 13:00 and dinners at 19:00. If you have dietary requirements, make them known to the hotel staff. Wine is included with lunch and dinner. Breakfast is from 7:30-9:00.

IAC Meeting: will be held in the Sala Semplicità on Wednesday followed by dinner. (By invitation only).

Other Meetings: Ask at the ICCF22 reception desk if you need a meeting room.

Questionnaire

In order to help future conference organizers, please answer the following questions:-

1. Was the conference good value for money?
2. Were sufficient details about location and transport provided?
3. Was the food adequate?
4. Did you like the open bar policy?
5. Were presentations of appropriate length?
6. Would you have liked more panel discussions?
7. Did you appreciate the excursion?
8. Did you learn something useful?
9. Did you make new friends?
10. Would you like to return to Assisi for a future conference?

Poster papers

Poster papers are an excellent method of communicating scientific results interactively. To encourage more poster papers, ISCMNS is offering a bronze medal to the principal presenter of the best poster. Participants can vote on the winner! Poster papers will be displayed in the hallways outside the lecture theatre.



The poster boards are 2m high and 1m wide. Each board is numbered and allocated to the presenter specified in the conference program.

Takahashi: Latest Progress in Research on AHE and Circumstantial Nuclear Evidence by Interaction of Nano-Metal and H(D)-Gas

Akito Takahashi^{1,2}, Toyoshi Yokose³, Yutaka Mori³, Akira Taniike³, Yuichi Furuyama³, Hiroyuki Ido², Atsushi Hattori², Reiko Seto², Atsushi Kamei², Joji Hachisuka²
¹Prof. Emeritus Osaka University, ²Technova Inc., ³Kobe University

Latest results on anomalous heat effect (AHE) by interaction of binary nano-composite metal powders and H (or D) gas, after the NEDO-MHE project (2015-2017), are reported in this paper. PNZ (Pd1Ni10/zirconia) and CNZ (Cu1Ni7/zirconia) powders by melt-spun and calcination methods were used, and were re-used by additional calcination.

80 to 400 W/kg level excess thermal power W_{ex} of sustainable continuity for several weeks have been reproducibly observed at elevated temperature around 300 °C, by using re-calcined PNZ-type samples with D-gas, significantly in net D-gas desorption mode. Specific reaction energy (η -value) per D-transferred was very large as 100 eV/D to over 1000 eV/D. Very weak (0.1-0.2 n/J level) neutron emission looked correlating with the rise-up heat hump of thermal power after joule heating started. These results can be of the circumstantial nuclear signature of the AHE by the nano-metal D-gas interaction.

Data of 50 to 140 W/kg level excess thermal power was repeatedly obtained by CNZ-type samples with H-gas at elevated temperatures after the saturation of H-gas absorption (endothermic) by sample. Excess thermal power of ca. 50 W continued for more than two weeks by 505 g CNZ7r (re-calcined) sample, with very strange behavior of the “cooled-flat and oscillating” TC4 RC upper flange temperatures (the effect has been investigated and concluded as a kind of turbulence gas-flow of up- and down-stream by strong local AHE). Big or small heat bursts were observed many times in the rise-up data after the start of external heating from room temperature. The η -values were obtained to be so large as more than 10,000 eV/H-transfer for CNZ7r sample runs, implying nuclear effect.

Anomalous Heat Effect (AHE) is repeatable by the interaction of H (or D) gas and Ni-based nano-composites metal powders. Reproducibility is established. In the rise-up phase by external heating, large thermal power humps happened repeatedly after H (or D) desorption modes. Conditions to realize the apparent equilibrium pressure with maximum dynamic H (or D) gas flux in both direction of desorption and sorption on surface of nano-composite metal particle are considered to be of key factor. Higher temperature than 300 °C for RC with homogeneous gas feed is to be tested.

Kasagi: Possible radiation from thin film metal surface with anomalous excess heat: Can we observe hot spots or Bremsstrahlung?

J. Kasagi¹, T. Itoh^{1,2} and Y. Iwamura¹

¹ Research Center for Electron Photon Science, Tohoku University, Japan

² Clean Planet Inc., Japan

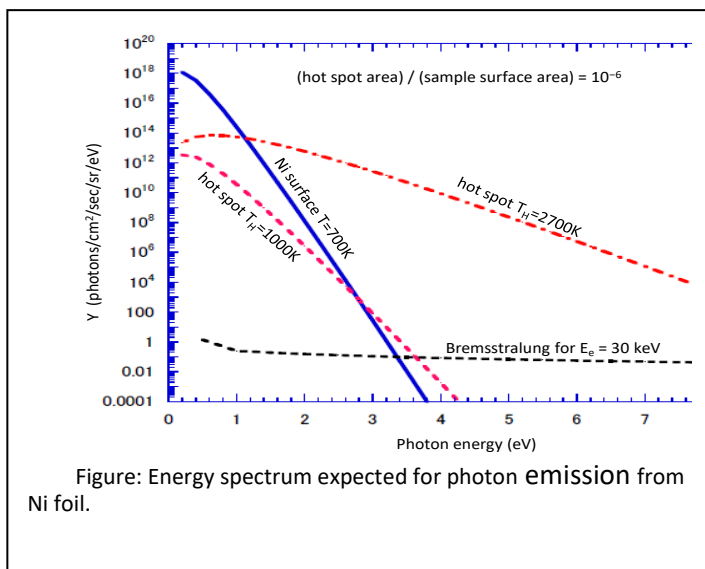
In the ICCF21, we reported that no radiations with photon energy higher than 50 keV were observed associated with the excess heat generation in NiCuZr-H₂ system. This means that the reaction does not produce energetic particles that undergo a secondary nuclear reaction with the material in the sample, nor does it produce radioactive nuclei. Then a question is ‘How is locally generated energy of above MeV transferred to the thermal energy of the sample?’

Here, we consider a naive situation in which the energy (Q) generated by the reaction is given to an extremely small region and is instantaneously transferred to kinetic energies of all conduction electrons there (the number of electrons is N_e). These electrons lose their energy by ionizing and exciting the substance during traveling a distance of the range (R), which may be a radius of a sphere of the hot spot. Then, the temperature of the hot spot rises by $\Delta T = Q/MC$ (M: mass of the hot spot, C: specific heat capacity).

For a thin Ni foil with Q = 1 MeV, a hot spot is formed only for the case of 500 < N_e < 1000; corresponding radius 38 > R > 16 nm and temperature 145 < ΔT < 2150 K. When the excess heat is 1 W, hot spots are repeatedly generated in the sample at a rate of 6.3 × 10¹² / sec. Although very rough, 10⁻³ to 10⁻⁴ of the total number of Ni are included in a hot spot portion. Thermal radiation should be observed from the hot spot on the film surface. An energy spectrum expected for photon emissions from the thin film surface is shown in Figure. Present are hot spots with ΔT = 2000 K (red dashed-dotted line) and 300 K (red dashed line) at the ratio of (hot spot area) / (sample surface area) = 10⁻⁶ on the surface of a film at T = 700K (blue solid line). One can say that if the temperature of the hot spot is high enough, visible light will reveal the presence of hot spots.

When N_e decreases (electron increases), Bremsstrahlung emitted might be visible. Figure also shows Bremsstrahlung emission by 33 keV generated when N_e = 30 (black In the visible light region, the not affected by the Bremsstrahlung measurement of keV region or essential in order to clarify the the Bremsstrahlung.

When N_e decreases (electron increases), Bremsstrahlung emitted might be visible. Figure also shows Bremsstrahlung emission by 33 keV generated when N_e = 30 (black In the visible light region, the not affected by the Bremsstrahlung measurement of keV region or essential in order to clarify the the Bremsstrahlung.



spectroscopy energy by electrons the expected electrons spectrum is at all. Thus, a higher is presence of We have just associated wide range of light) to keV surface is a

Grimshaw: LENR Research Documentation Initiative: Progress in Methods and Participants Oral & Poster

Thomas W. Grimshaw, Ph.D., The University of Texas at Austin

Cold fusion (LENR) became a pariah science when it was rejected within a year or so after its announcement in 1989. Consequently, few new researchers have entered the field in the past 30 years. Much progress has been made in understanding LENR and addressing the issue of adequate reproducibility. However, many of the long-term researchers are retiring and otherwise leaving the field. The loss of their research records would be a major blow to the field. Given the urgent need of society for a new source of low-cost, clean, and plentiful energy, the loss of LENR research and understanding would also be tragic for all of humanity.

The LENR Research Documentation Initiative (LRDI) is underway to mitigate the loss of LENR research records. It began with a successful pilot project with Dr. Ed Storms, which was reported at ICCF-21 in 2018. It is being conducted at The University of Texas at Austin and is built on a foundation of more than 10 years of contributions to the field. Methods used in the LRDI are as follows:

- Begin with an existing professional biography
- Make on-site visits as required
- Identify and describe (with memos) the components of the research record
- Conduct and transcribe interviews with the investigator and other knowledgeable persons
- Develop a timeline (phases) of LENR research
- Prepare reports based on the interviews and the memos for the components
- Make arrangements for long-term archiving

Typically the research record components include published papers and presentations, unpublished reports, lab notebooks, correspondence with other investigators, electronic files, hardcopy records, LENR library (books, papers, magazines, etc.), and conference proceedings (e.g. ICCF). Reports are normally prepared at key stages of each project: information collection, organization, and documentation.

Seven projects (including a supplement to the pilot project) are now underway in the LRDI:

- Edmund Storms supplemental project (Los Alamos National Laboratory, retired)
- Tom Claytor & Malcolm Fowler (Los Alamos National Lab, retired)
- Dennis Pease & Arik El-Boher (former SKINR, University of Missouri)
- David Nagel (George Washington University; Naval Research Lab, retired)
- Mahadeva Srinivasan (Bhabha Atomic Research Center, retired)
- Dennis Letts (LettsLab, Austin, Texas)
- Melvin Miles (Naval Air Weapons Station – China Lake, retired)

Component descriptions (memos), interview transcriptions, and draft reports have been prepared for each of these projects.

Conclusions and lessons learned for the LRDI are:

- The stepwise approach with memos followed by reports is verified.
- On-site visits are almost essential for establishing communication, collecting information, and conducting interviews.
- Reports are prepared at each milestone: collection, organization (timeline), and documentation.
- The records available for each participant are variable and depend on the amount of LENR work, recordkeeping practices, and availability to the project.
- Nondisclosure agreements have not proven to be a major obstacle so far.

The main future opportunities in the LRDI are to include more participants (and their records) and develop a long-term solution (Cloud?) for securing archived records. Future re-examination of records for new insights (“leaching the tailings”) is subject to intellectual property considerations. Comprehensive analysis and reporting of the LRDI encompassing current (and additional) participants may also be accomplished in the future.

Kotsyubynsky: Synthesis and characterization of Pd and Ni nanoparticles confined in microporous structures for the LENR applications **Withdrawn**

#Vladimir Dubinko¹, Volodymyr Kotsyubynsky², Pavlo Kolkovskiy², Volodymyra Boichuk², Oleksii Shvets³, Yevhen Kalishyn³, Valeriy Borysenko¹, Oleksii Dmytrenko¹ and Klee Irwin⁴

¹ NSC "Kharkov Institute of Physics and Technology", Kharkov, Ukraine

² Vasyl Stefanyk National Precarpathian University, Ivano-Frankivsk, Ukraine

³ L.V. Pisarzhevskii Institute of Physical Chemistry, Kyiv, Ukraine

⁴ Quantum Gravity Research, Los Angeles, USA

#Email: vdubinko@hotmail.com

The Coulomb potential barrier overcoming is the major problem the low energy nuclear reactions (LENR). One of the proposed ways to overcome the Coulomb barrier is based on time-periodic driving of adjacent potential wells occupied by hydrogen ions (protons or deuterons) [1]. Such driving may be provided either by *discrete breathers* (DBs) - large amplitude anharmonic oscillations of a small group of atoms or by fast phase transformation of quasicrystals (phasons) [1, 2]. Both these phenomena can create nuclear active sites. The ab initio molecular dynamics modeling (using VASP 5.5) of cuboctahedral (CUBO, 4-fold symmetry) and icosahedral (ICO, 5-fold symmetry) Pd-X and Ni-X clusters (X- "magic" atoms number, X=13, 55, 147, 309, 561) was performed [3]. It was determined that time-periodic driving is possible based on *reversible* phason flips of nanoclusters consisting of 13 Pd or Ni atoms from CUBO to ICO configuration with frequencies lying in THz range, which may be considered as potential drivers of fusion reactions between hydrogen isotopes confined in the clusters.

To test the proposed theory, the template synthesis of Pd and Ni nanoclusters was performed using different experimental protocols and matrixes. In particular, Pd nanoparticles were obtained using saturation of previously activated at 250°C microporous carbon (specific surface area of about 1100 m²/g) with tetrachloropalladous acid - acetone (1:2) and reduction procedures in H₂/Ar flow at 200°C for 4 hours. The Pd content (confirmed by XRF method) was about 9-10 wt.%. The average size of Pd clusters was about 1.5-1.6 nm (calculated from Scherrer equation from XRD data. The mean particle size calculated from the TEM image is about 3.5. nm but clusters localization in pores of carbon matrix causes a contrast decreasing and it can be argued that particles with smaller sizes were present. The obtained value is close to the size of Pd147 cluster (1.53 and 1.49 nm for CUBO and ICO symmetry, respectively). The zeolite (NaY modification) three-dimensional framework with cage's size up to 1.3 nm was also used as a matrix for the hexane-assisted synthesis of Pd nanoclusters with the average size starting at about 4 nm (XRD data). Mesoporous silica matrixes (SBA-1, SBA-3, SBA-15, MCM-41) allowed obtaining the palladium clusters with the average size starting at about 1.8-2.0 nm that is close to Pd309 cluster (2.06 and 2.01 nm for CUBO and ICO symmetry, respectively).

[1] V. I. Dubinko, D. V. Laptev, Chemical and nuclear catalysis driven by localized anharmonic vibrations. *Lett. on Materials* 6 (2016) 16

[2] V. Dubinko, D. Laptev, K. Irwin, Catalytic mechanism of LENR in quasicrystals based on localized anharmonic vibrations and phasons, *J. Condensed Matter Nucl. Sci.* 24 (2017) 1.

[3] V. Dubinko, D. Laptev, D. Terentyev, K. Irwin, "Nuclear Fusion of Hydrogen Isotopes Induced by the Phason Flips in Pd and Ni Nanoclusters" – to be presented at ICCF 22.

Dubinko: Nuclear Fusion of Hydrogen Isotopes Induced by the Phason Flips in Pd and Ni Nanoclusters

#Vladimir Dubinko¹, Denis Laptev², Dmitry Terentyev³ and Klee Irwin⁴

¹ NSC “Kharkov Institute of Physics and Technology”, Kharkov, Ukraine

² B. Verkin Institute for Low Temperature Physics and Engineering, Kharkov, Ukraine

³ CK•CEN, Nuclear Materials Science Institute, Mol, Belgium

⁴ Quantum Gravity Research, Los Angeles, USA

#Email: vdubinko@hotmail.com

Energy localization in bulk hydrides of Pd and Ni crystals manifest itself as *discrete breathers* (DBs), in which large amplitude atomic motion may result in time-periodic driving of adjacent potential wells occupied by hydrogen ions (protons or deuterons) [1]. This driving has been shown to result in the increase of amplitude and energy of zero-point vibrations (ZPVs) and in broadening of the wave packet [2]. Numerical solution of Schrodinger equation for a particle in a non-stationary double well potential, which is driven time-periodically, shows that the rate of tunnelling of the particle through the potential barrier separating the wells is drastically enhanced by the driving with a resonant frequency ranging from w_0 to $2w_0$, where w_0 is the eigenfrequency of the potential well [3]. Based on that, we demonstrate a drastic increase of the D-D or D-H fusion rate with increasing number of modulation periods evaluated in the framework of Schwinger model [4], which takes into account suppression of the Coulomb barrier due to ZPVs, which is further enhanced by the time-periodic driving in DBs. The resulting macroscopic fusion rate is determined by the concentration and lifetime of DBs, which should be sufficiently large to provide observable fusion rates.

We propose another possibility of time-periodic driving based on reversible phason flips of nanoclusters consisting of 13 Pd or Ni atoms. Phason flip (PF) is a phase transformation of a nanocluster from cuboctahedral (CUBO, 4-fold symmetry) to icosahedral (ICO, 5-fold symmetry) configuration or vice versa. Phason flips were modelled in Pd, Ni and Pd-H clusters consisting of 13, 55, 147, 309 and 561 atoms by LAMMPS techniques. The smallest clusters of 13 atoms demonstrate reversible PFs at temperatures close to zero K with frequencies lying in THz range, which may be considered as potential drivers of fusion reactions between hydrogen isotopes confined in the clusters. For larger metal clusters, icosahedral symmetry is more energetically favourable than cuboctahedral, but addition of hydrogen affects the final structure of the cluster, and the phase diagram of Pd-H clusters is constructed.

[1] V.I. Dubinko, D.V. Laptev, D. Terentyev, S. V. Dmitriev, K. Irwin, Assessment of discrete breathers in the metallic hydrides. *Comput. Mater. Science* 158 (2019) 389

[2] V. I. Dubinko, D. V. Laptev, Chemical and nuclear catalysis driven by localized anharmonic vibrations. *Lett. on Materials* 6 (2016) 16

[3] V. Dubinko, D. Laptev, K. Irwin, Catalytic mechanism of LENR in quasicrystals based on localized anharmonic vibrations and phasons, *J. Condensed Matter Nucl. Sci.* 24 (2017) 1.

[4] J. Schwinger, Nuclear Energy in an Atomic Lattice I. *Z. Phys.* D 15 (1990) 221.

Konagaya: Supercomputer simulation and experiment clarifying the maximum level of focusing compression due to pulsed supermulti-jets colliding: in weak cold-fusion engine (Fusine)

Remi Konagaya, Ken Naitoh: Waseda University, Tokyo, Japan
E-mail: k-naito@waseda.jp

Unsteady three-dimensional supercomputer simulations based on the CIP method (Yabe et al, JCP, 1985) and the BI-SCALES method (Naitoh and Kuwahara, FDR, 1992; Naitoh and Shimiya, JJIAM, 2011) applied for the stochastic compressible Navier-Stokes equation and theoretical considerations clarify that single focusing collision of 26-jets pulsed in supersonic regime has a potential of stable high compression at chamber center over 1,000 bar and 3,000 K, at conditions without chemical and atomic reactions, because this simulation model is validated by using lots of experimental data. (See Fig. 1.) This focusing collision of jets may be enough for weak cold fusion (low energy nuclear reaction).

Emphasis is placed on twice of focusing collision of 26-pulsed supermulti-jets of high-speed gases. After 26-pulsed jets of hydrogen-oxygen gases at level of 20 bar due to supercharging system or high-pressure tank are initially supplied into reaction chamber, first collision of 26-jets pulsed in reaction chamber will produce vapor water of temperature and pressure, much higher than 3,000 K and 1,000 bar due to focusing collision of jets and molecular chemical reaction. Next, after the first collision of jets, second injection of 26-jets pulsed of hydrogen (or deuterium) encloses the vapor water over 3,000 K remained around reaction chamber center, which will bring pressure over 1,000 bar and temperature over 7,000 K, even though heat release due to nuclear reaction based on nano-particles of palladium is not considered.

We will show four physical reasons why the focusing collision of jets is stable. Nobody has tested this type of engine which may continually generate both weak cold-fusion and combustion by focusing jets entering from outside. Further study based on the present computation model and experiments may lead to occurrence of weak cold fusion at energy level less than 10 times of combustion, with less radiation.

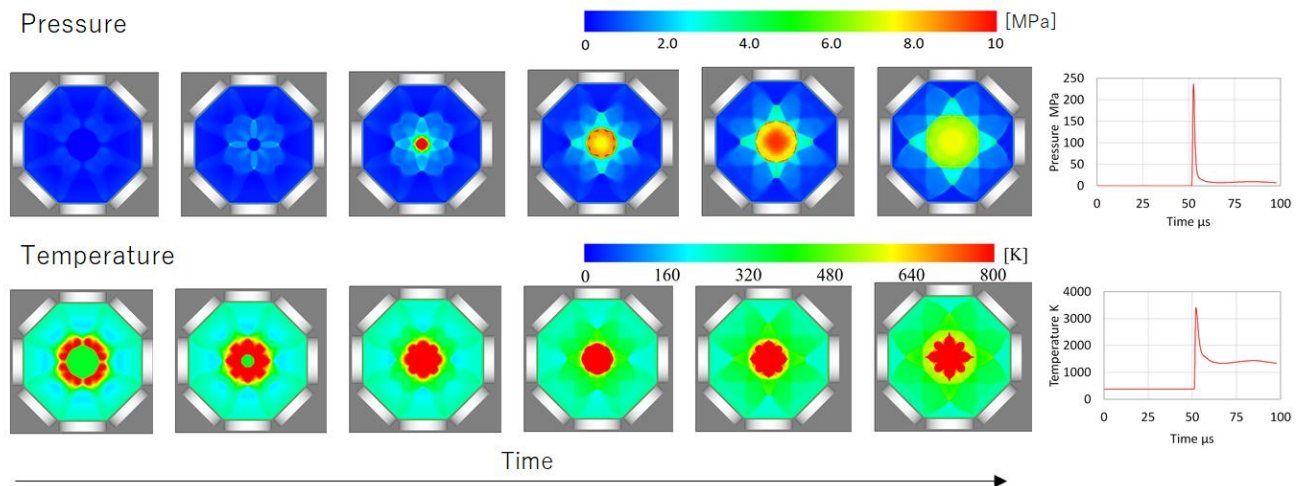


Fig. 1 Computational results of single focusing collision of 26-pulsed supermulti-jets with high speed. Spatial distribution of pressure and temperature, and time history of pressure and temperature at the collision point.

Konagaya: Development of weak cold-fusion engine (Fusine) assisted by molecular chemical reaction: based on double focusing-compression over 1,000 bar and 7,000 K due to pulsed supermulti-jets colliding

Remi Konagaya, Ken Naitoh, Tomotaka Kobayashi, Yoshiki Kobayashi, Hiroki Makimoto, Yohei Naridomi,
Yoshinari Wake: Waseda University, Tokyo, Japan
E-mail: k-naito@waseda.jp

Pressure around collision point of fourteen pulse-jets placed on a geometrical plane in an engine developed originally (Figs. 1a and 1b, Naitoh, patents, 2011-2015) is first measured by varying the pressure transducer position (of Kistler Instruments Ltd.), without chemical and nuclear reactions. High pressure ratio over 18:1 is reliably and stably occurred with variation of about 3% for peak pressure, while variation of intake pressure is less than 1%. Cases with strong disturbance also indicate stable and high compression. The single focusing collision of 14-pulsed jets injected with initial pressure increased by conventional supercharging system or high pressure tank brings the level of 1,000 K, which may be enough for achieving weak cold-fusion (low energy nuclear reaction).

Second, fast chemical reaction of hydrocarbon fuel and oxygen in the present engine using single focusing collision

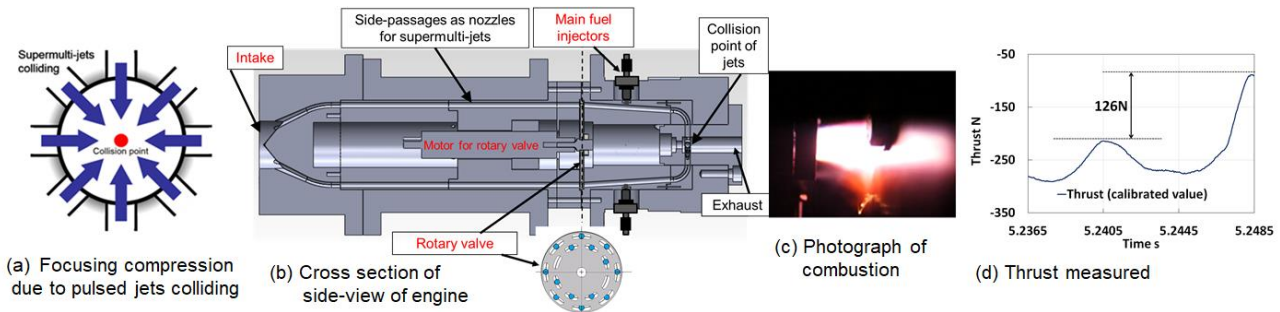


Fig. 1 Weak cold-fusion engine and photograph of combustion with high power

Then, experiments shown above and theoretical considerations clarify that chamber-center collision of “double”-pulsed supermulti-jets of high speed gases, i.e., two collisions during a short interval, brings potential of high compression over 1,000 bar and 7,000 K, when the number of jets is increased to twenty-six placed spherically and the double-pulsed collisions of the jets without nuclear reactions are done. This will be possible because the next engine modified by using the double-pulsed collisions of jets is repeatedly operated, so that second stage of focusing collision of pulsed supermulti-jets of hydrogen (or deuterium) encloses hot vapor water at level of 3,000 K generated by combustion from the first collision of jets of hydrogen and oxygen, leading to much higher temperature, i.e., which may bring weak cold-fusion and higher power if nano-particles such as palladium is added.

Thus, we here show fundamental experimental result on durability test of an additional injector for supplying small flow rate of nano-particles, while focusing collision of jets is absent. i.e., as a unit test of injector.

Moreover, we will release the outline of this new weak-fusion engine (fusine) to the public, because we must find a place in the world where this developed prototype engine can be safely tested, and because nobody has tested this type of engine which continually generates both weak cold-fusion and combustion by focusing jets entering from outside.

It is also stressed that nearly-complete air-insulation is obtained by encasing reacted gas around chamber center due to the supermulti-jets, which is important for heat resistance.

Greenyer: Leveraging observations of patterns in transmutation data from multiple experiments and nature to drive the development of a predictive tool **Poster**

R. W. Greenyer¹, P. W. Power²

¹ Martin Fleischmann Memorial Project, m.fleischmann.memorial@gmail.com

² Martin Fleischmann Memorial Project, pwpowernz@gmail.com

Patterns of the crustal abundance of elements and an understanding of radioactive decay processes are combined with key historical observations of CMNS researchers and the contemporary analysis of a range of similar processes. Simple logic derived from this aggregated data is used to develop an on-line predictive tool for researchers which has good accuracy at predicting outcomes. The evidence-led motivation behind the development of further tools, which have been integrated to allow researchers to explore their data and make informed decisions on possible fruitful future research avenues, is also presented.

Szumski: Initial Simulations Using The Least Action Nuclear Process [LANP] Computer Model for Electrode Design **Poster**

Daniel S Szumski ¹

¹ Independent Scholar, 513 F Street, Davis, CA 95616, USA, Danszumski@gmail.com

The Fleischmann-Pons excess heat effect appears to be related more to electrode composition than any other identifiable factor. This is most clearly seen in the experiments of Miley, Mizuno, and Iwamura where the variety of transmutation products, and deviations from natural abundance ratios, suggest that electrode impurities are fundamentally implicated in both nuclear and excess heat effects. These studies hint at a fundamentally new nuclear transmutation dynamic. This presentation will use Miley's data where the author reports *"...over 40 atom % of the thin film consists of these product elements, the remainder being the host Ni plus trace elements."*

This research uses the LANP model of cold fusion (Nickel Transmutation and Excess Heat Model using Reversible Thermodynamics, ISCMNS, vol. 13; The Atom's Temperature, ICCF-19) to predict both excess heat, and the appearance of new nuclear transmutation products. It will illustrate how the model provides both: an understanding of cold fusion experiments, and also a vehicle for electrode design.

The discussion begins, as it should, with cold fusion energetics. A brief overview describes how nuclear energy is accumulated and stored in the electrode. Energy storage is identified as the most fundamental process in cold fusion. Its stepwise increase during electrode loading initiates the Least Action Nuclear Process, leading to ignition. Continuing energy accumulation then sponsors a precise, stepwise sequence of nuclear transmutations, determined by electrode impurity concentrations, and the model's foundations in the laws of physics.

Energy calculations are the single most important element of the model. The sign of the energy change indicates the direction of heat flow. But more importantly, its absolute magnitude describes its place in the temporal hierarchy of nuclear reactions. Specifically, LANP assumes that the electrode's internal energy continually increases, and nuclear transmutations occur as their energy threshold occurs. Other ordering principles can be simulated by modifying the computer code.

The first of two programs, LANPDECAY, computes all possible decay pathways for all unstable isotopes. This uses data derived from Wikipedia. The program continually calculates the mass/energy changes along each known decay path, and then saves information on to the minimum mass/energy change for that isotope.

A second program, LANPDESIGN uses the data file prepared by LANPDECAY in a design process that adds and removes elements or specific isotopes from a candidate electrode. The front end of the program is user friendly and free formatted. A typical command sequence might be: INITIALIZE; ADD NI SI Fe Cu; CALCULATE; add zn; calculate; REMOVE Cu; CALCULATE; Make Pr; EXIT.

Some initial simulations will illustrate the kinds of insights that can be derived from LANPDESIGN including:

1. Typical excess heat calculations, an exercise in LANP energetics,
2. An electrode design procedure tailored to produce excess heat,
3. Electrodes that make specific elements or isotopes,
4. Changes in isotope abundance ratios,
5. Illustration of electrode sacrificial behavior,
6. Methods for partitioning electrode response to a specific cause

Szumski: The Least Action Nuclear Process [LANP] Computer Model of Cold Fusion Poster

Daniel S Szumski ¹

¹ Independent Scholar, 513 F Street, Davis, CA 95616, USA, Danszumski@gmail.com

Cold fusion research is entering a new phase where the emphasis is less dominated by the quest for excess heat, and more toward an understanding of its nuclear process. This is a very welcomed change. However, if this transition is to be successful, theorists will need to develop what could be a very complex theory into a mathematical model that can be tested not only at the level of observable effects such as excess heat or transmutation products, but also at the levels of process energetics and mass/energy conservation. The LANP model of cold fusion (Nickel Transmutation and Excess Heat Model using Reversible Thermodynamics, ISCMNS, vol 13; The Atom's Temperature, ICCF-19) is founded in these modelling principles, and only then does it theorize how its most fundamental process, energy storage, sponsors nuclear transmutations, and excess heat.

My graduate work and my first career were in mathematical modelling. This is a discipline that disaggregates a complex process into its component parts, describes each in mathematics, and then reassembles these into computer simulations that can be verified against observations. The model is then used as a predictive tool. This presentation will describe the methodology of mathematical modelling, and illustrate each model component with examples from the LANP model of cold fusion .

Models consist of four parts: system geometry, transport, forcing functions, and kinetics. All of these are model specific. Cold fusion's geometry consists of an electrode having specific dimensions, and then deeper layers of geometric definition including a liquid or gas boundary condition, the electrodes surface boundary layer, a host metal lattice configuration, and perhaps several deeper layers that are connected by the model's transport mechanisms.

Model transport describes movement between elements of the model geometry using mechanisms like advective movement, diffusion, dispersion, and phase change. It describes mass and energy transport, which might differ for different state variables. Mass and energy conservation are strictly managed.

Kinetics describes the self-reaction or interaction of state variables leading to changes in their concentrations or intensity. The rates of change are known from experiments or estimated from calculations. Reactions might be temperature or pressure dependent, or dependent on the intensity of other state variables. High energy radiation emissions decay immediately according to far-from-equilibrium blackbody kinetics.

Forcing functions describe the mechanics by which the overall system is propelled in the forward time direction. These might be additives such as deuteron mass loading rates, or energy input from an electrical current; or changes in boundary conditions; or even changes in other state variables such as temperature.

All of these factors can be estimated as steady state or time dependent, yielding different types of model output. Model predictions are then calibrated against experimental data to fine-tune the models ability to reproduce observations. It is then used to model conditions beyond those on which it was initially developed.

The LANP has been formalized into a computer model that simulates energy accumulation and nuclear transmutations according to LANP principles. However, the code is comprehensive enough to simulate other modeling frameworks that rely on known isotope decay sequences. For instance, the program has been used to simulate: fission, bound beta decay, and conditions where beta emissions decay to thermal motion.

Plans for experimental verification will be outlined.

[Kobayashi: Quasi-stability theory with multi-dimensional Taylor expansion: revealing transmutation of atoms in cold fusion](#)

#Tomotaka Kobayashi¹ and Ken Naitoh¹

¹ Waseda University, Tokyo, Japan.

#Email: winningshot1996@asagi.waseda.jp

Behavior around breaking up for two connected particles, which are assumed with flexible spheroids (or other shapes) and forces working between particles existing in various natural phenomena from subatomic particles to stars in the cosmos, are described by momentum equation (Eq.1) having stochastic term δ_{st} , while ε , γ_k , and \bar{t}_k denote size ratio of connected two particles and deformation rate of particle k and dimensionless time of particle k ($=1, 2$), with the other constants m and Δm of order of surface force and degree of indeterminacy of contact position of connected particles [1].

$$\frac{d^2}{d\bar{t}_i^2} \gamma_i = \frac{1}{Det} \left\{ \begin{aligned} & \left[\left(-\varepsilon - \varepsilon^4 + \frac{2}{3} \varepsilon E_{0j} \gamma_j^{-\frac{1}{3}} \right) B_{0i} + \frac{2}{9} \varepsilon^{4-2\Delta m} E_{0i} \gamma_i^{-\frac{4}{3}} \right] \left(\frac{d}{d\bar{t}_i} \gamma_i \right)^2 \\ & + \left(-\varepsilon - \varepsilon^4 + \frac{2}{3} \varepsilon E_{0j} \gamma_j^{-\frac{1}{3}} \right) C_{0i} \gamma_i^{\frac{5}{3} - \frac{2}{3}m} \\ & + \left[\frac{2}{3} \varepsilon^{2+m-\Delta m} E_{0i} \gamma_j^{-\frac{1}{3}} B_{0j} - \frac{2}{9} \varepsilon^{2+m-\Delta m} E_{0i} \gamma_j^{-\frac{4}{3}} \right] \left(\frac{d}{d\bar{t}_j} \gamma_j \right)^2 \\ & + \frac{2}{3} \varepsilon^{2+m-\Delta m} E_{0i} \gamma_j^{-\frac{1}{3}} C_{0j} \gamma_j^{\frac{5}{3} - \frac{2}{3}m} \end{aligned} \right\} + \delta_{st} \quad (1)$$

[for (i, j) = (1,2), (2,1)]

$$Det = -\varepsilon - \varepsilon^4 + \frac{2}{3} \varepsilon^4 E_{0i} \gamma_j^{-\frac{1}{3}}, B_{0k} = \frac{1}{3\gamma_k} \frac{\gamma_k^2 - 2}{\gamma_k^2 - 1/2}, C_{0k} = \frac{3}{8} \frac{2\gamma_k^{2m} - \frac{1}{\gamma_k^m} \gamma_k^m}{\gamma_k^2 - 1/2}, E_{0k} = 3 \frac{\gamma_k^{7/3}}{\gamma_k^2 - 1/2}$$

Quasi-stability is defined as condition that one term in the right-hand side of Eq. 1 approximated by Taylor expansion becomes zero, which is weaker than the neutral stability. By using this quasi-stability after performing one-dimensional Taylor expansion for Eq. 1, the bi-modal size ratios of 1:1 and about 2:3 for atoms produced in fission of uranium 235 is qualitatively revealed. [1]

In our previous report using multi-dimensional Taylor expansion [2], size distributions for biological molecules in DNA and protein are quantitatively explained.

Thus, in this report, we apply multi-dimensional Taylor expansion to predict size ratios of atoms produced in cold fusion, which results in quantitative predictions, especially for Li-Pt. (Fig.1)

[1] K. Naitoh, *Artificial Life and Robotics* 18, 133-143, 2013.

[2] T. Kobayashi, K. Naitoh, *J. Adv. Simulat. Sci. Eng.* 6, 80-93, 2019

Rusetskii: Investigation LENR Processes in Condensed Matter on the HELIS Setup - Overview and Prospects

A. S. Rusetskii¹, O. D. Dalkarov¹, M. A. Negodaev¹, B.F. Lyakhov², E.I. Saunin²
e-mail: rusetskijas@lebedev.ru

1. P.N. Lebedev Physical Institute, Russian Academy of Sciences, Leninsky pr. 53, Moscow, 119991 Russia
2. A.N. Frumkin Institute of Physical Chemistry and Electrochemistry, Russian Academy of Sciences, Moscow 119071, Russia

The report presents the results of studies LENR Processes in Condensed Matter using the ion accelerator HELIS.

The results of measurements of the DD-reaction yields from the Pd/PdO:D_x and the Ti/TiO₂:D_x structures in the energy range of 10 – 25 keV are presented. The neutron and proton fluxes are measured using a neutron detector based on ³He-counters and a CR-39 plastic track detector. Comparisons with calculations show significant effect of DD-reaction yield enhancement.

It was first shown that the impact of the H⁺ and Ne⁺ ion beams in the energy range of 10–25 keV at currents of 0.01–0.1 mA on the deuterated structures results in the appreciable DD-reaction yield stimulation.

It was also studied the neutron yield in DD reactions within a polycrystalline deuterium-saturated textured CVD diamond and Pd, during an irradiation of its surface by a deuterium ion beam with the energy less than 30 keV. The measurements of the neutron flux in the beam direction are performed in dependence on the target angle, θ , with respect to the beam axis. A significant anisotropy in neutron yield is observed. The results were explained by channeling of both deuterium ions and neutrons (DD reaction products).

It was shown that when exposed beams D⁺ ions on the target TiD_x heat generation is far superior heat production with beams of H⁺ and Ne⁺, depending on the concentration of deuterium in the target and beam current density of deuteron. The possibility of calorimetric studies and the search for promising materials for LENR processes are discussed.

Mastromatteo: LENR evidence with hydrogen and deuterium loading in thin palladium films

U. Mastromatteo

A.R.G.A.L.

Via S. Stefano, 27 – 20010 Bareggio – Milan – Italy

ubaldo.mastromatteo@libero.it

We have seen interesting evidence of Low Energy Nuclear Reactions (LENR) experimenting with hydrogen and deuterium loading in thin palladium films deposited on inert supports or on other metals such as Nickel or Titanium.

Nuclear signature

Several types of experiments were performed at the ARGAL laboratory in Bareggio, in particular using thin films of palladium in an H₂ or D₂ atmosphere at various pressures. The laboratory is equipped with instrumentation suitable for the detection of neutron and gamma emissions with a He3 detector and a multi-channel detector with a 3-inch NaI crystal.

All the experiments carried out have been monitored with these instruments and in many cases it has been possible to detect neutron emissions attributable to nuclear events inside the reactor. Some of these anomalous events were short-lived, others were prolonged for several minutes. Apart from one particular case, the events were modest. In any case, this evidence shows yet again the nuclear nature of LENR phenomena, in the past highlighted by clear episodes of nuclear transmutations in similar conditions where it had been possible to analyze the material with the appropriate techniques at the end of the experiment.

High Hydrogen absorption by Nickel at ambient temperature

A sample of nickel on which a thin layer of palladium was deposited electrochemically, immersed in a hydrogen atmosphere at a pressure of about 950 mbar, showed an unexpected ability to absorb hydrogen at room temperature, specifically at around 25 degrees Celsius.

A first exposure of the sample to hydrogen showed a decrease in pressure in the reactor higher than the predictable and very modest one attributable solely to palladium deposited on the nickel surface. Normally this absorption is monitored by a thin film palladium resistance placed in the reactor just to verify the presence of hydrogen or deuterium in the reactor. In particular the macroscopic absorption reduced the system pressure from 950 to 870 mbar. This can only be attributed to nickel substrate, since the ratio of atoms $\langle H \rangle / \langle Pd \rangle$ (few mg of deposited Pd) would have led to an absurd value of about 90. It should be noted that this initial absorption stabilized after about 3 days, showing a rather slow exponential progression. By subjecting the sample to vacuum degassing and subsequent loading cycles with hydrogen pressure, again at around 950 mbar, a marked increase in the speed of the phenomenon was observed (only 2 hours instead of 3 days), in addition to progressive increases in the volume absorbed. In the fourth cycle the pressure decrease was more than 300 mbar, such as to bring the ratio between hydrogen and nickel atoms to a value around 1.2, higher than the threshold considered for the activation of the LENR anomalies in the Palladium.

Excess Heat

The particular structure that showed this considerable absorption of hydrogen at room temperature did not show a similar behavior in a deuterium atmosphere, but it produced excess heat for about 20 minutes bringing the material from room temperature up to 130 degrees without any power input from the outside. The replication of the anomalies described is currently in progress.

Ruer: Experimental setup to detect hydrinos

Jacques Ruer
SFSNMC
Jsr.ruer@orange.fr

Hydrinos are particles whose existence is speculated by Randell Mills of Brilliant Light Power Inc.

According to the theory developed by this author hydrinos result from the shrinkage of hydrogen atoms and could represent the bulk of dark matter in the universe. It is rather difficult to detect hydrinos and Mills refers to several methods. This paper proposes a laboratory setup able to demonstrate if hydrinos are produced during the experiment.

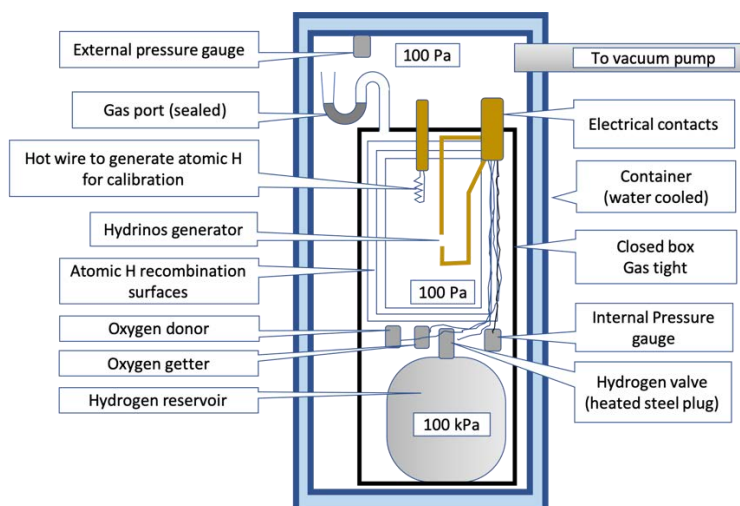
The basic idea comes from the statement that hydrinos are very difficult to confine and escape any container (1). This means that if hydrinos are produced within a closed box the inventory of hydrogen contained in this box will decrease progressively as more hydrinos are synthesized internally and escape into the environment. The possible embodiment of the experimental setup is shown.

A gas tight box is completely sealed. It includes a system to generate hydrinos by electrical discharges in low pressure (100 Pa) hydrogen as explained in (2). It also includes a reservoir of hydrogen to replenish the box atmosphere if the pressure drops too low. All the hydrogen used during the experiment is then embarked in the closed box before the start. The gas pressure inside the box is monitored to detect a loss of gas. Atomic hydrogen is also produced by the hydrino generator. Catalytic surfaces installed inside the box ensure that all atomic hydrogen is recombined so that no atomic form comes in contact with the wall of the box. A separate hot wire able to produce atomic hydrogen but no hydrinos makes it possible to check that hydrogen does not leak out of the box in the absence of hydrinos. The box is enclosed in a container at the same pressure to minimize the diffusion of hydrogen out of the box.

The experiment would include 3 phases:

- The box and container atmosphere is thoroughly flushed with hydrogen. The pressure is reduced to 100 Pa, then the box gas port is sealed by melting some solder in the gas port siphon.
- Generation of atomic hydrogen by the hot wire. H_2O vapor that poisons hydrogen dissociation would be first eliminated by an oxygen and water getter. The loss of hydrogen out of the box will be evaluated.
- Generation of hydrinos. H_2O that is said to be a catalyst for hydrino formation would be added thanks to an oxygen donor. The internal pressure will be monitored during a long period of operation.

A loss of mass exceeding any experimental error would be an indirect indicator of hydrino existence.



(1) Analytical presentation 040319.pptx – brilliantlightpower.com

(2) Validation of the Observation of Soft X-ray Continuum Radiation from Low-Energy Pinch Discharges in the Presence of Molecular Hydrogen – Gen3 Partners report – brilliantlightpower.com

Ruer: How LENR can change the World

Jacques Ruer
 President SFSNMC
 Email: jsr.ruer@orange.fr

Humanity consumes presently about 13850 tons oil equivalent per year. 81% of the primary energy is provided by fossil sources.

The advent of LENR energy will have a profound impact on the global energy market. The revolution will evolve progressively. This paper proposes a scenario for the development of the new source of energy. It is supposed that the applications will come stepwise following the temperature level of the heat delivered by the LENR reactors.

An analysis of the conversion processes to transform primary energy into final energy shows that complete domains of the industry will be progressively impacted as the LENR reactors reach some temperature levels:

- 100°C: heating purposes, district heating
- 200°C: Boilers, steam driven processes, paper mills, food processing, etc.
- 350°C: Steam turbines, electricity generation

This last threshold is sufficient to convert the generation of electricity from fossil fuels or nuclear fission to LENR.

An intermediate scenario is obtained. Fossil fuels share in primary energy falls to 35%. Their use is limited to high temperature combustion processes, chemistry, surface and air transport.

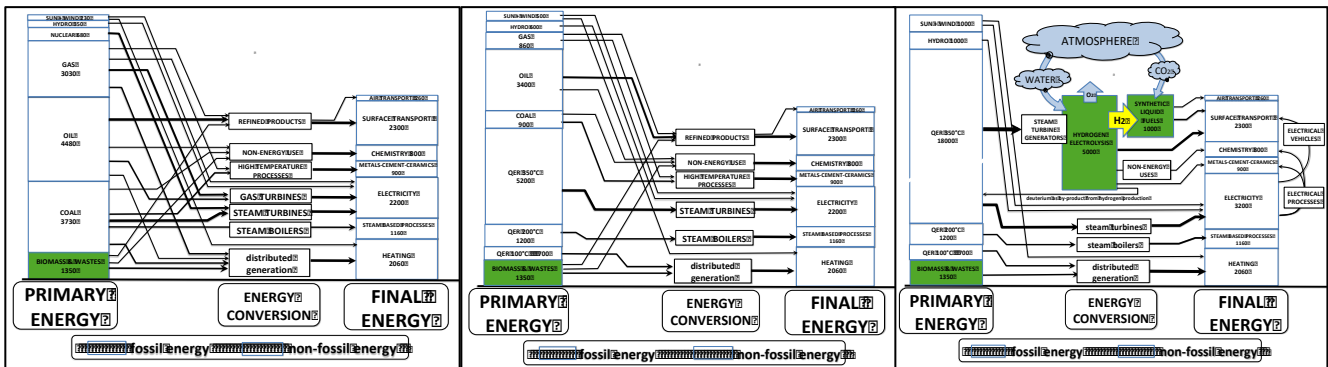
A further development is possible if LENR electricity generates hydrogen via water electrolysis. Hydrogen is used as an energy vector and synthetic fuels can be manufactured by reacting H₂ with CO₂ extracted from the atmosphere.

It is then theoretically possible to describe a final scenario without any need of fossil fuels.

The potential benefits of LENR energy are incommensurable. It would be available as a non-space invasive form anywhere at any time with a positive influence on climate change.

The annual theoretical consumption of hydrogen to cover all the primary energy consumed by humanity would be about 100 tonnes obtained via the electrolysis of 900 tonnes of water if normal hydrogen is a suitable input. If deuterium is required it could be extracted as a by-product of hydrogen production. The resource has virtually no limit.

Energy flowcharts of the present, intermediate and final scenarios
 QER: Quantum Effects Reactors (LENR reactors)



Carpinteri: Earthquake neutrons and Earth-Crust LENR: From seismic precursors to Geochemistry evolution

Alberto Carpinteri, Oscar Borla

Department of Structural, Geotechnical and Building Engineering, Politecnico di Torino C.so Duca degli Abruzzi 24, 10129 Torino, Italy
Corresponding author: alberto.carpinteri@polito.it

TeraHertz phonons are produced in solids and fluids by mechanical instabilities at the nano-scale (fracture and cavitation). They present a frequency that is close to the resonance frequency of the atomic lattices and an energy that is close to that of thermal neutrons. A series of fracture experiments on natural rocks has demonstrated that the TeraHertz phonons are able to induce fission reactions on medium-weight elements (in particular, iron and calcium) with neutron and/or alpha particle emissions. The same phenomenon appears to have occurred in several different situations and to explain puzzles related to the history of our planet, like the primordial carbon pollution (and correlated iron depletion) or the ocean formation (and correlated calcium depletion), as well as scientific mysteries, like the so-called cold fusion or the correct radio-carbon dating of organic materials. Very important applications to earthquake precursors, climate change, and energy production are likely to develop in the next future. In particular, three different forms of energy might be used as earthquake precursors. At the tectonic scale, Acoustic Emission (AE) prevails, as well as Electro-Magnetic Emission (EME) at the meso-scale, and Neutron Emission (NE) at the nano-scale. The three fracto-emissions tend to anticipate the next seismic event with an evident and chronologically ordered shifting: high frequencies and neutron emission about one week before, then lower frequencies and electromagnetic and acoustic waves. The experimental observations reveal a strong correlation between the three fracto-emission peaks and the major earthquakes occurring in the closest areas.

Regarding the cold fusion, despite the great amount of experimental results, the comprehension of these phenomena still remains unsatisfactory. On the other hand, as reported by most of the articles devoted to cold fusion, one of the principal features is the appearance of micro-cracks on the electrode surfaces after the experiments. A mechanical explanation is proposed as a consequence of hydrogen embrittlement of the electrodes during electrolysis. The preliminary experimental activity was conducted using a Ni-Fe anode and a Co-Cr cathode immersed in a potassium carbonate solution. Emissions of neutrons and alpha particles were measured during the experiments as well as evident chemical composition changes of the electrodes revealing the effects of fission reactions occurring in the host lattices. The symmetrical fission of Ni appears to be the most evident observation. Such reaction would produce two Si atoms or two Mg atoms with alpha particles and neutrons as additional fragments. In order to confirm the preliminary investigation, further electrolytic tests have been conducted using Pd and Ni electrodes. As for the early experiments, relevant compositional changes and the appearance of lighter elements previously absent have been observed. The most relevant process emerging from the experiments is the primary fission of palladium (decrement of 30%) into iron and calcium. Then, secondary fissions appear in turn producing oxygen atoms, alpha particles, and neutrons. The chemical composition changes were confirmed by four repetitions of the same experiment. An extensive evaluation of the heat generation has been carried out showing a positive energy balance in correspondence to the major neutron emission peaks.

McKubre: Thirty Years On.

Michael C.H. McKubre, Napier, New Zealand

Director of the Energy Research Center, SRI International, California (retired 2015).

When asked in 2009 by my colleague and good friend Vittorio Violante to provide my perspective [1] on the state of what then had become condensed matter nuclear science, CMNS, I concluded that:

1. Extensive review of literature generated since 1989 compels a conclusion that Martin Fleischmann and Stanley Pons uncovered evidence [2] of a new effect in physics.
2. This new effect requires a new mechanistic description and explanation that awaits exposition, although many paths remain open.
3. We would be best advised to seek advancement using quantitative predictive fundamental physics descriptions and experimentation, following the scientific method.
4. To do so we are going to have to engage the broader scientific community.

In the intervening decade little has changed my opinion of any of these conclusions. I will address all points but principally the last where significant progress has recently been made. This in my view is now the most important issue and has become increasingly timely for the CMNS community. Now 30 years on since 1989 [2] many or most of the scientific leaders whose work and inspiration allow me the state my first conclusion with confidence are no longer with us; all remaining from that “first generation” of “cold fusion” pioneers have diminishing output and influence. Unless we can inspire a “new generation” the effort to resolve the underlying physics and pursue application is destined to taper to nothing – perhaps, at best, to be re-started in some new “re-discovery”.

References.

1. M.C.H. McKubre, Cold Fusion (LENR) One Perspective on the State of the Science. in 15th International Conference on Condensed Matter Nuclear Science. 2009. Rome, Italy: ENEA.
2. M. Fleischmann, S. Pons and M. Hawkins, J. Electroanal Chem., 201, p.301 (1989); Errata, 263, p. 187 (1990). See also M. Fleischmann, S. Pons, M.W. Anderson, L.J. Li and M. Hawkins, J. Electroanal. Chem., 287, p. 293 (1990).

Bannister: The limits to growth: the intersection of energy and economics. Oral & Poster

Stephen C. Bannister, Ph.D., Department of Economics, University of Utah, Salt Lake City, Utah 84112, USA

steve.bannister@econ.utah.edu

The June 2007 Proceedings of the National Academy of Sciences (PNAS) article entitled “Global and regional drivers of accelerating CO₂ emissions” presented a seminal approach to analyzing the possibly existential issue of anthropogenic greenhouse gas emissions, focusing on the largest component, CO₂, of those emissions and its structural drivers.

The article’s findings were ominous, recalling that the growth rate of emissions had increased from 1.1%⁻¹ for 1990–1999 to > 3%⁻¹ for 2000–2004.

With ten year’s added data, and the underlying analytic power of the Kaya model defined in the PNAS article, we are in a position to step back and look at data and probabilities over the longer term.

The model presented here extends the Kaya framework to forecast decelerating CO₂ emissions, but likely not quickly enough to avoid significant climate change. This climate-change-negative outcome is because “upstream” system (and model) components are not decreasing either at all or fast enough. The system-driving culprit is the aggregate carbon intensity of primary energy sources. Its actual time path has been increasing since about 2000 in spite of all the hoped-for progress in renewable energy sources.

A strong conclusion is that if we are to avoid dangerous global warming (a position not shared by all scientists), we must eliminate carbon intensity as a system parameter entirely—that means completely eliminating all carbon-based primary energy sources. Many of the proposed policy responses to the threat have been to raise the carbon price. This has been both politically and economically challenging—the “price elasticity” of energy is low, so that only large price changes make much difference in consumption. A sufficiently large price change would likely raise the average cost of energy, thus curtailing economic output and living standards. And evoking great political resistance.

The energy technologies promised by Condensed Matter Nuclear Science (CMNS) offer a much better alternative—clean sources yielding energy costs that are both dramatically lower and more politically feasible. If sufficiently low cost, such sources would expunge carbon sources, perhaps even quickly. And no regulation would have to pass the fraught political processes as politicians almost always claim affinity for “market” forces.

Such very inexpensive clean energy sources will invoke other sets of problems—Schumpeterian “creative destruction” is one way economists frame the inevitable industrial and commercial turmoil—but this incipient energy revolution may indeed trigger a new Industrial Revolution at least as profound as the original one.

Thus, a realistic model, as attempted here, of our carbon future dramatically emphasizes the critical nature of the research conducted by CMNS scientists.

Meulenberg: Deep-level atomic orbitals and more

#A. Meulenberg¹, J. L. Paillet²

¹Science for Humanity Trust, Inc., USA

²Aix-Marseille University, France

Email: Mules333@gmail.com

The relativistic Schrodinger (Klein-Gordon or K-G) and Dirac equations for atoms predict the existence of electron deep orbits (EDOs) with radii in the low femto-meter range and with binding energies in the 500 keV range (in addition to the known atomic orbitals). However, they do not predict the kinetic and potential energies of these relativistic electrons. Models, based on these equations and on observations from successful cold fusion results and developed in prior work, now include both MeV and 100-MeV kinetic-energy levels. Earlier papers assumed the deep-orbit electrons to have kinetic energies in the 1 - 2 MeV range. This range was the minimum that would allow the D-D fusion to 4He without fragmentation. However, our recent work has replaced or augmented the low-MeV range with ~100 MeV values that satisfy the Heisenberg Uncertainty Relation (HUR) and the virial theorem as well. , Both models are consistent with predictions of the relativistic quantum-mechanical equations; nevertheless, both have problems with conventional thinking. The present work seeks to identify and explore further the dual (or multiple?) deep levels and their implications for cold fusion.

Since no direct experiment evidence for these deep levels has yet been found and an electron bound to these deep orbits would normally violate the HUR, little previous theoretical effort has been expended in looking at the interactions of a relativistic electron this close to the nucleus. The possibility of greatly enhanced conversion of a deep-orbit electron into a neutron and thereby of modifications to the weak interaction has implications for direct cold fusion (e.g., H-H to D) and for the many transmutations observed (without emitted hard radiation) in this new science. An examination of the potentials experienced by electrons in these deep orbits may shed light on the nature of a neutron and how to get atomic electrons to the EDOs and thus how to access the nuclear energies available.

Garai: Physical Model for Lattice Assisted Nuclear Reactions

Jozsef Garai

Department of Civil Engineering, University of Debrecen, Hungary

E-mail: jozsef.garai@fu.edu

Investigating the characteristic properties of the Hydrogen atoms it has been concluded that the electron in the vicinity of the nucleus transfers from point to surface charge [1]. The formed electron halo around the nucleus shields the repulsion of the proton and allows very close encounters of the nuclei. This physical phenomenon offers an explanation how fusion can occur at low atomic energies. In this study it is investigated how this electronic structure fits to Lattice Assisted Nuclear Reaction (LANR) experiments and theory. Based on literature review the conditions, required for successive LANR in the palladium–deuterium system, were collected. The theoretical objections against low energy nuclear reaction, raised by Huizenga and others, have also been collected. Analyzing the experimental and theoretical conditions it has been concluded that the nuclear reaction between the two atoms occur in the vacancy of the palladium. If this physical model for LANR is correct then the reaction should be enhanced by the resonance frequency of the Deuterium molecule. The calculated fundamental frequency of the vibrating Deuterium molecule in cavity is 21.65 THz. This frequency is almost identical with the observed “sweet spot” in the two laser experiments at 20.8 THz inducing the reaction [2]. Based on this coincidence it is suggested that this previously unidentified peak, inducing the nuclear reaction, relates to the self frequency of the Deuterium molecule in vacancy. The fundamental frequencies for HD and H₂ molecules in vacancies are also calculated. It is predicted that these frequencies in HD or H₂ systems should also activate the reaction and that these fundamental frequencies in cavities should remain unchanged regardless of the hosting lattice. These predictions are testable.

The article can be downloaded: <http://vixra.org/pdf/1901.0262v2.pdf>

References:

- [1] Garai, J.: The electronic structures of the atoms. *Physics Essays* 2017;30:455-60; preprint: https://dea.lib.unideb.hu/dea/bitstream/handle/2437/247192/0_9_Hydrogen_model.pdf
- [2] Letts, D., and Cravens, D.: Laser stimulation of deuterated palladium: past and present. *Proc. ICCF10*, 2003;159

Nagel: Review of Seebeck Calorimeters Used in LENR Experiments

Bengisu Sisik and David J. Nagel
The George Washington University

Low Energy Nuclear Reaction (LENR) experiments produce two major results, reaction products and heat energy. The transmutation products are scientifically useful, since they indicate which reactions might have occurred. They are measured with a wide variety of analytical techniques. The thermal energy has practical promise as a new source of clean energy. It is quantified by the use of calorimeters of various designs and properties. Mass Flow calorimeters have provided valuable data on the time history of thermal power production from LENR experiments[1]. Heat Flow calorimeters of two types have also been widely used. One class includes Isoperibolic calorimeters [2] and the other has Seebeck calorimeters [3-4]. They both require constant temperature surroundings to serve as a thermal sink and reference. This review considers reports where Seebeck calorimeters were used for quantification of LENR power.

Thermoelectric materials and devices are reciprocal, when they are configured properly. If they are powered electrically, they can pump heat from one location to another (the Peltier Effect). If they have different temperatures on two sides, a voltage will appear across the faces (the Seebeck Effect). Seebeck calorimeters are containers, the walls of which are covered with thermoelectric devices or thermocouples (both called TE elements). Experiments performed within them produce heat by (a) the electrolysis needed to produce protons or deuterons for LENR, (b) resistive heaters to provide calibrations before, during or after LENR runs, and (c) the LENR. The action of these heat sources raises the temperature of one side of the TE devices relative to the other side, which is heat-sunked to the exterior reference temperature. The voltages produced by individual TE elements are added by connecting them in series.

We have compiled information from 13 papers, where Seebeck calorimeters were used for LENR experiments, from 1990 to 2015. A table of their geometrical, physical and performance characteristics was completed. Plots of the quantitative features of the reviewed calorimeters have been produced. The reviewed Seebeck calorimeters have sensitivities that range from 1.1 to 190 mV/W. The results of this review might be useful to scientists considering the use of Seebeck calorimeters for LENR experiments. They also form the basis for the design of a new user-friendly Seebeck calorimeter being made for our laboratory.

[1] M. C. H. McKubre and F. Tanzella, "Mass Flow Calorimetry" in Proc of ICCF-14 (2008)

[2] M. Fleischmann and S. Pons, "Electrochemically Induced Nuclear Fusion of Deuterium", J. Electroanalytical Chemistry, Vol. 261, pp. 261-267 (1989) and Errata in Vol. 263.

[3] W.-S. Zhang "Construction, Calibration and Testing of a Decimeter-Size Heat-Flow Calorimeter." *Thermochimica Acta*, vol. 499, pp. 128–132 (2010)

[4] E. Storms, "The Method and Results Using Seebeck Calorimetry" in Proc of ICCF-14 (2008)

Hagelstein: HD/He-3 phonon-nuclear coupling matrix element Poster

Peter Hagelstein

Energy Production and Conversion Group, MIT Research Laboratory of Electronics

We have recently worked on the calculation of the phonon-nuclear coupling matrix element for the HD/He-3 transition. This matrix element is important in connection with excess heat in light water reactions, as well as low-energy nuclear emission in experiments with hydrogen (and some deuterium). It is also one of the simplest to analyze with nuclear models.

We have developed a reduction of the relativistic boost interaction for the lowest order meson exchange potential based on pseudoscalar and pseudovector interactions. The pseudoscalar interaction does not contribute, and we find a complicated but useful expression in the pseudovector case.

We have carried out a reduction based on the old Gerjuoy-Schwinger approach to wave function construction. This has advantages in terms of allowing for Mathematica to reduce the spin and isospin algebra, resulting in equations fully symmetric in particle coordinates. This makes things easier to evaluate numerically.

We have developed explicit expressions for the lowest-order boosted central and tensor potential interactions, which are readily evaluated to get numerical estimates.

Having a solid number for this phonon-nuclear coupling matrix element is by itself useful. However, an unexpected consequence of the analysis is that we may be able to say something important about the state of the HD molecule in the lattice if it is to have the strongest phonon-nuclear interaction -- that is we need a P-state rotational admixture.

Hagelstein: Recent Progress on Phonon Coupling Models

Peter Hagelstein

Energy Production and Conversion Group, MIT Research Laboratory of Electronics

There has been no agreement as to how excess heat is produced in the Fleischmann-Pons experiment over the past three decades. We have pursued ideas and models that relate to the interaction between nuclei and vibrations in the lattice, making progress step by step. During the past year some of the problems which have stood in the way have found solutions. We now have a picture that looks to address most if not all of the important issues.

The strongest interaction between nuclei and vibrations appears to come about due to the relativistic boost correction of the nuclear interaction for nuclei vibrating in a lattice. We have made progress in developing quantitative estimates for this interaction in some specific cases, and work is ongoing to calculate additional examples.

The transfer of excitation from one nucleus to another provides the basic engine within the theory for many anomalies. Excitation transfer due to direct nucleus-nucleus interaction is possible, but weak. A much stronger interaction is possible when many nuclei interact with a highly excited uniform THz vibrational model.

Excitation transfer and more sophisticated interactions are hindered by destructive interference in basic models. In previous years we relied on loss effects asymmetric off of resonance to break the destructive interference. Last year we found that this effect was insufficient to account for excitation transfer results in our lab, which meant that something else even bigger was happening. It seems clear at this point that the shift of nuclear levels off of resonance lies at the heart of the enhancements. Models including this effect appear capable of connecting quantitatively with experiment.

Off-resonant energy shifts of nuclear levels is expected to similarly eliminate much of the destructive interference associated with massive up-conversion and down-conversion needed for excess heat production, and for collimated x-ray emission within the models.

We also consider the connection between ongoing excitation transfer experiments and ion beam experiments in our lab to the models under development.

Metzler: Observations of delocalized gamma emission from Co-57/Fe-57 samples during application of mechanical stress

Florian Metzler

Energy Production and Conversion Group, MIT Research Laboratory of Electronics

The research presented is motivated by a host of experimental reports where radiation is observed but not conventionally expected and others where radiation is not observed but conventionally expected. Such reports raise questions about mechanisms for energy transfer into and out of atomic nuclei. Our group has pursued theoretical and experimental work to investigate the possibility of energy transfer into and out of atomic nuclei aided by the surrounding lattice. Here, we report on a series of experiments designed to demonstrate lattice-assisted transfer of nuclear excitation between nuclei. We refer to this mechanism as *nuclear excitation transfer*. Such nuclear excitation transfer follows from models in which multi-level systems (nuclei) are coupled to shared oscillators (phonons) – analog to electronic excitation transfer today widely studied in biophysics. The transfer of energy from excited nuclei to nearby ground state nuclei implies subsequent gamma emission from different places. If such transfer is fast enough to take place repeatedly before radiative decay, macroscopic changes of the spatial distribution of gamma emission from a sample are expected.

We present data from recent experiments that suggest delocalization of gamma emission on the order of several hundred microns, induced by mechanical stress. The experimental setup is as follows: Fe-57 nuclei in excited state (populated by beta-decaying Co-57) and Fe-57 nuclei in ground state are arranged on a steel plate; phonons are then generated in the steel plate via mechanical stress (in situ through thermal expansion of clamps). Correlated with such treatment we observe an increase of 14 keV gamma emission from plate regions with a high density of Fe-57 nuclei and a simultaneous decrease of 14 keV gamma emission from adjacent plate regions with a low density of Fe-57 nuclei. Energy-resolved spatial data are obtained via an Amptek X123SDD detector which repeatedly raster scans across the sample via two precision linear stages.

We interpret observed emission changes as effects of phonon-induced nuclear excitation transfer. Specifically, we propose to explain the emission increase in some pixels of the raster scan and the commensurate emission decrease in adjacent pixels of the raster scan as resulting from net energy transfer into and out of those pixels. Such net energy transfer can be expected across the border of a low-density and a high-density region of Fe-57 nuclei, within the range of the transfer – which is consistent with reported observations. As for the range of the transfer, we present early efforts to simulate the mechanism that match our results. The observed extent of delocalization of gamma emission is estimated to be on the order of 500 μm . For an individual transfer step of 10 nm (estimated from theoretical models) and with the assumption of a quantum walk pattern (as used in electronic excitation transfer studies), this suggests an average total number of 50,000 transfers before decay of the 14 keV state to ground state. With a 100 ns lifetime of the 14 keV state, this suggests a transfer step to take about 2 ps.

The new observations are consistent with earlier, preliminary results which will be summarized. Next steps and implications of these findings will be discussed.

Forbes: Initial report on low-energy ion beam experiments with various metal targets

Sadie Forbes

Energy Production and Conversion Group, MIT Research Laboratory of Electronics

This paper will discuss early results from a new experimental facility at MIT designed to accelerate deuterium, hydrogen, and argon ions at low energy onto metallic targets. Preliminary data includes observations of neutrons as well as charged particles at energies clustered at ~ 30 MeV during bombardment of a Ti plate with deuterons below 1 keV. In one case, we observed time-coincident neutrons and high-energy charged particles counts over a brief period (2-4 seconds).

Materials and Methods:

Deuterium, hydrogen, and argon ions can be accelerated to energies between 150 - 1000 eV with ion current flux of between 0.001 - 0.4 mA/cm² to impact metallic targets measuring 50x100mm. Targets include titanium, tungsten, lithium, and copper.

The experiment chamber is capable of UHV operation (primary baseline species $\sim 1 \times 10^{-9}$ Torr H₂ with H₂O typically below 5×10^{-10} Torr). HD, D₂, HDO and D₂O species are also present after D₂ is introduced to system. Recorded measurements include charged particle spectra from planar silicon charged particle detectors; neutron counts from a He-3 neutron counter, ion current as measured at the target, mass spectra of background and experiment gases by a residual gas analyzer.

Experimental protocols are still being developed. Goals include the creation of defects on the target surface, the implantation of hydrogen/deuterium nuclei in the metal target, the triggering of fusion events, and the subsequent phonon-assisted transfer of nuclear excitation to nearby lattice nuclei resulting in disintegration and host-material specific charged particle emission.

Background:

The observation of high-energy charged particles emitted from metal-hydrogen systems (such as in Chambers et al. 1990; Lipinski and Lipinski 2009) represents a puzzle. Conventional hydrogen fusion reactions would not result in charged particles with energies more than a few MeV. While D+D fusion results in released binding energy on the order of 24 MeV, much of that energy is conventionally expected to end up as binding energy in the reaction products. Therefore, the observation of high-energy charged particles above several MeV suggest the occurrence of a non-conventional fusion reaction or a secondary nuclear reaction.

In previous theoretical and experimental work our group investigated the possibility of nonradiative energy transfer of nuclear excitation to nearby nuclei. Such *nuclear excitation transfer* follows from models in which multi-level systems (nuclei) are coupled to shared oscillator modes (phonons) - analog to electronic excitation transfer today widely studied in biophysics.

We propose that nuclear excitation transfer can provide explanations for previous reports, as well as our own reports, of high-energy charged particles emitted from metal-hydrogen systems: instead of resulting in conventional fusion reaction products, the released nuclear binding energy from D+D fusion transfers to nearby lattice nuclei; the large quantum of energy thus accepted then results in the disintegration of such nuclei and the emission of alphas, protons, or neutrons characteristic of the acceptor nuclei. This conjecture can be tested by comparing measured charged particle energies from different target materials with the expected disintegration products from these materials when accepting excitation from hydrogen fusion reactions such as D+D. The latter is the overall goal of this experimental campaign.

S Dana Seccombe: Phonon Assisted Nuclear Fusion Mode

The paper presents a theoretical model for phonon assisted nuclear fusion. Though initially developed around experimental results in the Pd:D system, the results are applicable to the Ni: H system by changing model parameters.

The thesis of the paper is that the presence of phonons in the lattice provides an additional channel not present in plasma phase nuclear interactions. Using the model, one can compute a fusion threshold as a function of crystal size, temperature, and D doping,---and phonon spectra and lifetime--- which is itself a function of crystal doping , defect density, shape, orientation.

The theory doesn't require the postulation of exotic particles or new physics; it uses only previously well-known principles of solid state physics which has described multiphonon non-radiative transfers in phosphors; and a simple coupling mechanism between phonons and D-D wavefunctions.

The model starts with Fermi's Golden rule as further developed by Heitler for multi-state virtual transitions (here, $>10^9$ phonons) and *quantitatively* predicts a D-D transition rate to the He ground state as a function of known parameters. At the same time, calculation of Fermi's h_{fi} for traditional branching paths (to tritium or helium 3, or He4+gamma's) with near atomic sized D wave functions (deBroglie wavelengths) show those transitions will have low probability.

The model uses D probability amplitudes *between* lattice sites, and calculates the change in *nuclear energy* of overlapping D's as a function of optical phonon mode occupation. Though extremely small, these changes are the h_{fi} in Heitlers multi state/multichannel rate calculations. Though there are $>10^9$ sequential transitions (tending to dramatically lower rates), this is compensated for by the approximately $(2d)^{levels}$ parallel paths, where d is the number of degrees of freedom in a small crystal (say 10^{12}) and *levels* is the number of phonons (say $>10^9$). Those calculations show that, once a certain threshold is reached in a combination of crystal size, doping, and presence of coherent optical phonons, additional phonons are rapidly created, initiating a run-away situation in the crystal similar to that found in lasers above threshold. In both cases, the actual reaction then is limited by the availability of reactants, not the Golden Rule transition rate. [It is shown that Pd:D, in a "NaCl like" crystal lattice has a very narrow longitudinal optical spectrum that leads to coherency and long lifetimes.] The subsequent reaction will be steady state (life after death) if the reactants continue to diffuse into the reaction region at a rate high enough to sustain the necessary optical phonon population, whose size is dependent on the optical phonon lifetime. That lifetime is inherently longer in perfect PdD crystals (or crystals *near* stoichiometry and *nearly* defect free). If not, episodic reactions occur when a threshold condition occurs, then local reactants are again depleted in a relaxation phenomenon.

Any artificial means to create a larger population of optical phonons (electrical excitation of optical phonons, directly for example; or through plasmons) will tend to initiate fusion, given other factors are within a range that, combined with the phonon contribution result in exceeding threshold.

The model predicts/explains the following often observed effects:

- Why He with heat is by far the dominant pathway in Pd:D
- Why there is great variability in the success of experiments, including apparent "nuclear active entities"
- When and why "life after death" occurs
- Why there are "explosive" local reactions, and how they can be mitigated or controlled
- Why Ni:H and Pd:D reactions can occur
- Why Raman anti-Stokes lines are correlated with excess heat

Understanding of the phenomena via the model allows one to predict leverage areas for design of energy producing systems, and tools for materials control and analysis (for example, optical phonon lifetime and coherence as a function of material/process parameters and spatial inhomogeneity). Conversely, correlation of optical phonon lifetime and coherence (and other model parameters) allow a check on the model itself.

Uchikoshi: Laser Condensed-Matter Fusion Experiments. Oral and Poster

Takeru Uchikoshi, Shunsuke Ono, Yuki Nakashima, Yuta Kitagawa, Katsuaki Tanabe*
 Department of Chemical Engineering, Kyoto University, Japan
 *Email: tanabe@cheme.kyoto-u.ac.jp

The intensity and density of the triggering energy supplied to activate the nuclear fusion reaction are key factors to produce a smooth and reproducible initiation of the reaction. We previously proposed and numerically analyzed a scheme to provide high-density optical or electromagnetic energy to fusion-fuel materials by lasers and plasmonic field-enhancement effects, to significantly increase the reaction probability [1,2]. In another project, we experimentally observed temporal behaviors of heat generation unable to be explained by known chemical processes, and neutron signal peaks at timings corresponding to the accelerated temperature increases, in current-injected PdD_x [3].

In the present work, we have installed multiple kinds of lasers in the gas-phase D-Pd reaction system to irradiate the Pd samples, as an energetic stimulation support, potentially with a boosting plasmonic local field-enhancement effect [4]. The lasers are 405-nm and 594-nm continuous-wave semiconductor lasers with powers of 50 and 30 mW, respectively, and a 1064-nm pulsed YAG laser with a peak power of 10 MW. Similarly to our previous work, we have simultaneously observed a sudden temperature increase with an overshoot and a neutron signal (Fig. 1). Significantly, we have observed a clear signal of substantial-amount ⁴He generation from the Pd samples as a shoulder peak on the D₂ peak (Fig. 2), and a possible ³He signal, via in-situ mass spectroscopy. We have also observed a sudden burst of these gas species out of the Pd sample (Fig. 3). Our results might indicate a certain anomalous nuclear-related reaction in the D-Pd system. The experimental conditions and outcomes will be presented in detail at the conference.

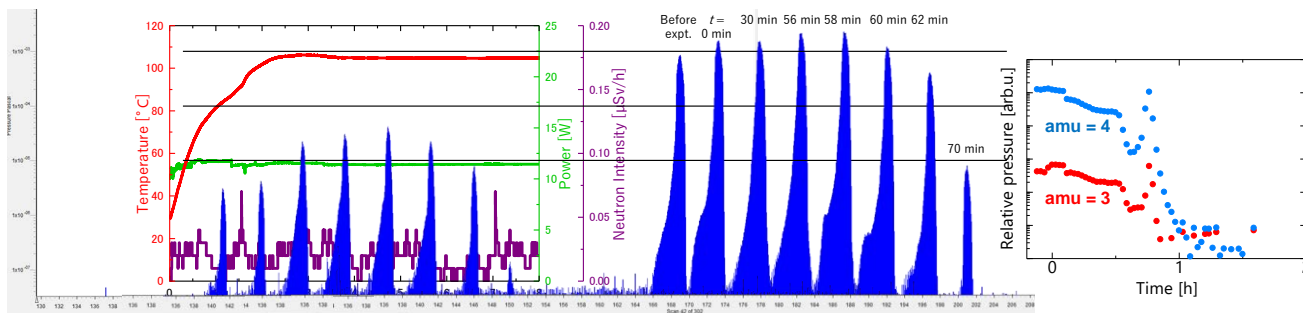


Fig. 1 Temporal behavior.

Fig. 2 Mass spectra for amu = 4.

Fig. 3 Pressure evolution.

(Note: Data are *not* from a single experimental run, but from independent ones for each of Figs. 1-3.)

This work was financially supported, in part, by the Thermal & Electric Energy Technology Foundation and the Research Foundation for Opto-Science and Technology.

- [1] K. Tanabe, "Plasmonic concepts for condensed-matter nuclear fusion," *ICCF-20*, X-4, Sendai, 2016 / *J. Cond. Matter Nucl. Sci.* **24**, 296, 2017.
- [2] K. Tanabe, "Plasmonic field enhancement on planar metal surfaces," *ICCF-21*, N-3, Fort Collins, 2018 / *J. Cond. Matter Nucl. Sci.* **27**, 152, 2018.
- [3] Y. Kitagawa, S. Ono, Y. Hayashi, E. Yamaguchi, K. Tanabe, "Direct Joule heating of D-loaded bulk Pd plates in vacuum," *ICCF-21*, K-3, Fort Collins, 2018.
- [4] N. Fukuoka, K. Tanabe, "Large plasmonic field enhancement on hydrogen-absorbing transition metals at lower frequencies: Implications for hydrogen storage, sensing, and nuclear fusion," *J. Appl. Phys.* **126**, 023102, 2019.

Miles: Thermodynamic Basis For The Power Term For Work in Electrochemical Calorimetry Poster

Melvin H. Miles
College of Science and Technology, Dixie State University,
St. George, Utah 84770, USA
email: mhmiles1937@gmail.com

Several varieties of work can be described by the First Law of Thermodynamics [1]. For the electrochemical electrolysis of D₂O in cold fusion experiments using open cells, both electrical work (Edq) and gas expansion work (-P_{ex}dV) are involved. The work done by the generated gases can be expressed by

$$w = -P_{ex}\Delta V = -nRT \quad (1)$$

where n (or Δn) is the number of moles of gas generated by electrolysis assuming Ideal Gas behavior ($\Delta V = \Delta nRT/P_{ex}$) [1]. For the D₂O electrolysis reaction per Faraday (F = 96485.3 A·s/mol electrons)



there are 0.75 moles of gas generated. The power term for work due to this gas generation is

$$P_w = dw/dt = -RTdn/dt = -RT (0.75 I/F) \quad (3)$$

where dn/dt = 0.75 I/F moles of gas generated per second. The negative sign for P_w is required because this gas expansion work is done by the cell on the surrounding for an open cell. For a closed cell, no gases escape (ΔV = 0) and P_w = 0.

This P_w term is generally small in most cold fusion experiments and was never reported in any Fleischmann-Pons publications. Perhaps they assumed that this small term could usually be incorporated into their cell constant calibrations. At typical cold fusion conditions for I = 0.200 A and T = 310 K, this work power term is P_w = -0.0040 W or -4.0 mW. However, at high cell currents (I = 1.000 A) and high cell temperatures (T = 360 K), this term is -0.0233 W or -23.3 mW and should not be neglected. For my Pd-0.5 B experiment at NHE in Japan, Fleischmann's calculations showed a mean negative excess power (-5.0 mW) on Day 61 where I = 1.00 A [2]. A negative excess power is not possible based on thermodynamics because the cell can never spontaneously operate as a refrigerator [2]. However, the addition of the P_w term increased the mean excess power for Day 61 to +17.3 mW.

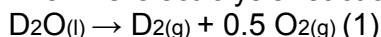
Some have erroneously suggested that the P_w term is included in the electrochemical power term, P_{EI} = (E - E_H)I. The thermoneutral potential for D₂O electrolysis, E_H = 1.527 V, is based solely on the enthalpy change, ΔH, for Reaction 2. Enthalpy is defined as H = U + PV, thus at constant pressure ΔH = ΔU + PΔV where ΔU = q + w = q - PΔV + w* where w* is any additional work other than P-V work. Therefore, ΔH = q + w* and does not include P-V work. For cold fusion experiments, the only power terms due to work are electrical (P_{EI}) and gas expansion (P_w). Both are required for open cells. The P_w term cannot be ignored at high cell currents. The use of E_H provides a convenient means for calculating the electrochemical power involved in splitting D₂O into D₂ and O₂ gases and the corresponding rate for this loss of chemical enthalpy from the cell.

1. P. Atkins and J. de Paula, "Physical Chemistry", 7th Edition, W.H. Freeman, New York, 2002, pp. 37-45.
2. M.H. Miles, M. Fleischmann and M.A. Imam, "Calorimetric Analysis of a Heavy Water Electrolysis Experiment using a Pd-B Alloy Cathode", Naval Research Laboratory Report, NRL/MR/6320-01-8526, March 26, 2001, pp. 78, 88-91

Miles: The Thermoneutral Potential In Electrochemical Calorimetry For The Pd/D₂O System Poster

Melvin H. Miles
College of Science and Technology, Dixie State University,
St. George, Utah 84770, USA
email: mhmiles1937@gmail.com

The thermoneutral potential (E_H) is used to determine the electrochemical power used to split D₂O molecules into D₂ and O₂ gases [1]. This D₂O electrolysis reaction



produces an enthalpy change of $\Delta H^\circ = 294,600 \text{ J/mol}$ of D₂O and yields a thermoneutral potential of $E_H^\circ = -\Delta H^\circ/2F = -1.527 \text{ V}$ at STP ($T = 298.15 \text{ K}$, $P = 101,325 \text{ Pa}$). Typical cold fusion experimental conditions for temperature, pressure (fugacity) and activity of D₂O in 0.1M LiOD do not significantly change this value for E_H . The electrochemical power applied to the cell in cold fusion calorimetry (P_{EI}) is then defined by $P_{EI} = (E - E_H)I$ where E is the cell voltage (V) and I is the cell current (A). This applies to any open calorimetric cell where the chemical enthalpy of the gaseous products of Reaction 1 are carried out of the cell to the surroundings and represents the rate of electrochemical work applied to the cell. There will be cell cooling if E is less than E_H , but this is never observed for the high cell currents typically used in cold fusion experiments.

The cell reaction will differ from Reaction 1 at the beginning of a cold fusion experiment where the loading of deuterium into palladium occurs. If all of the deuterium generated is used for palladium loading, then the cell reaction is



The enthalpy change (ΔH) for this reaction is $53,300 \text{ J/mol}$ of palladium, thus the thermoneutral potential is $E_H = -\Delta H/0.6 F = -0.921 \text{ V}$ rather than -1.527 V . The error in excess power (P_x) due to the use of $E_H = -1.527 \text{ V}$ rather than $E_H = -0.921 \text{ V}$ at the beginning of an experiment is given by

$$\Delta P_x = (1.527 - 0.921)I \quad (3)$$

Two recent experiments using a palladium cathode and a Pd-B cathode at different cell currents gave very early excess power effects in approximate agreement with Eq. 3 when $E_H = -1.527 \text{ V}$ was used (1,2). Early excess power results for these two experiments will be presented. The fraction of Reaction 2 versus Reaction 1 will decrease with time and E_H will increase in magnitude towards the normal value of -1.527 V . Measurements of the amount of gas escaping from the cell would be necessary to accurately determine the changing value for E_H during the loading period. It should be noted that any significant change from Reaction 1 within the cell will affect other calorimetric terms relating to gas evolution such as P_g and P_w in addition to changes in E_H [1]. Various experimental measurements of gas evolution by the author from cold fusion electrochemical cells using palladium rod anodes following deuterium loading were always in agreement with Reaction 1 where $E_H = -1.527 \text{ V}$.

1. M.H. Miles, "The Fleischmann-Pons Calorimetric Methods, Equations and New Applications", *J. Condensed Matter Nucl. Sci.*, 24 (2017) 1-14.
2. M.H. Miles and M. Ashraf Imam, "Excess Power Measurements for Palladium-Boron Cathodes", *J. Condensed Matter Nucl. Sci.*, 29 (2019) in progress.

Nagel: The LENRIA Experiment and Analysis Program (LEAP)

David J. Nagel¹, Chandraman Patil¹, Steven B. Katinsky², Melvin H. Miles³, M. Ashraf Imam¹
¹The George Washington University, ²LENRIA Corporations, ³Dixie State University

The field of Low Energy Nuclear Reactions (LENR) has three primary goals. The largest and most distant is the commercialization of generators based on LENR, which will provide a new source of clean energy in small, distributed units. The nearer-term goal is scientific understanding of the mechanisms that are active in LENR. Achieving understanding will take a combination of new theoretical and experimental results. The immediate goal is to get the field recognized and funded as a legitimate arena of research and development. This program and paper are aimed at this last goal.

LENR could get needed attention by any of a few possible events: (a) publication of a clear explanation of the mechanism(s), (b) a strong experimental demonstration, (c) a repeat of the 1985 Fleischmann-Pons meltdown experiment, (d) appearance of an LENR generator on the market, or (e) publication of papers with solid LENR results from several major international laboratories. Only the last approach can be controlled. So, the LEAP is taking that approach. The program goals include: (a) perform the same turn-key LENR experiment, which has been qualified to produce excess heat, at multiple major laboratories, (b) produce reports on the conduct and results of the experiments by each laboratory, and (c) coordinate simultaneous publication of the reports in a major scientific journal.

Phase I of the LEAP has been funded recently by the Anthropocene Institute. It seeks to demonstrate an experiment that reproducibly produces LENR energy with good signal-to-noise ratios. A key feature of the program is to exploit specific Pd-B alloys that have been shown to produce excess heat in multiple experiments with a high success rate. We have such materials, which were made over 20 years ago by one of us (MAI) at the Naval Research Laboratory [1]. Cathodes produced from those materials gave excess heat in nine of ten experiments with four different calorimeters in three laboratories in experiments by one of us (MHM) [2]. New Pd-B alloys have also been procured and characterized.

A simple, transparent isoperibolic calorimeter has been designed, built and tested. LabVIEW is being used for control of experiments, and for data acquisition, analysis and display. A Keysight E36313A power supply, which has three sources in one unit, provides electrolysis power. A Pico PT-104 unit, with four temperature sensors capable of milli-degree resolution, is being used. Two calorimeters can be run simultaneously in the same water bath.

This paper will provide the experimental and analytical results available at the time of the ICCF-22.

[1] M. A. Imam, D. J. Nagel and M. H. Miles, "Fabrication and Characterization of Palladium-Boron Alloys Used in LENR Experiments", Proc of ICCF-21, J. of Cond. Matter Nuclear Science (2019)

[2] M. H. Miles and M.A. Imam, "Excess Power Measurements for Palladium-Boron Cathodes", Proc of ICCF-21, J. of Cond. Matter Nuclear Science (2019)

Nagel: Comparison of the Theoretical Results of Kálmán and Keszthelyi with LENR Experimental Results

David J. Nagel

The George Washington University and NUCAT Energy LLC

Kálmán and Keszthelyi papers from 2013 dealt mainly with the enhanced deuterium fusion cross sections. Two basic papers showed the importance of 2nd, 3rd and 4th orders of standard quantum mechanical perturbation calculations for nuclear processes in solids. This review will concentrate on more recent works by the two theoreticians, which deal with LENR. A key paper that was revised in 2017 considers data from Fleischmann-Pons type of experiments, transmutations from LENR experiments, and data from an E-Cat report. Another 2017 paper emphasized the important mechanism of recoil-assisted nuclear reactions. In that concept, a third body, for example, a Pd nucleus, acts like a catalyst. It provides wave function mixing, resulting in enhanced nuclear reaction probabilities for two nuclei, such as a proton and deuteron, or two deuterons, which would otherwise have negligibly small reaction rates. The catalyst also carries off some of the reaction energy. That slow recoil of a heavy nucleus explains the lack of significant high energy x- and gamma-radiation from LENR experiments. This mechanism was more precisely restated in a 2019 paper. That paper also contained computed rates for many nuclear reactions. It topped off 15 years of theoretical efforts by Kálmán and Keszthelyi. Most recently, they predicted nuclear reactions for elements across the periodic table, and discussed the failure of the four year, \$10M Google program to achieve LENR. Some of the papers by Kálmán and Keszthelyi contain comparisons with LENR results.

A summary of the various theoretical explanations and predictions from these papers will be provided. More comparisons of some of the theoretical results with what is known about LENR will be made.

Roggeri : Opportunities and aid from the European community for the development of scientific cooperation projects: horizon 2020 and new horizon Europe programs

Riccardo Roggeri

The intervention will develop on three main themes:

- 1) New financing perspectives through instruments provided by the European community, for the last year of the horizon 2020 program. Examples of calls for the sectoral areas of interest.
- 2) Exploration of the main open international collaboration programs. In particular, analysis of the Europe-US-Japan and Middle East states programs.
- 3) Evaluation and exploration of the main differences that will occur in the new horizon Europe program. Europe that changes the perspective of communal aid for basic, applied research and the competitive development of companies and markets.

Tanzella: Mass Flow Calorimetry in Brillouin's Reactor

Robert Godes¹, Robert George¹, #Francis Tanzella²

¹ Brillouin Energy Corp., CA, United States

² Energy Research Center LLC, CA, United States

Email: consulting@tanzella.name

Brillouin Energy and Energy Research Center LLC have continued the calorimetry measurements on the Ni/ceramic/Cu coatings in a H₂ atmosphere performed earlier at SRI International. These sample tubes have been stimulated using nanosecond pulses applied between the Ni and Cu coatings. The reactive tubes (previously referred to as cores) have been described earlier [1]. We have been testing new electrical stimulation boards that have produced power and energy output in excess of that reported earlier. In addition, we have recently been testing new calorimetric methods that should allow us to determine the power gain relative to actual wall power.

As presented earlier, fast pulses of several hundred volts and tens of nanoseconds long cause the majority of the current to follow the “skin-effect” principle and concentrate at the Ni-ceramic interface before returning through the bulk of the Cu. The stimulation methods used previously have allowed us to determine the power produced by the core relative to the accurately measured power input directly to the tube. Recent advances in reducing the electrical losses in the supporting electronics have allowed us to increase the power input to the tubes by approximately an order of magnitude. In addition, we are removing the termination resistor used to measure the pulse current which now allows almost all of the pulse power input to either remain in or be reflected back into the tube. Hence, a higher percentage of wall power is input into the tube.

We have been using the System Identification (SID) model [2, 3] of the calorimeter with up to 10 coefficients to calculate the power reaching five temperature sensors during simultaneous continuous ramps of both heater (during calibration) and pulse powers. This model was conceived and executed working closely with the authors in references 2 and 3 who developed this technology. Figure 1 summarizes the coefficients of performance (COP) obtained during the last year.

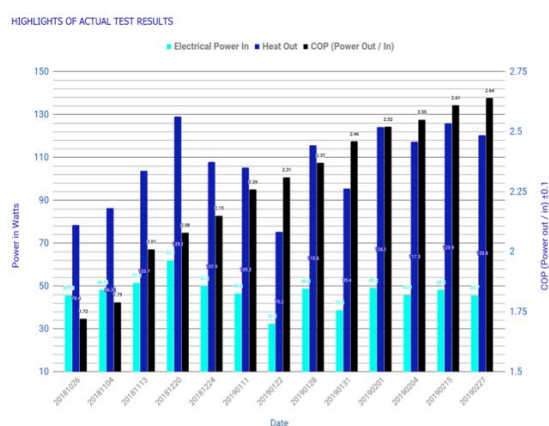


Figure 1. COP measurements over the past year

[1] F. Tanzella, R. Godes R., et al. “Controlled electron capture: enhanced stimulation and calorimetry methods”, *J. Condensed Matter Nucl. Sci.*, vol. 24, pp. 301-311, 2017.

[2] Berlinguette et al, “Revisiting the cold case of cold fusion”, *Nature Perspective*, <https://doi.org/10.1038/s41586-019-1256-6>

[3] B. P. MacLeod, D. K. Fork, et al, “Calorimetry under non-ideal conditions using system identification”, *Journal of Thermal Analysis and Calorimetry*, <https://doi.org/10.1007/s10973-019-08271-z> (2019)

Celani: Progress understanding LENR-AHE effects, using thin, long Constantan wires multi-elements coated, under D₂ gas mixtures at high temperatures, by DC/AC voltage stimulation in coiled coaxial geometry.

Francesco Celani^(1,2), C. Lorenzetti⁽¹⁾, G. Vassallo^(1, 3), E. Purchi⁽¹⁾, S. Fiorilla⁽¹⁾, S. Cupellini⁽¹⁾, M. Nakamura⁽¹⁾, P. Cerreoni⁽¹⁾, P. Boccanera⁽¹⁾, R. Burri⁽⁴⁾, A. Spallone^(1,2).

- 1) ISCMNS_L1, Via Cavour 26, 03013 Ferentino-IT;
- 2) INFN-LNF; Via E. Fermi 40, 00044 Frascati-IT;
- 3) DIID, University of Palermo, 90128 Palermo-IT;
- 4) IETCLaboratories, 6827 Brusino Arsizio-CH.

Our group has been studying LENR phenomena in Constantan (Cu₅₅Ni₄₄Mn₁) since 2011. In fact, this alloy captured our attention since it promotes efficiently the dissociation of molecular Deuterium (D₂) or Hydrogen (H₂) to the atomic state, followed by a remarkable absorption capability. Under certain conditions, this absorption is associated with exothermic phenomena exceeding by orders of magnitude the enthalpy of conventional reactions. Constantan is also much cheaper than Palladium, has better mechanical properties and it is found in an ample variety of applications. Similarly to the better studied Palladium, the occurrence of anomalous heat effects (AHE) in Constantan requires a loading with Deuterium or Hydrogen and conditions of non-equilibrium. When the latter are absent, AHE is either reduced or tend to decline with time. This observation led our group to investigate ways to increase non-equilibrium conditions. From 2016 we studied in particular the effect of surface modification of the Constantan wires with coatings comprising elements able to modify the absorption behavior (i.e. Fe) and oxides with low work function. We also developed certain geometrical arrangements of the wires (knots, capuchin knot and so-on) in order to induce local thermal gradients and hot-spots. Moreover, the polarization of the wires (initially as cathode) with a power supply proved to be a versatile approach to induce non-equilibrium conditions and AHE. In that respect, we have speculated that the electron emission from the wires may induce the movement of active species (similarly to the **Richardson** effect – data presented at MIT in March 2019). This hypothesis seems to be confirmed by the more recent finding that both the polarization of the Constantan as cathode or anode produces some AHE stimulus. The study of alternating currents followed (50 Hz, 600V), and proved to be an effective trigger as well. These results have been presented at the *ANV Meeting* in Assisi (17-19 May 2019), where we anticipated the findings of this presentation. In particular, we reported a remarkable AHE increase at reduced pressure, when a gas discharge closely matching the **Paschen**-law occurs. Because of the promising results with the AC fields, we assembled the wires in a different geometrical configuration, with the aim at maximizing the gas discharge phenomena (i.e. dielectric barrier discharges). This new geometry comprises a Constantan wire with a coaxial counter electrode (a Fe thin tube insulated by SiO₂ sheath). The Constantan wire is inserted inside a sheath comprising glass Type_e and SiO₂-Al₂O₃ fibers, and then coiled over the Fe counter electrode (ϕ=6mm) while keeping as low as possible the distance between the electrodes (<2.5 mm). The presentation discusses the results obtained with the new assembly and the effect of AC stimuli with Constantan wires of different thicknesses (ϕϕ 200, 350 ϕm) and length of 170 cm. The Constantan wires were studied up to 750 °C and gas pressures ranging from 100 to 2500 mbar.

Stankovic: Nuclear Transmutation with Carbon and Oxyhydrogen Plasma

Slobodan Stankovic¹, Prof. Emeritus Stewart K. Kurtz², Andy Mayers³

¹Swiss Oxyhydrogen Energy (SOHE), Morges, Switzerland

²Septor Inc., Kill Devil Hills, NC, USA

³State College, Penn State University, USA

Numerous experiments (Oshawa, Monti, Sundaresan and Bockris, Ransford) have been conducted with electric discharges between two carbon rods submerged in de-mineralized water, and some transmutation elements, such as Fe, Cr, Co and Zn, were subsequently found in the residues. In the present paper, a nuclear transmutation with a carbon rod and oxyhydrogen plasma was investigated. Oxyhydrogen gas obtained from water by an electrolyzer (developed by SOHE) was used as is, in order to obtain a plasma with a very low electron temperature (between 120 and 150°C). The plasma temperature was determined by a technique called *Moiré deflectometry* used to measure the temperature and electrons density distribution of the atmospheric arc plasma. An optical spectroscopy measurement was performed on the oxyhydrogen plasma alone, with a low-resolution Ocean Optics 2000 spectrometer (spectral range of 180-880nm), which indicated that only the OH radicals were present in the 280-330nm range. Graphite rod (99.9% pure carbon) was used as a testing element, and it was treated with the oxyhydrogen plasma. At the precise moment when the graphite rod was inserted into the plasma, we were able to see - besides the broad band spectrum center measured around 680nm - very strong Na D-lines at 589.0 and 589.6nm, as well as K lines at 766.4 and 769.9nm. Another measurement performed by a high-resolution spectrometer (constructed by SOHE), with a range of 4nm and a resolution of 0.01nm, confirmed the occurrence of the same lines. In addition, radiation measurements were carried out with a calibrated 360° Gamma Radiation Detector (made by SOHE), which did not indicate any radioactivity during the tests. The electric nature of the oxyhydrogen plasma enabled us to obtain nuclear transmutation by annihilating most of the graphite rod, and elements such as Si and Al were found in small transparent spheres (diameters between 10-100µm). Measured quantities by SEM/EDX of the Si and Al in those spheres were two to three times greater than the initial values measured in the graphite rod with the *Inductively coupled plasma mass spectrometry* (ICP-MS). The quantity augmentation of these elements could be explained by the “Kervran Effect”, named after the scientist Corentin Louis Kervran. It is important to highlight that all these elements were present in the graphite rod before the experiment, but in very small quantities measured under 0.014% weight concentration. Their presence is considered by Kervran to be “activator” of the creation of the supplementary quantity of the same elements. All of the aforementioned analytical methods (polarizing light and optical microscopy, radiation detector, Raman spectroscopy, SEM/EDX, ICP-MS) were used in order to characterize the graphite rod, and to identify and quantify different transmutation elements.

Keywords: Oxyhydrogen plasma, Nuclear transmutation.

Garai: Speculation on the size of the electron poster

Jozsef Garai

Department of Civil Engineering, University of Debrecen, Hungary

E-mail: jozsef.garai@fiu.edu

There is a discrepancy between the observed size of the electron and its measured magnetic moment or spin. Generating the observed Bohr's magnetic moment requires electron radius comparable to the atom. The size of the electron has not been measured, but experiments indicates that it should be 10^{-17} m or smaller.

Analyzing the known experimental data of the Hydrogen atom it has been proposed that in the vicinity of the atom the electrons transform from a small point like spherical object to a spherical halo around the nucleus [1]. This transformation can reconcile the size discrepancy and can explain the generation of the magnetic moment of the electron. Thus, in the vicinity of the atom, the size of the electron is equal with the size of the atom, and outside is much smaller.

The classical radius of the electron is calculated by assuming that the energy required for the charge formation is the same as the energy required for the mass formation. It is argued that this assumption is incorrect and the formation of the charge requires different energy than the formation of the mass. Using the energy of charge formation allows calculating the size of the electron. The results will be presented at the meeting.

[1] Jozsef Garai, The electronic structures of the atoms. Physics Essays 2017;30:455-60; preprint:
https://dea.lib.unideb.hu/dea/bitstream/handle/2437/247192/0_9_Hydrogen_model.pdf

Jaitner: Condensed Plasmoids – The Nuclear Active Environment in LENR Oral & Poster

Lutz Jaitner, lutz.jaitner t-online de,
www.condensed-plasmoids.com

LENR research was puzzled for a long time by the basic questions: How can nuclei fuse at low temperature? Why is the observed excess heat not accompanied with gamma radiation? Why is LENR producing helium-4 from deuterium, whereas D-D hot fusion is mainly producing helium-3, tritium and neutrons? How can LENR be technically optimized for commercial use?

To answer these questions, the author has built a quantum-mechanical model of the nuclear active environment in LENR. This environment is an ultra-dense plasmoid, i.e. a “condensed plasmoid”. The computed properties of CPs are so exotic, that CPs qualify as a previously unknown aggregation state of matter.

This document is first in describing the properties of CPs, the microscopic evidence of CPs in LENR experiments, how the properties of CPs help explaining a wealth of remarkable findings in LENR experiments, examples of nuclear reaction routes possibly enabled by CPs, the quantum-mechanical model of CPs, the computational results derived from this model, and an assessment on potential dangers of LENR. The mechanism, which suppresses gamma radiation in CPs, will also be described in this document.

The quantum-mechanical model of CPs is based on the cylindrical symmetry of a very thin (i.e. about 40 pm) plasma “wire” (The quantitative properties given in the abstract are depending on the configuration of the CP, they are just examples). The electrons of a CP are fully delocalized and decoupled from the nuclei. They are moving with high velocity (10 to 80% of light speed) against the nuclei. This is resulting in an intrinsic current of about 9 kA in the CPs, with a mean current density of approximately 2.5 A per square picometer.

The magnetic field from this current reaches 50 megatesla and creates a confinement pressure of more than 10^{21} Pa. The electrons are compressed by a z-pinch condition to a mean density of about 0.15 electrons per cubic picometer.

The creation of a CP is an endothermic process, which typically requires high voltages and high currents. Once created, CPs enjoy a lifetime, which can extend to hours. This longevity is likely not a result of the CP's stability, but is rather based on a self-sustained feedback of nuclear energy, countering the otherwise inevitable decay of the CP.

The minimum distance of hydrogen nuclei in a CP is only about 2 pm, which enables tunneling through the Coulomb barrier. The barrier is also much screened by the dense electrons.

The self-sustained growth of CPs can produce a dangerous and sudden release of nuclear energy, if the reaction rate is not properly fuel-limited.

Carat: Fiery Science of Cold Fusion comic book Poster

Ruby Carat, Coldscope

The *Fiery Science of Cold Fusion* is a comic book written by Ruby Carat and illustrated by Matt Howarth. Here the complex story of cold fusion is distilled into 32-pages. It is not "the" story of cold fusion, but "a" story of cold fusion. It begins with a brief historical review of human's evolution in energy use. Martin Fleischmann and Stanley Pons are then introduced as heroes who went against the prevailing paradigm, threatening the identity and funding of conventional nuclear physicists. Accompanied by a global cast of CMNS scientists, the development of a technology is assumed to give a happy ending for life on Earth. The only names used are those of Martin Fleischmann, Stanley Pons, and Steven Jones. All other characters are known only by the statements they make in the word balloons in the text and the drawing. When possible, actual quotes are used to propel the story. Characters from agencies and government are shown symbolically as icons, not individuals. It was not possible to put every story in this story. This comic book story is only a slice of the continuing drama of cold fusion. Here's page 7:

They worked secretly in the basement lab of the Henry Eyring Chemistry Building at the University of Utah, using \$100,000 of mostly Dr. Pons' personal savings.

I CAN HARDLY BELIEVE IT. WE ARE GETTING MORE POWER OUT THAN THE POWER WE'RE PUTTING IN.

EVEN IF EVERYTHING IN THE CELL REACTED CHEMICALLY, THAT WOULD NOT BE CLOSE TO THE ENERGY WE ARE MEASURING COMING OUT. IT MUST BE A NUCLEAR REACTION IN THE LITTLE PIECE OF METAL.

BUT IT'S NOT THE KIND OF NUCLEAR REACTION WE ARE FAMILIAR WITH --THERE'S NO DEADLY NEUTRONS OR GAMMA RAYS.

WE'RE STILL ALIVE--SO IS MARVIN HAWKINS, OUR GRADUATE STUDENT.

YES, I'M STILL ALIVE.

CONVENTIONAL NUCLEAR THEORY BASED ON HOT FUSION IN THE SUN SAYS THERE SHOULD BE A LOT OF DEADLY NEUTRONS TO GET THIS AMOUNT OF HEAT. WE'VE GENERATED SOME, BUT SO FEW--THEY ARE DIFFICULT TO EVEN MEASURE.

AND IT OFTEN TAKES MONTHS BEFORE A REACTION STARTS--IF IT STARTS. WE CAN'T SEEM TO TELL JUST WHEN IT'S GOING TO REACT.

WHAT'S GOING ON HERE?

S. Pons, M. Fleischmann, C. Walling, and J. Simpson International Patent Publication No. 90/10935 (1990)

Time (days)	Time (10 ⁵ s)	Cell Temperature (°C)
33.6	2.9	60
38.2	3.3	100

Once a current was applied, the temperature of the cell rose steadily, heating the water. Just over one month later, the temperature suddenly jumped 20 degrees--and increased exponentially toward boiling. Then just as suddenly, the temperature dropped back down, then continued to rise steadily. What made the temperature rise? What made the temperature drop? This was the question of the Anomalous Heat Effect.

Rothwell: Increased Excess Heat from Palladium Deposited on Nickel

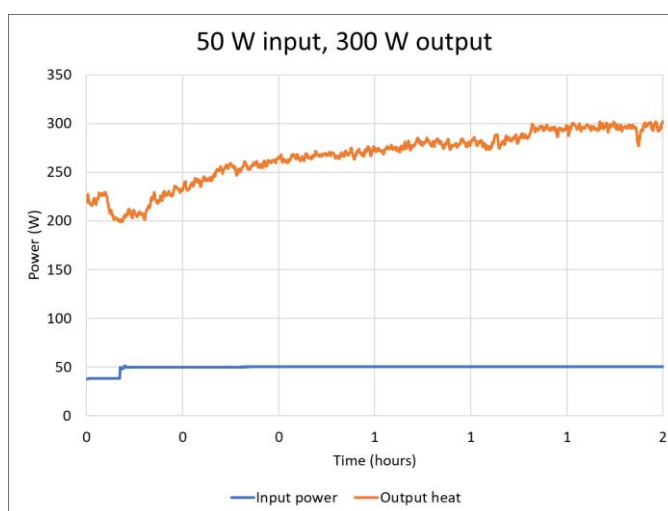
Tadahiko Mizuno

Hydrogen Engineering Application and Development Company, Kita 12, Nishi 4, Kita-ku, Sapporo 001-0012, Japan

Jed Rothwell

LENR-CANR.org, 1954 Airport Road, Suite 204, Chamblee, GA 30341, USA

We have developed an improved method of producing excess heat with nickel mesh coated with palladium. The new method produces higher power, a larger output to input ratio, and it can be controlled effectively. With 50 W of input, it produces ~250 W of excess heat, and with 300 W it produces ~2 to 3 kW. This paper is a comprehensive description of the apparatus, the reactant, and the method. We hope this paper will allow others to replicate the experiment.



Keywords: Air flow calorimetry, Deuterium gas, Excess heat, Nickel reactant, Pd coating, Simple method

Kovacs: The Zitterbewegung Orbit of Electrons

Andras Kovacs

Email: andras.kovacs@broadbit.com

At ICCF-21, I presented experimental data [1] pointing to the existence of a close-proximity electron-nucleus configuration, which catalyzes nuclear reactions by effectively shielding the proton's or deuteron's electric charge. The experimental support for such electron state is strong, but its theory has been lacking. Several researchers put forward theories of a close-proximity electron-nucleus configuration, referring to "deep electron orbit", "Rydberg hydrogen", etc. However, these preceding theories did not quantitatively account for all observed experimental data, and there was no specific guidance for experimental reactor designs.

This presentation discusses the physics of a meta-stable electron orbit at 0.383 pm average distance from the nucleus. This orbital is referred to as "zitterbewegung orbit", since it is related to the electron's zitterbewegung dynamics. Although its detailed understanding requires the knowledge of the correct electron structure, which is described in [2], the main concepts and results can be explained within the presentation.

As most important result, the calculation reveals that this meta-stable electron state establishment requires 35 eV and 80 eV electron energy around a deuteron and proton, respectively. When the kinetic energy of an ordinary electron orbital reaches this level, it may transition into zitterbewegung orbit state. Knowing this energy level is an important guidance for selecting LENR reactor materials or optimizing reactor designs. We go through several examples, such as nickel or calcium, where the reactor materials contain electron orbitals close to the critical energy level.

We review corresponding evidence from a broad range of experiments, which were considered unexplained and unrelated so far. The figures from left to right illustrate the following:

- Non-thermal IR emission during Pd-D experiments, which corresponds to the nuclear Zeeman energy-split upon zitterbewegung orbit establishment [3]
- "Runaway electron" production in hot fusion reactors, shooting out >10 MeV electrons when the plasma cools to certain temperature. The top part is the plasma current and the bottom part is the neutron count, produced by these energetic electrons. Experimenters give an estimated plasma electron temperature close to the expected 35 eV threshold.
- The 2.3 pm inter-nuclear distance measured in ultra-dense hydrogen producing experiments, which corresponds to the phase-coherence condition of the above described electron state [4]
- The triple-track carbon break-up patterns observed in Pd-D co-deposition experiments, which require >7 MeV particle energy. These are explained as energetic electrons carrying away the energy of D-D fusion, i.e. the same phenomenon as runaway electron production in tokamaks
- The measured flat power-spectrum RF emission from our past experiment, which corresponds to braking radiation of energetic electrons

[1] A. Kovacs, D. Wang, P. Ivanov "Investigation of Electron Mediated Nuclear Reactions", proceedings of the ICCF-21 conference

[2] A. Kovacs, G. Vassallo, A. O. Di Tommaso, F. Celani, D. Wang "Maxwell-Dirac Theory and Occam's Razor: Unified Field, Elementary Particles, and Nuclear Interactions"

[3] M. Swartz et al "Non-Thermal Near-IR Emission from High Impedance and Codeposition LANR Devices", proceedings of the ICCF-14 conference

[4] L. Holmlid and S. Zeiner-Gundersen "Ultradense protium $p(0)$ and deuterium $D(0)$ and their relation to ordinary Rydberg matter: a review", *Physica Scripta*, Volume 94, 7 (2019)

Kovacs: Maxwell-Dirac Theory and Occam's Razor: Unified Field, Elementary Particles, and Nuclear Interactions **Poster**

Andras Kovacs, Giorgio Vassallo, Antonino O. Di Tommaso, Francesco Celani, Dawei Wang
 Email: andras.kovacs@broadbit.com

1. Maxwell's Equations and Occam's Razor. We introduce and use the space-time Clifford algebra, showing that only one fundamental physical entity is sufficient to describe the origin of electromagnetic fields, charges and currents: the electromagnetic four-potential. We get a familiar form of Maxwell's equations: $DA=G$ and $DG=0$, where A is the vector potential, and D is the space-time differentiation operator. But G now incorporates electromagnetic fields, charges, and also currents. This perspective brings a new understanding of zitterbewegung dynamics.
2. Quantum Mechanics and Occam's Razor. Quantum mechanical relations follow naturally from this model, and we derive the electromagnetic formulation of the Dirac equation. The spinor field is shown to correspond to electromagnetic energy-momentum.
3. The Electron and Occam's Razor. We derive from the model all the essential features of the electron: its mass exactly corresponds to its electromagnetic energy, its charge surface is on a sphere at the classical electron radius, its zitterbewegung radius is the reduced Compton radius (in the rest frame), and we derive its relativistic increase of mass.
4. Detailed Analysis of Electron Dynamics 5. Zitterbewegung Orbit Our calculation shows the existence of a meta-stable electron state at 0.383 pm, requiring 35 eV and 80 eV electron energy around a deuteron and proton, respectively. The 2.3 pm inter-nuclear distance in dense hydrogen is also calculated.
6. The Electromagnetic Wave Equation Based Nuclear Model The same model can be applied to describe nuclear forces and nucleons, and a very large set of "anomalous" or unexplained experimental data suddenly make sense. The figures show data from particle collision experiments, probing the nuclear structure of light nuclei and the proton's internal structure.

Klimov: Power Balance in Water Plasma Reactor

Klimov A., Belov N., Klimova T., Temirbulatov V., Tolkunov B.
Technical State University “ MPEI”, Russia, Moscow, 111250, Krasnokazarmennaya str. 14
klimov.anatoly@gmail.com

Physical parameters and characteristics of a heterogeneous plasmoid (HP) created by pulse repetitive discharge in a water plasma reactor (PVR) have been considered in our previous works [1-3]. This work is continuation of the previous one. It was revealed that there is a large extra-power release in the HP in water at metal nano-cluster- hydrogen atom interaction (products of water molecule's dissociation and cathode's erosion). This thermal power was much higher than the electric power input in plasma. It was obtained that a specific energy value of this reaction was about 1 KeV/atom and higher. This HP creates intensive soft X-ray radiation. The typical quantum energy of this X-ray radiation was about of 1-10 KeV. Transmutation of the chemical elements inside the PVR was studied by chemical analysis and MS ICP method. The electric discharge parameters were measured. Water calorimeter was used to measure power balance in these experiments. The value COP was about 2-4 in these experiments. Hydrogen flow was recorded and measured in this experiment also.

References

1. Klimov A., Vortex Plasmoids Created by High_Frequency Discharges, Atmosphere and Ionosphere: Dynamics, Processes, Monitoring, Springer, Berlin, 2013, P.251
2. A. Klimov, A. Grigorenko, A. Efimov, et.al., High-energetic Nano-Cluster Plasmoid and Its Soft X-ray Radiation, // J. Condensed Matter Nucl. Sci, 19, P.1-10
3. Klimov A., Bityurin V., Grigorenko A., et.al, “Plasma Assisted Combustion of Heterogeneous Fuel in High-Speed Airflow”, AIAA Paper AIAA-2009-1411-250, P.11

Klimov: Review of the Proceedings of the 25th Russian Conference on Cold Nuclear Transmutation of Chemical Elements and Ball Lightning

(Adler-Sochi, 1-8 Oct 2018).

Klimov A.

Chairman of RCNT-25,

Technical State University “Moscow Power Engineering Institute”

Russia, Moscow, 111250, Krasnokazarmennaya str. 14

klimov.anatoly@gmail.com

28 leading scientists from Russia and foreign countries have took part in the RCNT-25 (Moscow-21, Sochi-2, Novosibirsk- 2, Armenia-1, Belgium-1, Czech- 1). Six works were presented by young scientists. Program of the key experiments and the theoretical model development in the field of LENR physics was considered and discussed. It was recommended to take into account the following important tasks and problems:

1. Registration and study of a soft X-ray radiation and neutron-like particle flux from LENR set up,
2. Ecological problem connected with LENR. Biological protection from the different type radiation created by LENR,
3. Stability of the new transmuted chemical elements,
4. Combustion and detonation of the LENR’s fuel,
5. Optimization of LENR’s reactor design and its parameters ,
6. “Strange radiation”. What is it?
7. LENR and ball lightning physics,
8. and others.

Klimova: Thermal Energy Release in a Swirl Heterogeneous Reactor at Pulsed Repetitive Electrical Discharge

Klimova T., Klimov A.

Technical State University “Moscow Power Engineering Institute”

Russia, Moscow, 111250, Krasnokazarmennaya str. 14

* E-mail: klimov.anatoly@gmail.com

Physical parameters and characteristics of a vortex plasma-chemical reactor (PVR) have been considered in our previous works [1, 2]. According our opinion these characteristic and PVR's power efficiency could be improved considerably by a pulsed repetitive electric discharge (PRD). Active metastable particles are accumulated during a pause time period between the current pulses. A hot massive cathode heats a gas flow mixture in the pause time period additionally. These two factors play important positive role in energy balance in the vortex plasma chemical reactor (PVR) operation. Second important task in this work: - a study of kinetics of the different active chemical species in the plasma-chemical reactor. These two tasks were studied in this work. The experimental researches of PRD were fulfilled in the set up PVR. A new power supply created PRD with the following parameters: - pulsed repetitive frequency $F < 100$ kHz, ratio pulse time / pause time $Q = 2 \div 10$. Experimental conditions were the followings: - tested gas flow mixture - argon: water steam, argon mass flow rate $q = 1,8$ G/s, initial gas flow temperature – 70 °C, operation regime – PRD' mode and continuous mode, pulsed current $I_d = 2-4$ Amp, mean electric power input in plasma $N_e \sim 1-2$ kW. A massive nickel cathode 20 mm diameter (140 G mass) and a thin nickel anode 5 mm diameter were used in these experiments. It was revealed, that the best regime of PVR's operation was realized at the following PRD's parameters: - the pulsed repetitive frequency $F < 10$ Hz and the value $Q = 2 \div 4$. A stationary gas flow temperature was measured during a pulse time period namely. One can estimate the power efficiency value COP at a continuous mode and PRD's mode: - $COP = Q_T / N_e$, where Q_T - thermal power of outcoming gas flow, heated by an electric discharge, N_e – electrical power input in a plasma. It's revealed that the COP at PRD's mode is $1,5 \div 2$ times higher than the one at a continuous mode. So, PRD regime is the best one and has a higher power efficiency. It is very important to note that there is a gas flow heating during the time pause period also. We suppose that this heating process is connected with the hydrogen ion-nickel atom interaction. Additional experiment with a pure nitrogen flow proves this conclusion. Additional gas flow heating between pulses was absent in this experiment.

References

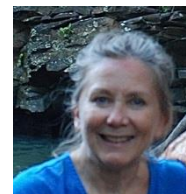
1. Klimov A., V. Bityurin V., Grigorenko A. et.al. *Plasma Assisted Combustion of Heterogeneous Fuel in High-Speed Airflow // AIAA Paper. 2009-1411.*
2. Klimov A., Kazanskii P., Belov N., Tolkunov B., Zavershinskii I., Molevich N. *Thermal Energy Release and Hydrogen Production in Swirl Heterogeneous Plasma-Chemical Reactor // Journal of Physics: Conf. Series. 2018. V.1112. 012024.*

Bowen: Primary and Secondary Reactions in a LENR with a Li Electrolyte Solution

N. L. Bowen

Colorado Mountain College, Glenwood Springs, Colorado, USA

nbowen@coloradomtn.edu



Conventional nuclear physicists claim that low energy nuclear reactions cannot exist because:

- Too much ^4He is produced, according to the reaction probabilities of a $^2\text{D}(^2\text{D}, \gamma)^4\text{He}$ reaction.
- The gamma radiation from the reactor is too small for the reactions that should be occurring.
- The ratio of excess energy to ^4He production is smaller than it should be.
- There are no neutrons coming out of the apparatus.

This paper will address those criticisms and show that these are incorrect misconceptions. These misconceptions are due to the fact that the secondary reactions inside the low energy nuclear reactor are not being taken into consideration by the naïve calculations.

The primary reactions occurring in the LENR are the two reactions of $^2\text{D}(^2\text{D}, n)^3\text{He}$ and $^2\text{D}(^2\text{D}, p)^3\text{H}$; each of these reactions occurring with a 50% relative ratio. These primary reactions occur within the palladium material of the LENR cell. While these primary reactions are important, the secondary reactions also play a critical role.

The most significant secondary reaction is that of ^6Li within the electrolyte solution interacting with the neutrons. For the $^6\text{Li}(n, ^3\text{H})^4\text{He}$ reaction, the thermal nuclear cross section of ^6Li is 942 barns [1, 2], an extremely large cross section. In this reaction, the ^6Li does not absorb the neutron, but rather uses the neutron to transform itself into an alpha and a tritium. The percentage of ^6Li in natural abundance is 7.59%, a relatively large abundance; which means this secondary reaction will be highly probable in a LENR with an electrolyte solution of lithium.

A calculation of the energy and the child products is made for a typical LENR. It is shown that the secondary reaction is not only very probable, but essentially eliminates all of the neutrons created in the primary reaction. Also, the resulting energy is much less than the predicted energy of the extremely improbable $^2\text{D}(^2\text{D}, \gamma)^4\text{He}$ reaction.

This calculation is made for the reactions involving of two pairs of ^2D ions--where the initial parent nuclides are four ^2D ions. Two of these ^2D ions will form $^3\text{H} + p$, and the other two ^2D ions will form $^3\text{He} + n$. Because of the extremely large thermal nuclear cross section in the secondary reaction, all of these newly-created neutrons will combine with the ^6Li in the electrolyte solution to form $^3\text{H} + ^4\text{He}$. In summary, in the total reaction involving both primary and secondary reactions, the parent nucleons are four ^2D ions, plus one ^6Li ion. The child products are $^3\text{H} + ^3\text{H} + ^3\text{He} + ^4\text{He} + p$. For every four ions of ^2D and one ^6Li ion, the net total energy output is much less energy than the improbable $^2\text{D}(^2\text{D}, \gamma)^4\text{He}$ reaction, with no neutrons and very little if any gamma radiation.

Thus by considering the secondary reactions taking place inside an LENR electrolyte cell, four of the more significant criticisms of the conventional nuclear physicists against LENR are easily answered. Due to the inclusion of the ^6Li nuclide in the total reaction, the released total energy is less. The probability of the reaction for the creation of ^4He is much higher than the $^2\text{D}(^2\text{D}, \gamma)^4\text{He}$ reaction. Furthermore in the reaction that includes ^6Li , there is very little, if any, gamma radiation created. The ratio of excess energy to ^4He production is much smaller than would be predicted by a naïve calculation, and there are essentially no neutrons escaping the apparatus.

[1] N. E. Holden, *Review of Thermal Neutron Cross Sections and Isotopic Composition of the Elements*, BNL-NCS-42224 (March 1989).

[2] Edgardo Browne, Janis Dairiki, and Raymond Doebler, editors Lederer and Virginia Shirley. *Table of Isotopes*, 7th edition, 1978, John Wiley and Sons.

[3] National Nuclear Data Center, information extracted from the NuDat 2 database, <http://www.nndc.bnl.gov/nudat2/>

Iwamura: Excess Energy Generation using a Nano-sized Multilayer Metal Composite and Hydrogen Gas

Yasuhiro Iwamura¹, Takehiko Itoh^{1,2}, Shoichi Murakami², Mari Saito² and Jirohta Kasagi¹

¹Research Center for Electron Photon Science, Tohoku University, Sendai, 982-0826 Japan

²CLEAN PLANET Inc., Tokyo, 105-0022 Japan

E-mail: iwamura@ins.tohoku.ac.jp

New excess heat experiments using a nano-sized metal multilayer composite and hydrogen gas have been performed. The multilayer thin film, fabricated by Ar ion beam sputtering method, was used as the nano-sized metal composite.

The experimental set-up is shown in Fig.1. Two nano-sized metal multilayer composite samples were placed in the chamber. After baking of the samples, H₂ gas was introduced into the chamber up to about 230 Pa at 250°C. Then, the Ni based multilayer thin films started to absorb H₂ gas. Amount of absorbed H₂ gas can be evaluated by the pressure measurement of the chamber. Typically, after about 50,000 sec, H₂ gas was evacuated and simultaneously the samples were heated up by the ceramic heater up to 500~900°C as shown in Fig. 1(b). These process triggers heat generation reactions. Anomalous heat generation was induced by heating up the metal multilayer thin film that absorbed hydrogen gas before heating.

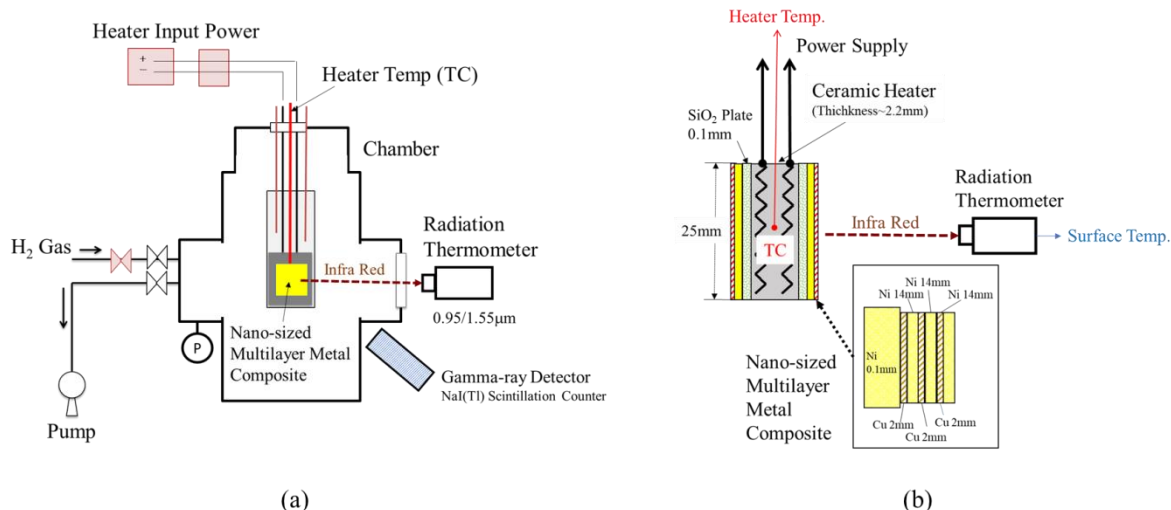


Fig.1 Experimental Set-up; (a) Schematic of experimental apparatus, (b) Detail drawing around Nano-sized Multilayer Metal Composite

Heat burst phenomena were simultaneously detected by a radiation thermometer looking at the surface of the multilayer thin film and a thermocouple located near the thin film. It shows that heat measurement by the thermocouple embedded in the ceramic heater correctly reflects surface temperature detected by the radiation thermometer.

Maximum released excess energy reached 1.1MJ and average released energy per absorbed total hydrogen was 16 keV/H or 1.5 GJ/H-mol. It cannot be explained by any known chemical process and suggests that the observed heat generation must be of nuclear origin.

Acknowledgement

This work was supported by CLEAN PLANET Inc., Research Center for Electron Photon Science of Tohoku University Electron Photon, Tanaka Kikinzoku Memorial Foundation and Thermal & Electric Energy Technology Foundation (TEET). We also acknowledge Mr. H. Yoshino and Mr. S. Hirano who are the members of CLEAN PLANET Inc., for their significant assistance.

Hatt: Cold Nuclear Transmutations Light Atomic Nuclei Binding Energy **Oral and Poster**

Philippe Hatt, independent researcher

Email: pcf.hatt@gmail.com

Several authors predict that α particle structures could be present in atomic nuclei. Convincing arguments of such structures are provided by systematics of the binding energies of the even-even nuclei with equal number of protons and neutrons. In that hypothesis, it is necessary to consider the binding energy of α particle as well as the binding energy between several α particles in order to determine the binding energy of a given nucleus.

The kind of binding energy existing within each α particle is a first point to consider. How to relate that binding energy to the deuterium binding energy, as well as to the tritium and He3 ones as these exist before the α particle is constituted? Also, could these structures be found within the nucleus as substructures linking the nucleons of one α particle with the nucleons of another α particle?

It will be shown that the hypothesis of α structures in the n- α nuclei can indeed describe the binding energy systematics for all nuclei. In such an approach the system in its ground state behaves like a crystal, with stationary configuration and shape and with defined bond values between the various α particles and the other substructures within a nucleus.

The hypothesis I develop finds its background in the structure of neutron/proton as well as α particle I propose in my document posted on the internet one finds under www.philippehatt.com According to that hypothesis the nuclei of the various elements are constituted out of α particles and other nucleons grouped in order to form sub nuclei bound together by four types of bonds called NN, NP, NNP, NPP.

The kinship which will be demonstrated between the binding energy distribution within the various nuclei or within isotopes of the same element is very important for LENR purposes, first because the difference between binding energies of the elements at the beginning and at the end of the LENR process determines the energy released, and second and more important because one can follow the shift between these binding energy distributions during the LENR process.

My purpose is not about looking for a new model of atomic structures. It is the reason I have favored a unidimensional approach trying to breakdown the binding energy value of each element and its isotopes in several clusters indicated above. As these clusters are 3 D structures the global structures are also 3 D, my binding energy approach looking only at unidimensional energy values expressed in MeV. Indeed, NP is the binding energy of Deuterium, NNP that one of Tritium and NPP that one of He3.

The element given as example is iron. The modifications in the binding energy distribution between each isotope of that element will be illustrated, from Fe 52 to Fe 61.

Tarassenko G.V., Demicheva E.A.

Caspian state university of technologies and engineering named after Sh. Yessenov, Kazakhstan
tarasenko-genadi@mail.ru

Planet Earth's core was the location for early thermonuclear synthesis which generated heat in the planet. New geological and-geophysical data show the possibility of rotation of geospheres from the core (or kernel) to the Earth's surface. It is suggested that rotation of the iron kernel of the planet is physically impossible, and instead assume that the kernel consists of plasma, like the gas-and-dust clouds from which planets are formed. This model of planet formation is now accepted. This 'plasma fireball' according to some sources rotates at a speed of 100,000 km/s. The dynamo effect of this plasma gives rotation to the planet. Friction of geo-spheres creates static stress which accumulates in the terrestrial electro-condenser with a capacity of 1 Farad. A result of this charge accumulation between subsoil and the planetary surface can be electric discharges, which in turn create channels filled with heated gas, perhaps, formed and filled with high velocity plasma, which escapes in the form of volcanoes, earthquakes, even a tsunami.

Based on laboratory and field researches of electromagnetic emission of minerals and rocks, V.N. Salnikov puts forward the hypothesis of electromagnetic unloading of the lithosphere in the form of electromagnetic systems representing a closed electric and magnetic field (field quasi crystals). At the exit to the surface of such quasicrystals, pits, tubes, diatremes or forest falls are formed (Tungus and Petrozavodsk phenomena). It is the trap of charged particles that determines the dipole of the earth's geosphere, and not some exotic permanent magnet in the center of the Earth, the shape and size of which has not yet been invented. It is the quasi crystalline ordering of the interior of the Earth that determines the need for the existence in the center of the Earth of the so-called "black hole", the space of which is not inherent in the inextricable continuity of real space. Figuratively speaking, a black hole is a "torricellian void" in the void of real space. The shape of the black hole in the crystal structure of the void is a concave hexahedron, resting its vertices on the centers of the faces of the octahedral structural composition of the real space. It is into this black hole that charged elementary particles rush, forming telluric closed shifts of the electric field along each face of the quasi crystalline structural compositions of the Earth. The hypothesis of plasma chemical origin of oil and natural combustible gases was also proposed.

The scientific community's adaptation to new knowledge is never easy. The current paradigm of physics does not support effects such as cold nuclear fusion. The situation is complicated by the fact that the ambitious and expensive attempts to find a solution to the problems of controlled thermonuclear fusion, which have lasted for more than half a century, have gone too far for a quiet termination. The most famous attempt for thermonuclear fusion is an Inter-national Project ITER. Currently, the Project is huge and extremely expensive. Realists have estimated that construction of the ITER reactor and the possibility of its launch will be completed no earlier than 35–50 years. The ITER project is seen as a purely scientific investigation, and if it can work, then it would only be in a cyclic mode. After its launch, there are plans to build an even more enormous structure - an industrial tokamak DEMO. In this case, the huge financial and material costs will continue for another half century. Global fuel and the oil and gas industry welcome this development.

Narita: Investigating Thermal Behavior of Pd Foil Coated with Metal Membrane in Deuterium Diffusion Poster

#S. Narita, M. Endo, S. Kikuchi, K. Negishi, K. Ota
Iwate University, Morioka, Japan
E-mail: narita@iwate-u.ac.jp

It has been reported that anomalous excess heat generation have been observed when charging deuterium into nano-composite Pd-Ni supported by ZrO_2 [1,2]. It is supposed to be difficult to explain the phenomena by known chemical processes, which could potentially be attributed to specific characteristics of deuterium diffusion in the metal complex, as well as the nano-sized fine structure of the sample. Yamaguchi et al. observed excess heat and helium production in controlled deuterium diffusion from multi-layered Au/Pd/SiO₂ fabricated by depositing Au and SiO₂ membranes onto a Pd foil surface [3]. Considering the experimental result, we performed a deuterium desorption experiment using a multi-layered Pd-Ni complex sample and investigated thermal as well as deuterium diffusion behavior. We also examined a multi-layered sample with a fine-structured surface and investigated the deuterium diffusion in dependence of the surface condition.

The samples were prepared using the following procedure. Pd foil (10 mm x 10 mm x 0.1 mm, 99.95 % pure) was annealed at 900 °C for 10 h. After annealing, the surface contaminants were removed using aqua regia. Then, a Ni membrane was deposited onto the sample surface using Ar ion beam sputtering. The thickness of the membrane was ~ 100 nm. Here, we prepared samples with a fine structure at the interface of the binary metal. The fine structure was obtained by Ar ion beam etching. Then, the samples were exposed to deuterium gas for 24 h at 5 atm. The sample weight was measured before and after loading, and the loading ratio was calculated from the weight difference. The loading ratios were typically 0.65–0.70. After loading, the sample was placed into a chamber evacuated by a Turbo-Molecular-Pump ($\sim 10^{-4}$ Pa). In the chamber, the sample was heated by supplying direct electric current to stimulate the deuterium diffusion. The sample temperature and chamber pressure were continuously monitored for ~24 h and measured with a thermo-couple and an ionization gauge, respectively. The current and the bias applied to the sample were also recorded during the experiment.

Short-period temperature fluctuation was often observed, lasting for 2-4 h at the beginning of the desorption phase for the Pd-Ni sample with fine structure at the interface. It is possible that deuterium diffusion from Pd to the membrane and from the membrane to Pd occurred frequently in the period, and that endothermic and exothermic phenomena associated with the heat of solution repeatedly occurred owing to deuterium transport between the two metals. We also tested other samples of Pd coated with a metal membrane, such as Pd-Ni, Pd-Ag, and Pd-Ti. Similar temperature behavior was observed for the Pd-Zr sample. Additionally, an instantaneous large heat evolution was occasionally found in the desorption period for Pd-Zr. Although a quantitative analysis for the heat balance in the temperature behaviors is underway, these distinctive thermal and deuterium diffusion properties for the surface coated binary metal might be related to the anomalous excess heat observed in the experiment with nano-composite Pd-Ni-ZrO₂.

References

- [1] A. Kitamura et al. "Collaborative Examination on Anomalous Heat Effect Using Nickel-based Binary Nanocomposites Supported by Zirconia" J. Condensed Matter Nucl. Sci, 24, pp. 202-213, 2017.
- [2] Y. Iwamura et al. "Replication Experiments at Tohoku University on Anomalous Heat Generation Using Nickel-based Binary Nanocomposites and Hydrogen Isotope" J. Condensed Matter Nucl. Sci, 24, pp.191-201, 2017.
- [3] E. Yamaguchi, H. Sugiura, "Excess Heat and Nuclear Products from Pd:D/Au Heterostructures by the 'In vacuo' Method" Proc. of 7th International Conference of Cold Fusion, pp. 420-424, 1998.

Jacques Ruer
SFSNMC
Jsr.ruer@orange.fr

Air flow calorimetry appears as a relatively simple method to measure the amount of heat released by a LENR reactor. This technology can be applied to large units and is well suited when the LENR device surface temperature is high. It is cheaper to build than calorimeters using water-cooled elements.

Basically, the calorimeter is designed in order to make sure that all the heat produced by the device under test is transferred to a known mass flow of air. According to the first principle of thermodynamics the rise of temperature of the air flow between the inlet and the outlet of the calorimeter makes it possible to calculate the heat input.

Although the basic principle is simple, the accuracy of the method is influenced by many factors. This paper proposes an overview of the main parameters involved in air flow calorimetry and the possible problems that may affect the accuracy during the testing of LENR devices.

The flow rate of air must be precisely known. Several measurement methods are reviewed and discussed. The heat capacity of a given volume of air depends on its density, hence on the air pressure and temperature, and marginally on its vapor content.

How the heat is transferred from the hot device to the air is detailed. Conduction, radiation and convection must be taken into account. Air is almost transparent to infrared and heat transfer mainly occurs by conduction and convection. Any heat that is not carried away by the air flow is not measured directly. A good thermal insulation of the calorimeter enclosure is required to minimize the heat losses as well as its tightness. The energy input of the air blower must be accounted. External conditions like room ventilation or direct sunlight can also have an influence. Other features of the calorimeter may have some impact on the accuracy. For example, if the air inlet and air outlet are installed at different locations on the calorimeter enclosure the temperature distribution inside the air box is affected and heat losses are modified.

Any fluctuation of the inlet temperature results in an error of the heat flow measurement. The heat storage capacity of the whole system introduces a time lag on the readings.

For a given heat power there is an optimum combination of flow rate and temperature rise in order to maximize the accuracy.

It is absolutely necessary to quantify the heat lost by the system in order to correct the measurements. Fortunately, it is in general possible to calibrate the calorimeter, provided some precautions are observed for the calibration process.

The theoretical accuracy of air flow calorimetry is discussed based on the fractions of heat carried away by the air flow and heat losses and the precision of the instrumentation.

Albertini: ^{228}Th , ^{63}Ni , ^{57}Co : three anomalous decays suggesting the feasibility of radionuclide neutralization

Gianni Albertini

Università Politecnica delle Marche (UNIVPM), Via Brecce Bianche, 60131 Ancona, Italy

Radioactive waste is a major problem nowadays. The deactivation usually consists in incorporating the waste into a large volume of material, thus decreasing the activity per unit volume or unit mass. This way, larger and larger deposits are required and the possibility of accidental release, mainly due to corrosion, increases with time. The neutralization, which consists in decreasing the mean-life of the radioactive elements by Deformed Space Time reactions, is considered not feasible.

We shall present and discuss three cases, reported in literature, which suggest the feasibility of radionuclide neutralization. In all these cases an anomalous decay of a radioactive material was observed after ultrasound irradiation.

HuangC: Temperature Dependence of Maximum Excess Power in 3 New Experiments (Letts, Parkhomov, & Mizuno)

S.X. Zheng*, G.S. Huang, Z.M. Dong, C.L. Liang, B. Liu, S. Chen, J. Tian, X.Z. Li
 *Dept. of Engineering Physics & Dept. of Physics, Tsinghua University, Beijing CHINA

At ICCF-21, the resonant surface capture model was proposed to relate the inelastic process (Excess heat) to the elastic process (Diffusion); then, we are able to derive the straight line behavior in the semi-logarithmic plot. Three sets of experimental data supported this model as Fig.1 (Ed. Storms, M. Fleischman, and Tsinghua Univ.). After ICCF-21, three new sets of data are available (Letts, Parkhomov, and Mizuno) to test this model (Fig. 2, 3, & 4). The agreement is very well, but only the maximum excess power for each temperature follows this straight line behavior. It implies a hidden variable which controls the excess power at each given temperature. Only if this hidden variable matches the optimum value; then, the system might reach its Optimum Operation Point as named by M. Swartz.

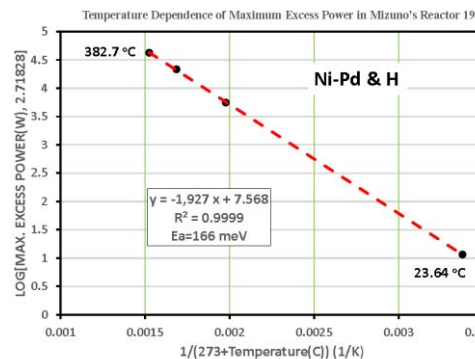
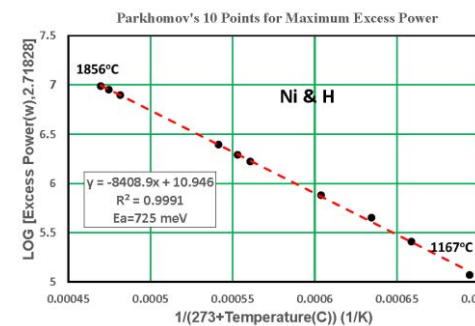
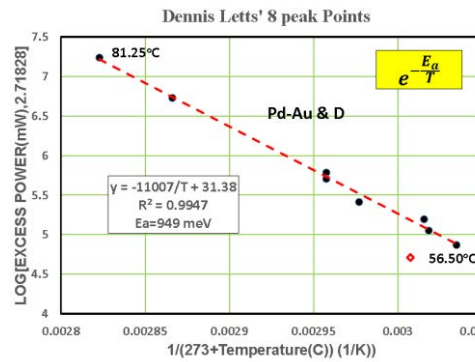
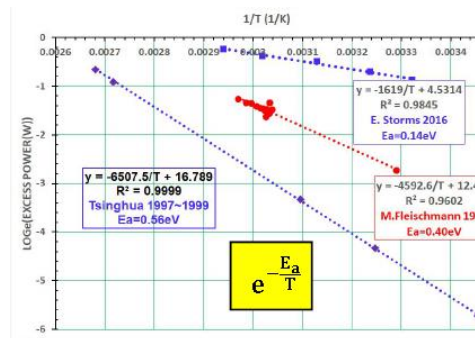
(1)**Dennis Letts'** Pd cathode heavy water tunable laser was used to trig the excess heat in gold coating. Only if the thickness of the gold coating peak of excess power appeared as a function of laser Among 9 peaks, 8 peak points (black) are on the from 56.5 °C to 81.25 °C.

(2)**Parkhomov's** Ni-H gas-loading system. Only temperature was higher than 1000°C, excess power measurable. For each given temperature the excess it maximum in the early period of operation. After fuel was exhausted, and no excess power was points are on the straight line from 1167 °C to 1856°C.

(3)**Mizuno's** Ni-Pd gas-loading system (R-19 During 92 days operation with H₂ gas, among 55 data maximum power were found on this straight line from 382.7°C.

This resonant surface capture model is based on energy model (the weak interaction) and Nuclear stripping reaction model (the strong therefore, there is no strong neutron or gamma accompanied with excess heat, and it may work for materials to explain Miley, Iwamura, Biberian and B. transmutation data as well.

Many thanks to Drs. Letts, Parkhomov, and their kindness to make their data available in advance.



electrolysis. A parallel with a was right, a frequency. straight line

if the power was reached 225 days, the measurable. 10

reactor). points only 4 23.64 °C to

Bethe's solar Oppenheimer's interaction); radiation high Z Liu's nuclear

Mizuno for

Varaprasad: Experiments to observe Excess Heat in Ni-LAH, Ni-H₂, D₂ systems **Poster**



Pd-

Prahlada Ramarao, Shree Varaprasad N S, Shashank G Dath,
Mohankumara P B and Ankith Y A
Centre for Energy Research (CER),
Swami Vivekananda Anusandhana Samsthana(S-VYASA),
Bangalore, India,
prahlada.ramarao@gmail.com

The efforts to generate excess heat by triggering LENR by various combinations of nano Ni and Pd with D₂/H₂ gas continued since ICCF-21. This is not only towards replicating the experiments of Parkhomov and Stephanov, but through independent combinations derived by the CER Team. But the outcome was not supportive of the results obtained earlier. This made the group to try different approaches with continuous improvements in the reactor design, fuel preparation and instrumentation.

The research team tried following fuel compositions – Ni + TiH₂, Ni + Pd + D₂, Ni + Pd + LAH, Ni + Li + LAH + ZrO₂, Ni + LAH + ZrO₂, Ni + LAH + TiO₂, Pd + D₂ + H₂, Pd + D₂, Ni + H₂ etc. Different particle sizes of Ni and Pd nano powders were used. Though some of the experiments showed some intriguing results, the same were not observed, while repeating. In this paper, we are going to discuss the procedures followed to clean and activate the fuel for the generation of excess heat and also different designs of the ceramic/SS reactors. Some of the designs had provision for having either D₂ or H₂ gas under pressure.

With the experience in conducting more than 120 experiments with different designs, processes, protocols and materials, this team also believes that the experiments on generation of excess heat is to be continued [5].

Acknowledgement: The research team thank “Science & Engineering Research Board”, Govt. of India for the financial support under ‘High Risk High reward’ scheme.

[1] Parkhomov AG, "A Study of the High-Temperature Heat Source Analog of Rossi", Journal of Emerging Areas of Science, vol. 3, No. 7, pp. 68–72, 2015

[2] I.N. Stephanov, Yu. I. Malahov, Chi Nguyen Quoc “Experimental Measurement of Excess Thermal Energy Released from a Cell Loaded with a Mixture of Nickel Powder and Lithium Aluminum Hydride,” Journal of Emerging Areas of Science, vol. 3, no. 9, 2015.

[3] Focardi, S., Habel, R. and Piantelli, F., Anomalous heat production in Ni–H systems. Il Nuovo Cimento, vol. 107A, pp.163–167, 1994.

[4] T. Itoh, Y. Iwamura, J. Kasagi, “Anomalous Excess Heat Generated by the Interaction Between nanostructured Pd/Ni Surface and D₂ Gas” Journal of Condensed Matter Nuclear Science, vol. 24, pp. 179-190, 2017.

[5] C. P. Berlinguette, Yet-M. Chiang, J. N. Munday, T. Schenkel, D. K. Fork, R. Koningstein and M.D. Trevithick, Revisiting the Cold Case of Cold Fusion, Nature, vol. 570, pp45–51, 2019.

Kaal: Nuclear Transmutation and Mass Defect explained with the Structured Atom Model (SAM) Oral & Poster

J.E Kaal (Edo) , James A. Sorensen, Jan G. Emming
<https://etherealmatters.org/sam>

The Structured Atom Model (SAM) has been under development since 2016. In this period, we have identified the geometric configurations of all elements of the PTE, including multiple isotopes of elements. As the model becomes more sophisticated, we continue to discover new features and are starting to appreciate its ability to predict key properties of the elements, such as whether its geometry represents a metal, a halogen or a noble gas, and whether it is stable, or decays radioactively, what the spin value is etc. Furthermore, identifying the geometry allows us to plausibly explain certain effects that cannot easily be explained using current concepts and mathematical approaches contained in the existing models of the nucleus. In the field of Low Energy Nuclear Reactions (LENR), we believe that at least some of the experimental findings can be understood based on the visualizations created by this model.

The paper makes a comparison between Norman Cook's FCC (Face-Centered Cube) model and the Structured Atom Model for several nuclei, showing how the structure between the two differs, which can be characterized as the difference between a crystal and a tree with several branches, particularly at the higher Z-numbers. Cook [1] has shown how the FCC model enables calculation of the binding energies of all stable/near-stable isotopes based on knowing the Cartesian coordinates of every nucleon in the nucleus. The Structured Atom Model also assigns precise coordinates to every nucleon in the nucleus and thus the same rationale for being able to calculate precise binding energies, applies to SAM. Binding energies for SAM are currently based on the number of "lines" between nucleons, which already provides new insight in the gross properties of the nuclei.

The current paper addresses the persistent problem of predicting the distribution of the various fission products released in nuclear fission. Existing standard models such as the Liquid Drop Model and the Shell Model, predict a virtual symmetrical split of U235 for example. SAM on the other hand, predicts an asymmetrical split of the fission products in accordance with observations, for reasons that are discussed in some detail. Another example of the utility of SAM is the explanation of the fission/transmutation of palladium and nickel, as observed by researchers such as the SAFIRE team, Mizuno [2] and Iwamura [3].

Binding Energy has been calculated with the SAM model for most elements and the comparison with known values is summarized in a chart. We find a divergence from the known mass-defect curve above iron, which we attribute to energy inherent in the progressive distortion of the structure as more nucleons are added, to the point that the nuclei become unstable. This store of energy, apparently invisible to the standard models, appears to be associated with the amount of energy potentially available in a fission reaction.

On the 150th anniversary of the Periodic Table, we are submitting two companion papers as poster papers:

- 1) A new Rendition of the Periodic Table that shows the corresponding structure for each element
- 2) SAM in a nutshell - Basic concepts, Nuclear Reactions and nuclear Binding Energy

References

- [1] The "Renaissance" in Nuclear Physics: Low-energy nuclear reactions and transmutations [presented](#) at ICCF-21, 2018.
- [2] Tadahiko Mizuno, Nuclear Transmutation: The Reality of Cold Fusion, Infinite Energy Press, translated by Jed Rothwell, 1998. Kindle edition, loc. 1455 of 2726.
- [3] Iwamura Transmutations Summary – in Steven B. Krivit, Hacking the Atom: Explorations in Nuclear Research, Vol. 1 (1990-2015) Kindle edition, loc.3120 of 8055.

Wytenbach: SO(4) Physics and LENR poster

Dr. J. A. Wytenbach
Independent researcher

juerg@datamart.ch; <https://www.researchgate.net/project/Nuclear-and-particle-physics-20>

There is no longer any doubt that $SO(4) = SU(2) \times SU(2)$ is the best suited mathematical space to describe dense condensed matter. The all (10) digits exact Hydrogen model given in version 2.1.5 of NPP2.0 was the first final illuminating proof and the “simple” derivation of the gravitation constant in version 2.1.7 was the ultimate revelatory highlight. No other model is able consistently unify all four forces.

The new understanding of mass being effectively all EM mass has lead to a deeper understanding of particle structures. Roughly all mass components of particles can be divided into 2,3,4(5) rotation equivalent EM mass. For dense mass the $(2 \times 2) \times (2 \times 2)$ 4 rotation mass builds the core of roughly 99% of the total mass. 1FC, 2FC, 3FC are the relative force constants for adding more rotations to a relativistic mass.

Core to the model is the proton mass structure given by 4,3,2 rotation components.

$$(1) M_p = \mu_p^2 * 4 * \pi * 100000 / (\alpha * \pi * r_{pr}^3 * e * (3FC * 2FC * 1FC)^3 * (1 - (\alpha / (\pi * 16))))^2$$

$(1 - (\alpha / (\pi * 16)))^2$ is the so called 4D potential factor of the proton.

From the above formula the so called relativistic proton radius r_{pr} can be calculated from the measured proton mass and magnetic moment as being 0.837653007352fm. At this radius we can give an exact mass equivalence formula for the proton/electron pair.

The proton relativistic mass M_{pr} in eV is the same formula without the 2 perturbative masses.

$$(2) M_{pr} = \mu_p^2 * 4 * \pi * 100000 / (\alpha * \pi * r_{pr}^3 * e) = 926'603'083.3eV$$

$$(3) \text{Perturbative proton 3D/4D mass } m_{pp34} = (1 / (3FC * 2FC * 1FC)^3 - 1) * M_{pr} = 11'396'588.8eV$$

$$(4) \text{Proton 4D/1D potential mass } m_{ppo} = M_p * (1 - (1 - (\alpha / (\pi * 16))))^2 = 272'409.8eV$$

$$(5) \text{Proton total perturbative mass } m_{pp} = 11'668'998eV$$

$$(6) \text{electron mass (CODATA) } m_e = 510'998.9eV$$

$$(7) \text{Perturbative electron mass } m_{ep} = 1183.1eV = m_e * (1 - 1/e_g^2)$$

$$(8) \text{relativistic free electron mass } m_{er} = 509'815.8eV = m_e - m_{ep}$$

$$(9) \text{relativistic bound electron(charge) mass } m_{erb} = 508'632.7eV = m_{er} - m_{ep}$$

A typical LENR D-D (deuterium) fusion event releases in total 23'846'533eV. This is equivalent to 2 times the proton perturbative mass (23'337'993.5eV) plus a relativistic bound electron mass m_{erb} . The tiny difference can also be explained by SO(4) physics. This mass disposal must happen because in fusion the relativistic core masses do join and flux that did stay in the 2 joined dimensions can no longer hold perturbative mass. The same explanation holds for charge conservation as the SO(4) physics model shows that q^2 is proportional to mass*radius. Because the radius doubles ($p \rightarrow {}^4\text{He}$) only half of the charge generating perturbative mass is needed. The additional release of the m_{erb} mass is a consequence of charge (mass) migration between the two neutrons of the fusing D-D pair. In a neutron the 2 symmetric charge bound masses are bound to a 2 rotation orbit where as in dense mass it is a 3 rotation orbit and thus only 3 out of 4 charge equivalent masses are needed for the force balance.

The first step in a Hydrogen fusion reaction is the forming of e.g. H^*-H^*/D^*-D^* pairs (Hydrino, dense Hydrogen ..) as shown by Mills/Holmlid. This process can be explained by the weak force equivalent constant 1FC that forces the two joining perturbative proton masses on one more rotation orbit. The charge corrected calculated net potential of 495.8eV is in perfect agreement with 496eV measured by R.Mills in the H^*-H^* case.

Further we will show a model how the D-D fusion energy is thermalized.

Bowen: An Examination of the Updated Empirical Data in Support of the Shell Model

N. L. Bowen

Colorado Mountain College, Glenwood Springs, Colorado, USA
nbowen@coloradomtn.edu

This paper is a re-examination of the experimental data, as is currently known in 2019, in support of the Shell Model and its concepts. The Shell Model of the nuclear force was proposed in 1955, and it has since been accepted as the fundamental quantum model of the nuclear force, especially with regards to the modelling and simulation of nuclear behavior. [1,2] The Shell Model was based on the experimentally-known data at that time, supporting the concept of nuclear shells--a concept similar to the quantum atomic shells formed by electrons. Most textbooks, even the current ones, present this outdated experimental data from the 1950's when discussing the validity of the Shell Model. [3] Much nuclear data has been collected over the past 60 years, and a re-examination of the experimental data in support of the Shell Model is overdue.

Using the latest and most updated databases for nuclear data, the diagrams, graphs, and other empirical evidence in support of the Shell Model are re-constructed. [4, 5] These updates include the supporting data for nuclear binding energy, the number of stable isotopes, separation energies, quadrupole moments, and other empirical indications of nuclear shells.

There are some unanticipated results, suggesting that certain magic numbers may not be as cogent as previously assumed. The paper concludes with a discussion of what changes the newer data imply with regards to the empirical evidence and substantiation of the Shell Model.

Vysotskii: Anomalous LENR effects and its justification based on the method of coherent correlated states

Vladimir Vysotskii , Mykhaylo Vysotskyy
Kiev National Shevchenko University, Ukraine; e-mail: vivysotskii@gmail.com

A number of successful LENR experiments in a few last years and their qualified independent analysis (e.g., Lugano expertise 2014) confirm a high efficiency of low-energy reactions without any exotic optimization methods and simultaneously indicate the necessity of the development of their adequate theoretical model.

This model should justify the efficiency of these reactions and explain a number of anomalies observed in such reactions: a) very large probability at low energies of particles; b) complete absence of radioactive isotopes in reaction products; c) very strong suppression of gamma radiation, which should inevitably accompany these reactions according to the standard concepts and practice of high-energy nuclear physics.

Numerous independent attempts to develop highly specialized variants of the theory of such processes each applicable only to a particular experiment, a particular pair of interacting nuclei, and a particular type of an active material medium (gas, plasma, liquid, amorphous, or crystal medium) were focused only on the search for a mechanism responsible for their high probability and did not concern the other LENR anomalies.

We believe that all these processes should occur through a common universal mechanism, which makes it possible not only to describe all detected anomalies in the studied reactions at low energies, but also to predict the properties of similar reactions involving other nuclei in other media under other experimental conditions.

In [1–12], it was shown that low energies of interacting particles could be combined with a high probability of the tunnel effect (and, as a result, with a high total probability of corresponding nuclear reactions) owing to the use of coherent correlated states of these particles. Such states are formed through the self-similar establishment of optimal phase relations between different eigenfunctions of the superposition state of a particle through monotonic unidirectional [1-5], periodic [4–12] or instantaneous [9,10] change in the parameters of a weak external force field determining the superposition state of this particle. A typical example of such an action is the modulation of the parameters of a harmonic oscillator acting on the particle under consideration. Such an oscillator can be formed, e.g., in nonstationary microcracks in metal hydrides [4-6], when a charged particle is subjected to a natural or laboratory pulsed magnetic field [10], the corresponding crystal matrix containing interacting nuclei is irradiated by weak terahertz radiation [5-9], and slow protons move through the crystal matrix or in the field of free molecules [11]. These states are most clearly characterized by the Robertson–Schrodinger uncertainty relations for coordinate and momentum as well as for energy and time

$$\delta q \delta p \geq \hbar^* / 2, \quad \hbar^* = \hbar / \sqrt{1 - r_{pq}^2} \equiv G_{pq} \hbar, \quad r_{pq} = \{ \langle qp + pq \rangle / 2 - \langle q \rangle \langle p \rangle \} / \sqrt{\langle q^2 \rangle \langle p^2 \rangle}$$

$$\delta E \delta t \geq \hbar^* / 2, \quad \hbar^* = \hbar / \sqrt{1 - r_{Et}^2} \equiv G_{Et} \hbar, \quad r_{Et} = \{ \langle Et + tE \rangle / 2 - \langle E \rangle \langle t \rangle \} / \sqrt{\langle E^2 \rangle \langle t^2 \rangle}$$

taking into account the corresponding correlation coefficients ($|r_{pq}|, |r_{Et}| \leq 1$) and coefficients of correlation efficiency $0 \leq G_{pq}, G_{Et} < \infty$. In the above physical systems under real experiment conditions, these coefficients reach values $G_{pq}, G_{Et} \geq 10^4$, which ensures the existence of very large energy fluctuations $\delta E \geq 30 \dots 100 \text{ keV}$ at low ambient temperature and anomalous long duration of existence of such fluctuations.

In the report it is shown that the correct interpretation of these relations combined with detail analysis of the time and energy characteristics of any LENR involving the tunnel effect allows the unified quantitative explanation of both a high probability of such reactions at low energies and a fundamental difference (including the exclusion of the formation of daughter radioactive isotopes and the suppression of accompanying gamma radiation) in nuclear reactions involving charged particles at low average energies of interacting particles [13].

1. V. I. Vysotskii, S. V. Adamenko, Tech. Phys. **55**, 613 (2010).
2. V. I. Vysotskii, M. V. Vysotskyy, S. V. Adamenko, J. Exp. Theor. Phys. **114**, 243 (2012).
3. V. I. Vysotskii, S. V. Adamenko, M. V. Vysotskyy, J. Exp. Theor. Phys. **115**, 551 (2012).
4. V. I. Vysotskii, M. V. Vysotskyy, Eur. Phys. J. A **49**, 99 (2013).
5. V. I. Vysotskii, S. V. Adamenko, M. V. Vysotskyy, Ann. Nucl. Energy **62**, 618 (2013).
6. V. I. Vysotskii, M. V. Vysotskyy, J. Exp. Theor. Phys. **118**, 534 (2014).
7. V. I. Vysotskii, M. V. Vysotskyy, J. Exp. Theor. Phys. **121**, 559 (2015).
8. V. I. Vysotskii, M. V. Vysotskyy, Curr. Sci. **108**, 524 (2015).
9. V. I. Vysotskii, M. V. Vysotskyy, J. Exp. Theor. Phys. **120**, 246 (2015).
10. V. I. Vysotskii, M. V. Vysotskyy, J. Exp. Theor. Phys. **125**, 195 (2017).
11. V. I. Vysotskii, M. V. Vysotskyy, S. Bartalucci, J. Exp. Theor. Phys. **127**, 479 (2018).
12. S. Bartalucci, V. I. Vysotskii, M. V. Vysotskyy, Physical Review AB, **22**, # 5, 054503 (2019).
13. V. I. Vysotskii, M. V. Vysotskyy, J. Exp. Theor. Phys. **128**, 856 (2019).

Vladimir Vysotskii , Mykhaylo Vysotskyy
Kiev National Shevchenko University, Ukraine; e-mail: vivysotskii@gmail.com

The “traditional” method of the analysis of the processes of interaction of slow moving particles (including LENR) is based on their description in the form of unbounded in space plane waves. A more correct analysis of such processes can be made in the case of describing particles in the form of bounded (Gaussian) normalized wave packets with the full wave function $\Psi(x,t)$, initial structure $|\Psi(x,0)|^2$ and initial spatial width $\Delta x_{t=0} = u$:

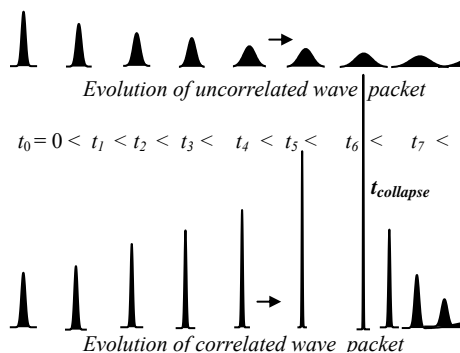
$$\Psi_{uncorr}(x,t) = \left\{ \left(u + \frac{i\hbar}{mu} \right) \sqrt{\pi} \right\}^{-1/2} \exp \left\{ \frac{-(x-v_0t)^2}{2u^2(1+t^2\hbar^2/m^2u^4)} \right\}, \quad |\Psi_{uncorr}(x,0)|^2 = \left\{ \pi u^2 \right\}^{-1/2} e^{-x^2/u^2}.$$

Such packets have constant velocity v_0 , momentum $p = mv_0$ and energy $T = mv_0^2 / 2$. During their space-time evolution synchronous decrease of amplitude and widening of the spatial width $\Delta x \approx \sqrt{u^2 + (i\hbar / mu)^2}$ occur (see Fig., upper row). These packets correspond to uncorrelated states of particles.

For LENR experiments more efficient are coherent correlated packets with initial and full wave functions:

$$\Psi_{corr}(x,0) = (\pi u^2)^{-1/4} \exp \left\{ -x^2 g / 2u^2 + ip_0 x / \hbar \right\}; \quad g = 1 + i\rho;$$

$$\Psi_{corr}(x,t) = \left[\left(u + i\hbar g / mu \right) \sqrt{\pi} \right]^{-1/2} \exp \left\{ \frac{-(x-v_0t)^2 g + i \left[g^2 \hbar x^2 t / mu^2 + mv_0(2x-v_0t)u^2 / \hbar \right]}{2u^2(1+g^2 t^2 \hbar^2 / m^2 u^4)} \right\}.$$



Such packets are characterized by correlation coefficient $r = \rho / \sqrt{1 + \rho^2}$ and they have identical to $|\Psi_{uncorr}(x,0)|^2$ initial space structure. The space-time evolution of correlated packet is shown in the Fig. (lower row). The motion of a correlated packet leads to its spatial collapse (spontaneous supercompression) over time $t_{collapse} = \rho mu^2 / (1 + \rho^2) \hbar$ in a distant area $x_{collapse} = v_0 t_{collapse}$. This collapse is characterized by a significant decrease of the packet width from the initial value $\Delta x_{t=0} = u$ to a minimum value $\Delta x_{min} = u / \sqrt{1 + \rho^2} \ll u$ in the case the coefficient of correlation

efficiency $G = \sqrt{1 + \rho^2} \gg 1$ [1-6]. Immediately after the collapse the width of wave packet quickly increases $\Delta x_{t > t_{collapse}} \approx \hbar t G / mu$ and its amplitude very quickly decreases. These features allow the use such coherent correlated states for a targeted localized action. Another important characteristic of the correlated packet is connected with its energy. In our previous works it was shown that the momentum dispersion $\sigma_p = \langle (p - \langle p \rangle)^2 \rangle = \hbar^2 |g|^2 / 2u^2 \approx G^2 \hbar^2 / 2u^2$ and the corresponding rms fluctuation of the kinetic energy $\delta T = \sigma_p / 2m = G^2 \hbar^2 / 4mu^2$ of correlated packet sharply increases with an increase of correlation efficiency coefficient. For example, if the proton is represented as a wave packet with a longitudinal size $u = 0.1 nm$, in the uncorrelated state the energy fluctuation of such moving packet is limited to $\delta T_{uncorr} \approx 10^{-3} eV$ and in the correlated state with realistic value $G = 10^4$ [1-6] it increases to $\delta T_{corr} \approx 100 keV$! Such energy significantly exceeds the average energy $T = mv_0^2 / 2$ of proton longitudinal slow motion in LENR experiments, where average energy can be equal to several units or tens of eV [6,7].

The report also presents several possible methods for the formation of correlated states of slow particles with a high correlation efficiency coefficient (for example the case of motion in a periodic weak magnetic field [4,5]).

1. V. I. Vysotskii, M. V. Vysotskyy, Eur. Phys. J. A **49**, 99 (2013).
2. V. I. Vysotskii, S. V. Adamenko, M. V. Vysotskyy, Ann. Nucl. Energy **62**, 618 (2013).
3. V. I. Vysotskii, M. V. Vysotskyy, Curr. Sci. **108**, 524 (2015).
4. V. I. Vysotskii, M. V. Vysotskyy, J. Exp. Theor. Phys. **120**, 246 (2015).
5. V. I. Vysotskii, M. V. Vysotskyy, J. Exp. Theor. Phys. **125**, 195 (2017).
6. V. I. Vysotskii, M. V. Vysotskyy, S. Bartalucci, J. Exp. Theor. Phys. **127**, 479 (2018).
7. S. Bartalucci, V. I. Vysotskii, M. V. Vysotskyy, Physical Review AB, **22**, # 5, 054503 (2019).

Gaydamaka: THE POSSIBLE ROLE OF LENR IN DENTISTRY (EFFECTS AND PREVENTION)

Poster

A.A.Kornilova¹, V.I Vysotskii², S.N. Gaydamaka¹, A.A.Bolotokov³, A.I.Panchishin¹

¹Lomonosov Moscow State University, Russia

²Kiev National Shevchenko University, Ukraine

³LLC "Amtertek", Moscow, Russia

The traditional field of research of effects of LENR is limited, as a rule, by model physical systems. A more detailed analysis has shown that such effects can successfully occur in microbiological systems [1-3] and, as will be shown below, even in the human body. One of the best examples is dentistry. In the practice of dentistry it is well known that dental implants made of titanium have a negative effect on the teeth, which is manifested in the form of "leaching" of calcium from the composition of the teeth and leads to their destruction. This effect is well known in dentistry, but has no scientific basis.

We have conducted experiments to study the effect of standard titanium implants on the state of calcium in the laboratory in a liquid medium, representing a solution of natural saliva, which fully corresponds to the human oral cavity. Experiments conducted in a fixed volume with a strictly controlled composition showed that in the presence of such a titanium implant a very substantial (by 21% in 12 days) reduction in the total amount of calcium contained in saliva actually occurs. The analysis also showed that simultaneously with the decrease in calcium, the concentration of molybdenum on the surface of the titanium implant increases.

This process may be associated with a nuclear reactions $Ti^x + Ca^y = Mo^{x+y}$ conducted with participation of different isotopes of Ti and Ca. The mechanism for optimization of this reaction may be due to two important circumstances.

1). We have previously shown (and convincingly confirmed many times) that growing microbiological associations are a very effective catalyst for nuclear reactions [1-3]. Such objects in abundance are in the saliva of a person.

2). Coherent correlated states of at least one of the interacting nuclei (Ti or Ca) can be a real and very effective physical catalyst for such reactions [4,5]. Such states are automatically formed in dynamic nanocavities formed in natural biological phenomena (cell division, DNA replications, processes on the surface of membranes, etc.) during the growth and development of microbiological cultures. Such states are characterized by very large energy fluctuations, which can reach 30–50 keV and more.

As a result of detailed studies, we determined which of the stable isotopes of titanium and calcium play a leading role in the course of these molybdenum synthesis LENR reactions.

We have also shown that the exclusion of this "key" isotope from the composition of titanium used for the manufacture of dental implants leads to a practically complete suppression of the negative effect of dental implants on induced calcium deficiency.

1. Vysotskii V.I., Kornilova A.A. Nuclear fusion and transmutation of isotopes in biological systems, *Monograph, Publishing House "Mir", Moscow, 2003, 302 p*
2. Vysotskii V.I., Kornilova A.A. Nuclear transmutation of stable and radioactive isotopes in biological systems. Book, *Pentagon Press, India, 2010, 187 p.*
3. Vysotskii V.I, Kornilova A.A. Transmutation of stable isotopes and deactivation of radioactive waste in growing biological systems. *Annals of Nuclear Energy*, 2013, v. **62**: 626-633.
4. V.I.Vysotskii, M.V. Vysotskyy. *European Phys. Journal A*, 2013, **49**, 99.
5. V.I.Vysotskii, S.V.Adamenko, M.V.Vysotskyy. *Annals of Nuclear energy*, 2013, **62**, 618.

VysotskiiV: Distant behind-screen generation, X-Ray stimulation and LENR action of undamped heat waves

Alla A. Kornilova¹, Vladimir I. Vysotskii², Peter L. Hagelstein³, Timofey B. Krit¹

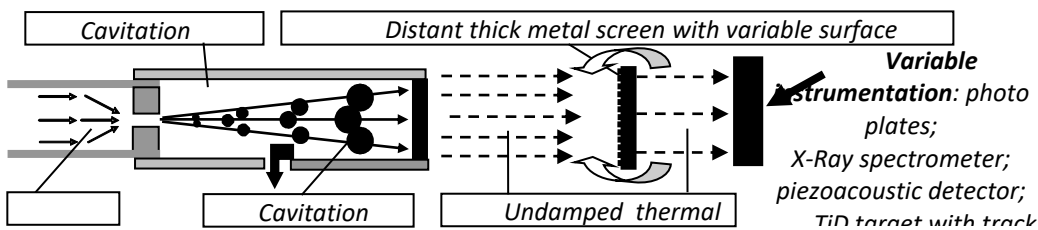
¹Moscow State University, Russia

²Kiev National Shevchenko University, Ukraine

³Massachusetts Institute of Technology, USA

It was shown (e.g. [1]) that the "standard" heat conduction equations of classical thermodynamics are incorrect in the analysis of very fast thermal processes. This is due to the fact that these equations do not take into account the final (non-zero) local thermal relaxation time in the material propagation medium. In these equations, the process of heat transfer is considered as a transition between a between infinitely small cells, each of which is always in equilibrium state. If we correct this incorrect assumption, then the solution of the exact equations of thermodynamics leads to the possibility of the existence of undamped thermal (temperature) waves that can be generated and propagated only at certain frequencies $\omega_n = (n + 1/2)\pi / \tau$ (τ - local relaxation time). For air, the minimum frequency of such waves depends on pressure and temperature and lies in the interval 75-85 MHz. The process of reflection of these waves from any boundary (e.g., air-metal) was theoretically considered in [2]. It was shown that the transmission coefficient depends on thermophysical parameters of both media, as well as on the quality of the input surface (small for a polished surface and large for inhomogeneous (unpolished) surface). Earlier we investigated the process of the excitation of these waves and their detection at a long distance without an additional screen [2-4], as well as their influence on LENR in remote targets [5].

In the first part of the report we present the results of a study the process of the passage of these waves through remote thick LiNbO₃ crystal (~10 mm) and steel (3 mm) screens with different quality surface treatment

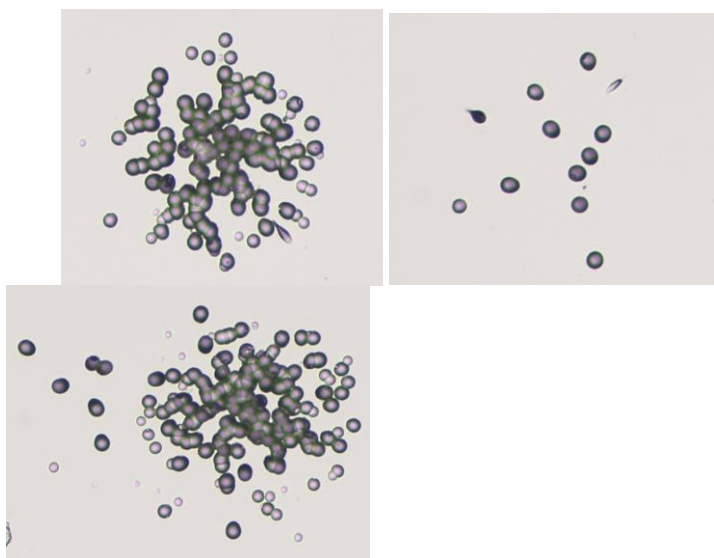


(**polished** surfaces and ground _____ face (**unpolished**)), and X-Ray generation behind this metal screen (see Fig.1).

During these studies, we found complete agreement between the experimental results and theoretical calculations (optimal X-ray generation occurs when the metal screen is oriented with the **unpolished** side towards the cavitation chamber, with generation of directional (forward) high-frequency (~83 MHz) temperature waves in the case of a

metal screen, and the generation of two differently directed temperature waves (~83 MHz) for LiNbO₃ crystal).

In the second part of the report the effect of these temperature waves on LENR processes is presented. In this case instead of X-Ray and piezoacoustic detectors (Fig.1), a TiD target (similar to



that used in the work [5]: length - 10 mm, diameter - 7 mm, saturation ~150%) was installed together with a nearby track detector. Several fragments of this detector with many alpha-tracks after three-hour experiment are

shown in Fig.2. The mechanism of stimulation of $d+d=He^3+p$ and $d+d=He^4$ reactions by action of temperate waves is discussed in the report. This mechanism is associated with the influence of these waves on the dynamic structure of TiD target and, possible, on formation of coherent correlated states of interacting particles during such structural and topological processes in the target lattice, which leads to very large controlled fluctuations of proton energy (up to 30-100 keV and more (e.g.[6])).

These processes are also associated with the phonon-nuclear coupling mechanism of LENR (e.g. [7]).

1. V.I.Vysotskii, V.B.Vassilenko, A.O.Vasilenko, Intern. J. of Sci.: Basic and App. Research (IJSBAR), v.12, 160 (2013).
2. V.I.Vysotskii, A.A.Kornilova, A.O.Vasilenko, V.I.Tomak. J. Surf. Investigations, v.8, 1186 (2014).
3. V.I.Vysotskii, A.A.Kornilova, A.O. Vasilenko. Current Science, v.108, No.4, p. 114 (2015).
4. V.I.Vysotskii, A.A.Kornilova, T.B.Krit, M.V.Vysotskyy. J. Surf. Investigations, v.11, 749 (2017).
5. A.A. Kornilova, V.I.Vysotskii et al., Engineering Physics, №5, 13-22 (2018) (in Russian).
6. V.I.Vysotskii, M.V.Vysotskyy. European Physical Jour. A, v.49, 2013, issue 8: 99, p.1-12.
7. F. Metzler, P.L.Hagelstein, S. Lu. JCMNS, v.24, 98-113 (2017).

Vysotskii: Periodic structure of Fe-Mn natural geology crusts with anomalies of the isotopic ratio as the results of self-controlled global biostimulated isotope transmutation in oceans and lakes

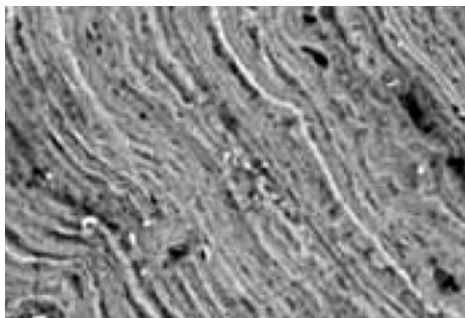
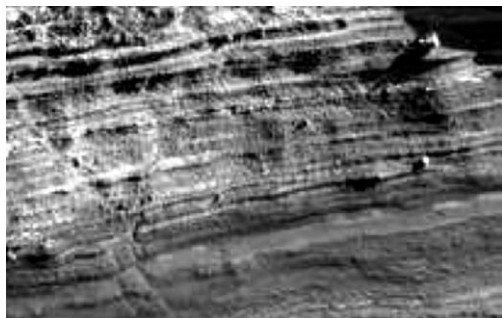
V.I.Vysotskii¹, A.A.Kornilova², S.N.Gaydamaka², A.A.Novakova²,
D.S.Novikov², N.V.Kim², A.G. Sverchkov³

¹Kiev National Shevchenko University, Ukraine

²Moscow State University, Russia

³ Center of Expert Technologies at Moscow State University, Russia

It is well known that Fe-Mn crusts are among of the most mysterious geological objects. The world reserves of iron and manganese in these structures are 3000 billions of tons. The internal structure of crusts is characterized by a rhythmic alternation of contrasting Fe and Mn thin layers (see typical Figs of crusts cross-sections). The traditional description of such



anomalous structures is connected with the action of volcanoes. However, such a hypothesis is unlikely due to the fact that crusts are found in different places of the Earth and the main parts of these places have no relation to volcanoes. In addition, the strictly periodic structure of such crusts and the approximate constancy of the

period, regardless of their location, also confirm that they are not connected with the random volcano activity. Even more mysterious is the violation of the "standard" isotope ratios in all samples of crusts (regardless of the location in the oceans and lakes): in all cases the relative concentration of Fe⁵⁷ isotope decreases in comparison with Fe⁵⁴ and Fe⁵⁶ [1,2]. It is also very important that these objects are always connected with water sources (they are located in a bottom of swamps and lakes, along the coast of seas and oceans, and they are never located on high mountains with no water sources).

There is no reasonable explanation for these anomalies and the typical summary in many articles is the following: "to determine which of these processes is the preponderant isotope fractionation observed in hydrogenous ferromanganese crusts requires additional studies"[1].

The possible and the most realistic explanation of the origin of such anomalous structures and abnormal isotope rates is natural nuclear transmutation $Mn^{55}+p=Fe^{56}$ and $Na^{23}+P^{31}=Fe^{54}$ of Mn⁵⁵, Na²³ and P³¹ isotopes dissolved in water into iron isotopes under the influence of the natural biological syntrophic microorganisms, which grow in a bottom area of any lake or sea. On the other hand, the reaction $Mn^{55}+d=Fe^{57}$ for a similar Fe⁵⁷ fusion under natural conditions is practically impossible because of the extremely low concentration of deuterium in water. It is very important that layered crusts are found only in middle and equatorial latitudes and are absent in cold seas! It is the additional confirmation of the biogenic mechanism of isotope transmutation.

We have repeatedly shown that the process of such transmutation takes place in the aquatic environment in the presence of appropriate isotopes and the presence of syntrophic microbiological associations [3-6]. The characteristic feature of such transmutation is self-limiting and self-control: the process starts to be inhibited when a large amount of toxins (as metabolic products) are released and when the local environment is depleted with the necessary isotopic components. Under laboratory conditions, these factors can be controlled and corrected by periodical adding of appropriate chemical components. Under natural conditions, a sufficiently long time is needed to re-launch the transmutation process, during which a natural self-purification of the near environment from toxins takes place and the necessary isotopic composition is restored. Such a self-similar process justifies the periodicity of iron synthesis and the formation of thin layers of this element. The paper considers the dynamics of this process and shows that it can be used for the local geological chronology.

1. Levasseura S., Franka M., Heinb J.R., Halliday A.N. *Earth and Planetary Science Letters*, 2004, v. **224**, p. 91– 105.
2. Rouxela Olivier, Dobbeka Nicolas, Luddena John, Fouquet Yves. *Chemical Geology*, 2003, v. **202**, p. 155–182.
3. Vysotskii V.I., Kornilova A.A. Nuclear fusion and transmutation of isotopes in biological systems, *Monograph, Publishing House "Mir", Moscow, 2003, 302 p*
4. Vysotskii V.I., Kornilova A.A. Nuclear transmutation of stable and radioactive isotopes in biological systems. *Pentagon Press, India, 2010, 187 p.*
5. Vysotskii V.I, Kornilova A.A. *Annals of Nuclear Energy*, 2013, v. **62**: p.626-633.
6. Kornilova A.A., Vysotskii V.I. *RENSIT*, 2017, v. **9**, No. 1, p.52-64

Alla A. Kornilova¹, Vladimir I. Vysotskii², Sergey N. Gaydamaka¹¹Moscow State University, Russia²Kiev National Shevchenko University, Ukraine

Intensive studies conducted over 25 years have confirmed the possibility of using the effect of the isotope transmutation in growing biological systems for solving various fundamental and applied problems of biology and nanotechnology, nuclear physics and other fields of science [1-3]. In some of these areas (in particular, in nuclear physics during transmutation of radioactive isotopes), optimization of LENR related biotechnology has achieved very significant progress - reducing of the deactivation time of the long-lived (30 years) radioactive Cs¹³⁷ isotope from initial 310 days [2,3] to 14 days in last experiments. Such a significant optimization allows the use of this technology today to solve urgent problems of deactivation of industrial radioactive water at NPP.

On the other hand, less attention and efforts did not allow achieving the same significant results in areas related to the transmutation of stable isotopes, which can be used to solve important problems in agriculture, medicine and nanotechnology. It should be noted also that the actual concentration of radioactive isotopes (even with very high activity) is usually substantially lower than the typical concentrations of stable isotopes in real applications.

This report presents the results of optimizing the transmutation process with the ultimate goal of bringing them to the pre-industrial level. When solving such problems, a more fundamental study of factors that lead to the possibility of transmutation and which impede this process is necessary. We have previously shown that biological culture, which is put on the brink of survival by the absence of a number of nutrients in the nutrient medium and nonspecific growth conditions, synthesizes the chemical elements necessary for the growth of new cells. This process is based on nuclear reactions involving, as a rule, the elements present in the liquid nutrient medium on the basis of conventional water or deuterium [1-3].

To achieve control of the transmutation effect, it is necessary to solve as purely biochemical, as nuclear problems. In our experiments, we have used fast-growing syntrophic associations resistant to various toxicants, i.e. communities, in which there are more than three thousand different types of microorganisms, protozoa, bacteria and fungi. From biomass, micro- and macro-elements were maximally desorbed, and in nutrient media, a rational change was made in the composition of biogenic elements. At this stage, to solve the problem of maximization the efficiency of the transmutation process, we conducted 3 experiments:

- 1) synthesis of a rare potassium isotope on the base of reaction $\text{Ca}^{40} + \text{p} = \text{K}^{41}$ in deionized water;
- 2) synthesis of Fe⁵⁶ isotope from manganese on the base of reaction $\text{Mn}^{55} + \text{p} = \text{Fe}^{56}$ in deionized water;
- 3) synthesis of a rare iron Mossbauer isotope on the base of reaction $\text{Mn}^{55} + \text{d} = \text{Fe}^{57}$ in deuterium water.

These experiments, taking into account their planned pre-industrial character, were carried out much longer (12 days) and much more effective than it was in our initial works (e.g. [4,1]). The buffer component in nutrient solutions was absent; therefore, to stabilize the process, glucose was added in small portions. The intensive character of transmutation process clearly illustrates the change of pH in nutrient medium in all experiments.

days:	1	2 (morning)	2 (evening)	3	4	8	10	11	12
1 (pH)	4,81	5,00	5,10	3,69	3,70	3,14	2,94	2,92	2,90
2 (pH)	5,10	5,10	4,88	3,85	4,18	3,88	7,66	8,03	7,71
3 (pH)	5,46	5,50	5,87	6,80	5,86	4,35	3,26	2,62	2,59

At the end of the experiments, samples of the original nutrient medium, initial biomass, as well as supernatants and biomass from 3 parallel experiments were separated to analyze isotope ratios for K³⁹, K⁴¹, Ca⁴⁰, Mn⁵⁵, Fe⁵⁴, Fe⁵⁶ and Fe⁵⁷ isotopes. These results are presented and discussed in the report. They demonstrate very high (close to maximum) transmutation efficiency.

From the results of such an analysis it follows that the use of special combined adjustments of the composition and parameters of the "bioreactors" made it possible to dramatically increase the efficiency of the synthesis (by tens or more times) and bring it closer to industrial level - e.g. for production of rare isotopes similar to Fe⁵⁷ (natural concentration 2.1%).

1. Vysotskii V.I., Kornilova A.A. Nuclear fusion and transmutation of isotopes in biological systems, *Monograph*, Publishing House "Mir", Moscow, 2003, 302 p

2. Vysotskii V.I., Kornilova A.A. Nuclear transmutation of stable and radioactive isotopes in biological systems. Book, *Pentagon Press*, India, 2010, 187 p.

3. Vysotskii V.I., Kornilova A.A. Transmutation of stable isotopes and deactivation of radioactive waste in growing biological systems. *Annals of Nuclear Energy*, 2013, v. 62: 626-633.

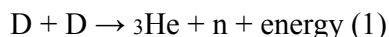
4. Vysotskii V.I., Kornilova A.A., Samoylenko I.I. Experimental discovery and investigation of the phenomenon of nuclear transmutation of isotopes in growing biological cultures. *Cold Fusion and New Energy Technol.*, 1996, v.2, № 10, 63-66.

Alexandrov: Cold nuclear fusion in lithium compound alloy

Dimitar Alexandrov
Lakehead University, Canada
Email: dimitar.alexandrov@lakeheadu.ca

Experiments about cold nuclear fusion reactions in lithium compound alloy have been performed and explained theoretically. The results are presented in this paper.

The experiments were performed in vacuum chamber in order precise measurements to be achieved and due to the relatively low concentrations of the interacting gases the amounts of the generated helium and of the generated energy (heat) were relatively low. In fact D₂ gas in environment of H/H₂ gas in the chamber was directed to a specimen of lithium compound alloy placed on sample holder and significant generation of both ³He and ⁴He was observed in all experiments as it was supported by the following facts: *i*) Mass analysis shows relatively high amount of ³He; *ii*) Mass analysis shows relatively high amount of ⁴He/D₂ and relatively significant amount of ⁴HeH that confirms relatively high amount of ⁴He; *iii*) Mass analysis shows absence of H₃⁺ (stable positive ion of three hydrogen molecule), DH (deuterium hydride) and D₂H⁺ (stable positive ion of deuterium-deuterium hydride molecule); and *iv*) DC plasma spectroscopy shows peaks typical for both ³He and ⁴He. Based on the experiments it was concluded that the following cold nuclear fusion reactions have had place:



Where n is neutron released in a cold nuclear fusion reaction (1). Also the author assumes that the released neutrons may cause nuclear fission reaction where lithium atoms of ⁶Li belonging to the crystal lattice of the lithium compound alloy participate. However the Author considers that additional experiments must be performed in order the above nuclear fission reaction to be confirmed.

The temperature of the sample holder was measured during the experiments and cyclic dependence on the time was found and also it was found that this dependence correlates with changes in the amounts of both ³He and ⁴He in the time. In some experiments external heating of the sample holder was performed and it was found increase of the amounts of both ³He and ⁴He with increase of the temperature. Radiation (including gamma rays and neutrons) was measured in all experiments and no increase of the radiation above the normal background was found. (Absence of increase of the radiation is due to either: *a*) The low amounts of gases used in all experiments give a radiation, which is very small and cannot be detected by the used devices; or *b*) There is no external radiation at all due to the low kinetic energies of the interacting D nuclei in solids and due to a fact that the released neutrons in (1) do not leave the solid.)

The experimental results provided above are explained with a previously developed quantum mechanical theory based on interaction of D nuclei with heavy electrons that are localized in solids. The theoretical outcomes are consistent with the above experimental results and they provide proof that two nuclear fusion schemes in the lithium compound alloy specimen have places: *i*) D+D→³He+n+energy; and *ii*) D+D→⁴He+energy. Also the theory explains increase of the amounts of both ³He and ⁴He with increase of the temperature of the specimen. The theory is valid for all solids, however it determines that the above nuclear fusion reactions can have places only in solids having certain properties as the lithium compound alloy is a solid satisfying these requirements and the released helium is much bigger than in similar experiments using others solids (including palladium).

Collis: An Empirical Global Calculator of Atomic Masses

William Collis
billcollis (at) iscmns org

In our previous works we dramatically improved the accuracy of so called “local relations” (relying on local masses) first pioneered some 50 years ago¹. From these, global formulas were developed noticing that the best local relations appeared to satisfy a high order differential equation of this form:-

$$\frac{\partial^{p+q}M}{\partial Z^p \partial N^q} = b(-1)^{N+Z} \quad \text{for some arbitrary constant } b \quad (1)$$

The right hand side is any two valued odd / even function.

Which has the general solution:-

$$M(N,Z) = f_1(Z) + \dots + N^{q-1}f_q(Z) + g_1(N) + \dots + Z^{p-1}g_p(N) + k(-1)^{N+Z} \quad (2)$$

where $f(Z)$, $g(N)$ are arbitrary functions of their integer arguments, and k is a constant parameter, all determined by least squares regression.

For $p=q=3$ some 800 parameters would have to be determined (compared with some 2700 observations of experimentally measured atomic masses). In this paper we explore how the number of parameters can be substantially reduced and accuracy of the mass predictions improved. The better RMS errors in the predictions are about 101 keV with 545 parameters.

References

1. G. T. Garvey et al., Rev. Mod. Phys. 41, S1 (1969).
2. W. Collis, AIP Conf. Proc. 1165, 116 (2009).
3. G. Audi et al., Chin. Phys. C 36, 1603 (2012).
4. Z. He et al., Phys. Rev. C 90, 054320 (2014).
5. J. Janecke and E. Comay, Nucl. Phys. 108, 436 (1985).
6. J. Janecke and P. Masson, At. Data Nucl. Data Tables 39, 265 (1988)
7. P. Masson and J. Janecke, At. Data Nucl. Data Tables 39, 273 (1988).
8. J. Piekarewicz et al., arXiv:0905.2129 [nucl-th]. 1745024-3
9. W. Collis “New global atomic mass formulas”, Int. J. Mod. Phys. B 2017.31.

Zeiner-Gundersen : Electricity production from ultra dense deuterium

Sindre Zeiner-Gundersen

Abstract not submitted.

Huang BJ: Excess Energy from a Vapor Compression System

Bin-Juine Huang*, Ming-Li Tso, Ying-Hung Liu, Jong-Fu Yeh
 Department of Mechanical Engineering, National Taiwan University, Taipei, Taiwan
 Corresponding author: bjhuang@seed.net.tw

In a vapor compression system using reciprocating compressor (Figure 1), we found that excess energy output over the energy input can occur. This vapor compression system does not include a conventional evaporator which absorbs heat from surroundings as in air conditioning system. Hence, the coefficient of performance COP (ratio of total heat released to total energy input) of the vapor compression cycle will never be greater than 1, according to the law of energy conservation. The compressed hot refrigerant vapor at the compressor outlet (controlled around 150°C) is used to heat the water in a “CIF steam generator”. This may cause a violent cavitation phenomenon of water and produces a hot steam output. We continuously run a vapor compression system built with a 2.75 RT R22 compressor. The measured COP is greater than 1 as shown in Table 1, ranging 1.5~7.0 determined from the heat balance on cold water in a tank mixing with the output hot steam with or without heat loss (COP_{HL} or COP_{HO}), or from the output dry steam heat (COP_{max}). The repeated experiments reveals the excess energy output from this machine. We attribute this to the phenomena of CIF (cavitation induced fusion) created by violent cavitation and heat absorbing/releasing of water inside the tiny water/vapor channels [1-5]. The properties of water condensed from the output steam are also found changed, consisting of copper ion and dissolved hydrogen etc. The optimization of the vapor compression system is underway.

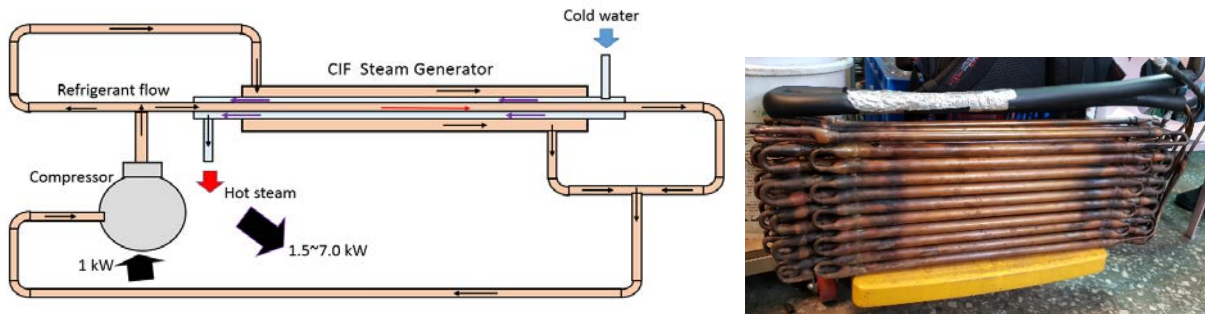


Figure 1. Schematic of vapor compression system (left) with CIF steam generator (right).

Table 1. Test results.

Test date	2019/5/2 9	2019 /6/1
Output hot steam temperature (°C)	155	155
Initial cold water temperature in tank (°C)	41.1	44.7
Final hot water temperature in tank (°C)	90.9	96.3
Hot steam generation rate (kg/min)	0.613	0.598
Total electrical energy input (kWh)	2.4	2.7
Total heat released (including heat loss) (kWh)	3.74	3.94
COP_{HL} including heat loss (measured)	1.56	1.46
COP_{HO} without heat loss (estimated 20%)	1.87	1.75
COP_{max} (assuming dry steam output)	7.01	6.25

References

1. Max I. Fomitchev-Zamilov. Cavitation-Induced Fusion: Proof of Concept. Natural Philosophy Alliance Vol 9, 2012. 1-14
2. Taleyarkhan, R., West, C., Cho, J., Lahey, R., Nigmatulin, R., & Block, R. (2002). Evidence for Nuclear Emissions During Acoustic Cavitation. *Science*, 295 No.5561, 1868-1873.
3. Taleyarkhan, R., Cho, J., West, J., Lahey, R., Nigmatulin, R., & Block, R. (2004). Additional evidence of nuclear emissions during acoustic cavitation. *Physical Review E*, 69 (3), 036109
4. Wu, C., Roberts, P. (1993). Shock-wave propagation in a sonoluminescing gas bubble. *Physical Review Letters*, 70 (22), 3424-3427.
5. Alan J. Walton, Geo. T. Reynolds “Sonoluminescence”, *Advances in Physics*, 33(6), 595-660, 1984.

Greenyer: Nickel-hydrogen heat generator continuously working for 7 months

A.G. Parkhomov¹, V.A. Zhigalov¹, S.N. Zabavin¹, A.G. Sobolev², T.R. Timerbulatov¹

¹ **OKL KIT**, Moscow, alexparh@mail.ru

² **Lebedev Physical Institute** of the [Russian Academy of Sciences](#), Moscow

A nickel-hydrogen heat generator was created that continuously worked for 225 days with a heat dissipation power exceeding the consumed electricity from 200 to 1000 W (thermal coefficient 1.6 - 3.6). Completion of the work is connected with the exhaustion of fuel energy resource. Total excess energy generation of about 4100 MJ. The fuel used in the heat generator is hydrogen-saturated nickel powder weighing 1.2 g. Energy release per 1 nickel atom 2.1 MeV. Changes in the elemental and isotopic composition of fuel and structural materials are analysed.

Greenyer: LENR as Appearance of Weak Interactions Poster

A.G. Parkhomov¹

¹ **OKL KIT**, Moscow, alexparh@mail.ru

Low mass of neutrinos (antineutrinos) makes possible their intensive generation as a result of matter particles collisions during thermal motion. Arising neutrinos (antineutrinos) have energy of about 0.1 eV. With such energy, de Broglie length is about 5 microns. It means that a huge number of atoms are involved in weak nuclear interactions, which makes the effects of nuclear transformations with the participation of neutrinos (antineutrinos) really observable. Consideration of thermal generation of neutrinos as the basis of nuclear transformations in the LENR process allows us to explain a number of features of this phenomenon.

Hatt: Cold Nuclear Transmutations Theoretical basis for the calculation of binding energy. Poster

Philippe Hatt, independent researcher
Email: pcf.hatt@gmail.com

1. In order to determine the binding energy of the various elements, five types of bonds are necessary according to the author's theory:
 - Deuterium like bond, called NP with value 2.2246 MeV, linking a neutron of one α -particle with a proton of a second α -particle, or a neutron or proton outside an α -particle to that α -particle.
 - Tritium like bond, called NNP with value 8.4818 MeV, linking three nucleons of three different α -particles, or one or two nucleons outside an α -particle to one or two α -particles.
 - ^3He like bond, called NPP with value 7.718 MeV, having a similar function as NNP.
 - A dineutron bond the author called NN, with value 4.9365 MeV and linking two neutrons not being located within the same α -particle. This bond value is deduced from the α -particle binding energy.
 - The α -particle bond with value 28.325 MeV ($E_B \alpha$).

Remarks:

 - The NN and NP are the most used bonds. Generally, they oscillate to form an "A" bond equal to $(NN/2 + NP/2)$.
 - The NN value (4.9365 MeV) is comparable to the mass of quark down (4.8 MeV) and the NP value (2.2246 MeV) is comparable to the mass of quark up (2.4 MeV).
2. It will be seen that the bonds of α type, as well as ^2_1H , ^3_1H , ^3_2He and NN are sufficient to explain the binding energy of all nuclei, which pleads for predominance of α -particles in the nuclei. The atomic nuclei are therefore constituted of sub-nuclei, essentially ^4_2He but also ^2_1H , ^3_2He and ^3_1H or simply of N or P, somewhat like molecules, being understood that the bonds can be more or less strong.
3. The results are obtained by comparing binding energy values of several nuclei, especially isotopes of the same element and by breaking down these values in NP, NNP, NPP and α -particle binding energy values. For instance, in case of ^{16}O the figure is based on four α -particles bound by four equal bonds the author calls "A", actually a simplification for $NN/2 + NP/2$. If a neutron is added it becomes ^{17}O . So, the author looks for a bond linking the new neutron and two nucleons located within two α -particles. The author has the choice between NNP and NPP. It is NPP which fits, so the author takes that one arbitrarily.

Hatt: Cold Nuclear Transmutations - Examples of Fe Isotopes Binding Energies Poster

Philippe Hatt, independent researcher. Email: pcf.hatt@gmail.com

In order to determine the binding energy of the various elements, five types of bonds are necessary according to the author's theory:

- Deuterium like bond, called NP with value 2.2246 MeV, linking a neutron of one α -particle with a proton of a second α -particle, or a neutron or proton outside an α -particle to that α -particle.
- Tritium like bond, called NNP with value 8.4818 MeV, linking three nucleons of three different α -particles, or one or two nucleons outside an α -particle to one or two α -particles.
- ^3He like bond, called NPP with value 7.718 MeV, having a similar function as NNP.
- A dineutron bond the author called NN, with value 4.9365 MeV and linking two neutrons not being located within the same α -particle. This bond value is deduced from the α -particle binding energy.
- The α -particle bond with value 28.325 MeV ($\text{EB } \alpha$).

Remarks:

- The NN and NP are the most used bonds. Generally, they oscillate to form an "A" bond equal to $(\text{NN}/2 + \text{NP}/2)$.
- The NN value (4.9365 MeV) is comparable to the mass of quark down (4.8 MeV) and the NP value (2.2246 MeV) is comparable to the mass of quark up (2.4 MeV).

It will be shown that the basic rule valid for the stable elements which are at the center of the periodic table (case of Iron), is:

$$\text{EB } n = x \text{ EB } \alpha + (x + y) \text{ EB } (\text{NN} + \text{NP})$$

(x = number of α particles, y = number of N and P supplementary into one nucleus).

One will see that (NN + NP) bonds could be replaced by NNP or NPP bonds which have a higher value. As well, some bonds are not completed, $(\text{NN}/2 + \text{NP}/2)$ being replaced by NP. This happens in case of non-stable isotopes.

The results are obtained by comparing binding energy values of several nuclei, especially isotopes of the same element (presently $_{26}\text{Fe}$) and by breaking down these values in NP, NNP, NPP and α -particle binding energy values. This method is not based on a theory. The author makes mind experiments: he has the choice to use a few bonds each time a new neutron or proton is entering a nucleus. So, the author chooses that one which fits. This is comparable to the work of a chemist looking for several solutions in his experiments and validating that one which fits best. Moreover, the author is looking at the compliance of the solution for one nucleus with the solution for another nucleus in order to avoid discrepancies, especially between isotopes. The author is also taking care of symmetry within a given nucleus and between nuclei.

Swartz: Superhyperfine Structure of the Deuteron Line Emission from Active ZrO₂PdD Heralds an FCC Vacancy

Mitchell R. Swartz

AC1ER Nanortech, Inc. June 29, 2019 ©

Analysis of non-Zeeman superhyperfine line (SHFL) splitting in LANR-induced RF DLEmissions [1] yields insight into the LANR active site not otherwise available [Figure 1]. The SHFL emitted at 327.37 MHz from an active ZrO₂PdD component [2] have been analyzed for asymmetry, amplitude and position as a function of frequency. The asymmetry is 7-15% (1st through 3rd closest positions); smaller than the ~50% noted for some Zeeman splittings [3]. Most importantly, the SHFL arise from resonance broadening (RB) which occurs from perturbing deuterons in other vacancies through energy exchange processes. RB impact was derived for the first four closest neighbor sites. The RB interaction decreases as $1/r^3$. Figure 1 demonstrates the better overlap of the expected FCC locations in the midgraph, unlike the BCC lattice. The coordination numbers (CN) also better match for the FCC lattice. Thus, analysis of the CN and RB sideband positions as a function of frequency strongly suggest that the location of the excited state deuterium is a palladium (Pd) vacancy within a slightly modified FCC lattice. The modification shows a multiplet near the second nearest neighbor which might indicate nearby zirconia at a rhombic corner (isoequivalent to a FCC vacancy) or an atom of zirconium (or impurity) within the PdD lattice. The results in nickel are more complex and demonstrate a range of FCC and body centered cubic (BCC) vacancies, possibly heralding new metallurgic phases. This discovery adds semiquantitative material science support to theories that cite vacancies [4] as the site of the desired LANR reactions. Figure 1 – Lattice Analysis of Active PdD Component's Frequency-Time Plot This top shows the actual SHFL sideband structure for Nanor®-type component #7-4, driven at ~10 volts. This is a 'waterfall' plot and intensity is shown as a function of frequency. The middle and bottom of the fig. show the expected results for two different gendanken active sites, face and body centered cubic (FCC, BCC) respectively: both the coordination numbers (height) and expected deviation (to the right for frequency).

[1] Swartz M., Atomic Deuterium Produces 327.37 MHz Superhyperfine RF Maser Emission (ICCF-22, 2019) [2]

Swartz M. R., Verner, G., Hagelstein, P., Imaging of an Active NANOR®-type LANR Component using CR-39, J. Condensed Matter Nucl. Sci. 15, (2015), p 81; www.iscmns.org/CMNS/JCMNS-Vol15.pdf

[3] J. E. Mack and O. Laporte, Asymmetric Zeeman Effect Patterns in a Complex Spectrum, Physical Review Journals Archive, Phys. Rev. 51, 291 (February 1937); DOI:<https://doi.org/10.1103/PhysRev.51.291.2>

[4] Swartz M., Catastrophic Active Medium (CAM) Theory of Cold Fusion, Proc. ICCF4 4, (1993), p 255

[5] The author thanks David Nagel, Bo Gardmark, Dennis Craven, Peter Hagelstein, Michael Staker, and Louis Dechiaro

Swartz: Atomic Deuterium in Active LANR Systems Produces 327.37 MHz Superhyperfine RF Maser Emission

Mitchell R. Swartz AC1ER JET Energy, Inc. June 21, 2019

Active lattice assisted nuclear reaction (LANR) systems, both aqueous and dry nanomaterial, emit very narrow bandwidth radiofrequency (RF) emission peaks (circa 327.37 MHz), in the Deuteron-line (“DL”; 327.348 MHz) region. Figure 1 shows RF maser emission from a preloaded ZrO₂PdD Nanor®-type LANR component [1,2] operated below its avalanche voltage in a well-grounded resonant Fabry Perot chamber. The high Q [$> 1.2 \times 10^6$] and Zeeman response indicate maser activity. There are superhyperfine sidebands. Nearest neighbor resonance analysis of those superhyperfine emissions heralds reactions occurring in a Pd lattice palladium face center cubic vacancy. D-loaded active nickel is far more complex. Figure 1 –Software Defined Radio Identification of LANR D-Line Maser Emission In this dual graph, there are two regions; in both, the frequency increases from left to right. The upper portion shows RF intensity peaks as a function of frequency (horizontal) at a single moment in time. On the bottom, each peak appears as a dot on a line for each one moment in time, and time increases from top to bottom, as in a waterfall. The DL RF CF/LANR maser emission line is indicated in both portions of the display.

[1] Swartz M. R., Verner G., Tolleson, J, Energy Gain From Preloaded ZrO₂–PdNi–D Nanostructured CF/LANR Quantum Electronic Components, JCMNSci. 13, 528 (2014).

[2] Swartz, M. R. G. Verner, J. Tolleson, P. Hagelstein, Dry, preloaded NANOR®-type CF/LANR components, Current Science, 108, 4, 595 (2015)

Swartz: Buoyant heat transport can produce unreliable estimates of heat generation

Mitchell R. Swartz, MD, ScD,
EE JET Energy, Inc. USA

Many aspects of flow calorimeters used to detect putative CF/LANR reactions [1-6] have been discussed. Issues include thermometry, electrical grounding, crosstalk, thermal mixing, sensor positioning problems, and recombination. The potential impact of a buoyancy error is usually not considered despite its demonstrated significance [7-12] and relevance to heat and mass flow [13] and Bernard instability [14]. In the absence of thermal (ohmic) controls, derived flow equations cannot always be trusted, especially when the input and output temperatures are taken without consideration of possible thermal stratification which only increases at higher input powers. Therefore, the derived indicated output from calculations, in the absence of ohmic controls, should be suspect if the temperatures are not taken at the same elevation. Such cold calculations, even if thermometry is correct, deviate from the actual Navier-Stokes heat and mass flow calculations which demonstrate significant problems when there is thermal-created buoyancy inversion of water or air [“Bernard instability”], especially at low flow rates. Figure 1 demonstrates the impact of misunderstanding the falsity of indicated data, which increases significantly at higher values of ηB . The non-dimensional number ηB is the ratio of heat transported by the buoyant forces to the heat transported by the applied air or solution convection. Thus, an improved estimate of the incremental power gain in an experiment then becomes: . Figure 1 – The indicated uncalibrated outputs from flow calorimetry can be magnified in an unwarranted fashion if temperature probes of the “input” and “output” area (deliberately) taken at two different elevations (“levels”, “heights”) in the absence of ohmic controls and/or buoyant correction.

Swartz: Pulsing Sideband at 327.37 MHz May Herald Movements within an Active Loaded PdD Lattice

Mitchell R. Swartz, MD, ScD, EE AC1ER JET Energy, Inc.

July 14, 2019 © 2019

Active LANR (lattice assisted nuclear reaction) systems, both aqueous and dry nanomaterial, emit very narrow bandwidth radiofrequency (RF) emission lines (circa 327.37 MHz) in the Deuteron-Line (DL) region [1]. The maser line can include sidebands which appear by resonance broadening and energy exchange processes [2]. The superhyperfine sideband line (SHFL) structure (Figure 1) has been analyzed for the aqueous nickel MOAC system in its active mode [3]. In that light, the pulsatile superhyperfine RF line (PSHFL) is evident with periods of minutes. It is unlike everything else examined over two years from Earth and galactic origin, and only associated with XSH from an ordinary water nickel CF/LANR system. This is not mode-locking [4]. Laser mode locking involves hundreds of half-wavelengths, enabling interaction of different mode orders; but this 327 MHz LANR maser has only single-mode (half wavelength) operation. Laser mode locked pulses are separated by the Fabry-Perot cavity transit time but the 327 MHz LANR maser pulsing sideband is characterized by times which are minutes. Finally, laser mode locked pulses have a Gaussian or a hyperbolic-secantsquared (sech²) pulse shape but the 327 CF/LANR maser's pulses appear as near step functions. What this is, instead, might be new information obtained from these unique pulsing RF bands which may herald deuteron density movements between, and to other, lattice regions, as revealed by the PSHFL (and interpreted, depending upon the model used: Band States, Bose Einstein condensates, and other quasiparticles). It is a fact that thirty years of data demonstrate that deuterons loaded into Group VIII metals DO work together in active LANR systems to generate de novo 4He. There are inverted populations of atomic D [1] with RF D-line emission sidebands [2] and this RF pulsing from active LANR systems might indicate part of an active-necessary deuteron redistribution in the lattice. Is such redistribution a sine qua non for successful movement through the Coulomb barrier? Efforts are underway to examine this further, including intensities, pulsations and transfer-movements; which together suggest a need for an intralattice kinoscope. Figure 1 – Pulsatile RF Emissions in a Background of other RF SHF Lines The Radiofrequency Superhyperfine D-L spectrum of hydrogen loaded nickel MOAC during its active state [40 volts, 200 milliamperes]. This is a 'waterfall' plot and intensity is shown as a function of frequency. Note the arrow appears to almost be a horizontal mirror axis.

[1] Swartz M., Atomic Deuterium in Active LANR Systems Produces 327.37 MHz Superhyperfine RF Maser Emission (ICCF-22, 2019)

[2] Swartz M., Superhyperfine Sideband Structure of the Deuteron Line Emission from the ZrO₂PdD Active Site May Herald an FCC Vacancy (ICCF-22, 2019)

[3] Swartz, M. R, C. Haldemann, A. Weinberg, B. Ahern, Possible Deuterium Loss During Excess Heat From Ordinary Water-Carbonate Electrolyte using Nickel, J. Condensed Matter Nucl. Sci. (Proc. ICCF-21, 2018)

[4] Herman A. Haus, Mode-Locking of Lasers, IEEE J Sel. Topics in Quantum Electronics, 6, 6, (2000) , 1173

[5] The author thanks David Nagel and Bo Gardmark.

Fredericks: Elliptical tracks: evidence for superluminal electrons?

Keith Fredericks

Restframe Labs, West Lafayette, IN, USA

In the literature of Low-Energy Nuclear Reactions (LENR), particle tracks in photographic emulsions (and other materials) associated with certain electrical discharges have been reported. Some Russian and French researchers have considered these particles to be magnetic monopoles. These tracks correspond directly to tracks created with a simple uniform exposure to photons without an electrical discharge source. This simpler method of producing tracks supports a comprehensive exploration of particle track properties. Out of 750 exposures with this method, elliptical particle tracks were detected, 22 of which were compared to Bohr-Sommerfeld electron orbits. Ellipses fitted to the tracks were found to have quantized semi-major axis sizes with ratios of $\approx n^2/\alpha^2$ to corresponding Bohr-Sommerfeld hydrogen ellipses. This prompts inquiry relevant to magnetic monopoles due to the n^2/α^2 force difference between magnetic charge and electric charge using the Schwinger quantization condition. A model using analogy with the electron indicates that the elliptical tracks could be created by a bound magnetically charged particle with mass $m_m = 1.45 \times 10^{-3} \text{ eV}/c^2$, yet with superluminal velocities. Using a modified extended relativity model, m_m becomes the relativistic mass of a superluminal electron, with $m_0 = 5.11 \times 10^{-3} \text{ eV}/c^2$, the fine structure constant becomes a mass ratio and charge quantization is the result of two states of the electron.

Beyond hydrogen loading

Gianni Albertini

Università Politecnica delle Marche (UNIVPM) Via Brecce Bianche, 60131 Ancona, Italy

and

Massimo Rogante

Rogante Engineering Office, Contrada San Michele 61, 62012 Civitanova Marche, Italy

While experimental and technological attention is focused on the operational methods for hydrogen loading in metals and on the observed anomalies with respect to well-established rules, we aim to remark that these methods and these consequences can be seen as a part of a more general problem. In fact, most of the experiments and deductions of material sciences are based on the assumption that space-time is flat and isotropic (Minkowskian). After discarding this assumption, a theory of Deformed Space Time (DST) was developed in the last decades. Following this theory, experimental results were obtained which are not predicted by the Standard Model. The DST-theory concerns the fundamental interactions and in particular the nuclear ones, that can play the main role in the observed anomalies.

In order to consider a nuclear reaction as a DST-reaction, four main phenomenological features were deduced: occurrence of an energy threshold; change of atomic weight; absence of gamma radiation; anisotropic emission of nuclear particles in intense beams having a very short life span.

From the experimental point of view, rather than looking for fortuitous events that produce the conditions for DST-reactions, more systematic research can be undertaken by following the above reported four general rules. In particular, the occurrence of a thresholds can correspond to a latency time, necessary to reach the energy density necessary to deform space-time. The absence of gamma radiation cannot be considered as a sign that nuclear reactions are not present; in fact, in absence of detected gamma radiation elements were found which were not present before the reaction. The nuclear emissions, which are anisotropic and impulsive, can be difficult to detect with the traditional methods, thus inducing incertitude on the occurring reactions. Finally, a rapid variation of energy density is an experimental common factor of DST-reactions.

Thus, the DST-theory can be the leading theory in the design of the experiment and in the interpretation of its experimental results.

Paillet: Highly relativistic deep electrons and the Dirac equation

#Jean-Luc Paillet¹, Andrew Meulenberg²

¹Univ. Aix-Marseille, France, jean-luc.paillet@club-internet.fr

²Science for Humanity Trust, Inc., USA

Our works on the Electron Deep Orbits (EDOs) are motivated by the need to develop and complete a theoretical model to explain [1] some of the outstanding questions about low-energy nuclear reaction (LENR) results. These results, such as the quasi-absence of high-energy radiation and ejection of particles, require an understanding of the nuclear processes involved as well as the means of influencing them from a lattice. Moreover, a better understanding of EDOs and its interaction with nuclear fields will hopefully lead to a practical means of populating these deep levels in a nuclear region from which they can alter nuclear properties (e.g., transmutation and nuclear-decay processes) and facilitate electron capture. Over the last 3 years, we have analyzed results based on the use of relativistic quantum equations, because it was to be expected that an electron required to mediate fusion of two nuclei must maintain its high-probability of being between them and therefore must be relativistically or otherwise confined. That is why we particularly analyzed and extended [2] the results of [3] and validated [4] the need for Relativity. In our more recent works, we took the question of the EDO from a different angle, by studying in a semi-classical way, the possibility of a local minimum of total energy for an electron in the vicinity of the nucleus. For this, we consider combinations of attractive and repulsive potentials [5], as well as the action of radiative corrections, such as the Lamb shift, while satisfying both the Heisenberg Uncertainty relation (HUR) [6] [7] and virial theorem. Facing for the first time the thorny question of the HUR for electrons confined in deep orbits, we were able, not only to evaluate the coefficient g of these highly relativistic electrons, but also to show that a strong relativistic correction to the Coulomb potential leads to an effective potential capable of confining such energetic electrons.

In the present work, being equipped with these new insights and methods, we come back to a important and subtle theoretical question encountered during initial EDO calculations with the Dirac equation, which showed a significant overlap of the electron wavefunction with the physical nucleus: Should the energy levels, usually obtained with the Dirac equation solved while considering a point-like nucleus, be modified and how? In fact, computation of the energy of a deep-orbit electron from its probability-density distribution, allows us to adjust its initial energy level by applying a fixed-point method. Moreover we improve the semi-analytical solutions of the radial equations, to obtain wavefunctions having continuous derivatives on the femto-meter scale, including the surface delimiting the inside and outside of the nucleus. Doing this, we study how to preserve the initial coupling between the two components of Dirac solutions for EDOs. Finally, we give some approaches on the probability of presence of EDO states.

- [1] A. Meulenberg and J-L Paillet, "Implications of the electron deep orbits for cold fusion and physics," Proc. 20th Int. Conf. on CMNS, Sendai 2016, J. Condensed Matter Nucl. Sci. **24** (2017) 214-229, http://coldfusioncommunity.net/pdf/jcmns/v24/214_JCMNS-Vol24.pdf
- [2] Paillet, J.L., Meulenberg, A., "Electron Deep Orbits of the Hydrogen Atom", Proc. 11th Int..W. on Anomalies in Hydrogen Loaded Metals, Toulouse 2015, JCMNS 23, 62-84, 2017. http://coldfusioncommunity.net/pdf/jcmns/v23/62_JCMNS-Vol23.pdf
- [3] Maly J.A., Va'vra J "Electron transitions on deep Dirac levels II," Fusion Science and Technology, V.27, N.1, pp.59-70, 1995, http://www.ans.org/pubs/journals/fst/a_30350
- [4] Paillet, J.L., Meulenberg, A., "Special Relativity, the Source of the Electron Deep Orbits", Foundations of Physics, 47(2), pp. 256-264, 2017, Springer, Heidelberg.
- [5] Paillet, J.L., Meulenberg, A., "Advance on Electron Deep Orbits of the Hydrogen Atom", Proc. 20th Int. Conf. On CMNS, Sendai 2016, JCMNS 24, 258-277, 2016. http://coldfusioncommunity.net/pdf/jcmns/v24/258_JCMNS-Vol24.pdf
- [6] Paillet, J.L., Meulenberg, A., "Deepening Questions about Electron Deep Orbits of the Hydrogen Atom", Proc. 12th Int..W. on Anomalies in Hydrogen Loaded Metals, 2017, Asti. JCMNS 26, pp. 56-68, Oct. 2018, http://coldfusioncommunity.net/pdf/jcmns/v26/56_JCMNS-Vol26.pdf
- [7] Paillet, J.L., Meulenberg, A, On highly relativistic deep electrons, Proc. of ICCF21, 21th Conf. on Cond. Matter Nuclear Sci., Fort Collins (CO, USA), 3-8 June 2018, to be published in JCMNS 29, (2019).

Bowen: The Electromagnetic Considerations of the Nuclear Force

N. L. Bowen
Colorado Mountain College, Glenwood Springs, Colorado, USA
nbowen@coloradomtn.edu

The examination of the electromagnetic energies and forces within a nucleus is able to answer many questions about nuclear behavior. By incorporating the electromagnetic principles into nuclear theory, this model is able to achieve predictions of binding energy better than any accepted-current model and doing so using only one variable instead of five, as is used in the currently-accepted liquid drop model.

By applying the laws of electromagnetics to the quarks inside of the nucleus, the lowest energy configuration of hundreds of nuclei, from ${}^2\text{H}$ to ${}^{238}\text{U}$, have been determined, computer-modeled, and simulated. The binding energies of these nuclei have been calculated and compared to experimental data; the calculated binding energies agree with the experimental binding energies within a few percent. No other currently-accepted model of the nuclear force has been able to demonstrate such a tight prediction of binding energy with only one variable. This model is based on recent theoretical and experimental advances related to quarks and clustering.

In 1964, the existence of quarks was revealed by Nobel Prize winner Dr. Gell-Mann, changing the concepts of protons and neutrons from what was believed in the 1950's [1]. Since the concept of quarks was introduced, we now know that the electrical charge and magnetic moments of a nucleon are confined to the quarks, rather than being homogeneously distributed throughout the nucleon. A proton has three valence quarks, two up quarks and one down quark. A neutron also has three valence quarks, two down quarks and one up quark. Up quarks have an electrical charge which is $+2/3$ of an elementary charge. Down quarks have a charge which is $-1/3$ of an elementary charge.

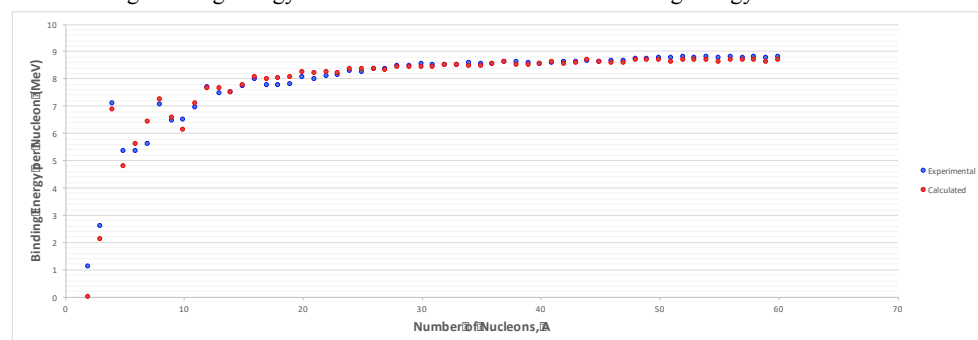
As a result of the experimental confirmation of quarks, recent nuclear theories postulate that the residual chromodynamic force bonds a quark in one nucleon to a quark in another nucleon, thereby binding the two nucleons together. In other words, the residual chromodynamic force is an internucleon quark-to-quark force. However, using the residual chromodynamic force to compute the binding energy is mathematically too complex to be useful [2].

Research regarding the clustering model of nuclei has recently shown that clustering structures do indeed exist within nuclei. Clustering is observed as a general phenomenon at high excitation energies in light alpha-like nuclei and is also a general feature observed in other nuclei as well, such as light neutron-rich nuclei. The alpha-cluster model has now been extended beyond just the alpha nuclei, with much study and research in the field of cluster structure and of so-called "nuclear molecules". These nuclear molecules can be thought of as being built from building blocks or segments, which are linked together in chain-like structure, to form the various nuclei [3, 4]. This recent research in the clustering structure of nuclei further corroborates the experimentally-observed collective motion of nuclei, and strongly supports the concept of an internal nuclear structure.

The residual chromo-dynamic force model postulates that the nuclear force is due to the attractive chromodynamic properties of the quarks. However, if this attractive force is dependent upon the electromagnetic attraction of the up-to-down quarks instead of the chromodynamic forces, then many questions can be readily answered with very simple mathematics. We know from electromagnetics, that a down quark is attracted to an up quark, but not to another down quark. Similarly, an up quark is attracted to down quark, but not to another up quark. Given this, it is quite possible that the nuclear force is the attraction of the up quark in one nucleon to the down quark in another nucleon. It is an internucleon force between two quarks, similar to the residual chromodynamic force.

Using electromagnetic equations, the lowest energy configurations are found for each nuclide. The lowest energy configurations for nuclei is, indeed, a chain-like structure very closely resembling those described in the cluster model. Only one variable needs to be selected for the best fit to the experimental binding energy data—the minimum distance between the two internucleon quarks. The Liquid Drop model uses five variables and a conditional logic statement to achieve its mathematical curve-fitting. The electromagnetic model of the nuclear force is able to get comparable results with only one variable. The value for the minimum distance between quarks was selected to be $2.11082 \cdot 10^{-16}$ meters. Hundreds of nuclides have been computer modeled and simulated using this method to calculate the binding energy based on electromagnetics. Using the lowest energy configuration, the electromagnetic energy is calculated and the resulting binding energy is determined.

The resulting bonding energy curve is shown. The calculated binding energy is shown in red circles, and the experimental binding energy is



shown in blue circles. These calculations have been done all the way out to ${}^{238}\text{U}$; however, the figure shows only the points from $A=2$ to $A=60$ for ease of viewing the details of this curve. As can be seen, there is excellent agreement in the reproduction of the experimental data. However, as the mass number becomes larger, the error becomes slightly larger as well.

- [1] M. Gell-Mann, The Eightfold Way:A Theory of Strong Interaction Symmetry, *DOE Technical Report*, Report Number TID-12608, 1961.
- [2] R. Machleidt, Nuclear Forces. *Scholarpedia*, 9(1):30710, 2014. doi: 10:4249/scholarpedia.30710.
- [3] L. R. Hafstad and E. Teller, The alpha-particle model of the nucleus, *Phys. Rev.* 54: 681, 1938.
- [4] M. D'Agostino, Focus: rod-shaped nucleus, *Phys. Rev. Focus*, 28: 10, 2011.